
Selected Methods for non-Gaussian Data Analysis

Krzysztof Domino

Foreword

The primary goal of computer engineering is the analysis of data. Such data are often large data sets distributed according to various distribution models. In this manuscript, we focus on the analysis of non-Gaussian distributed data. In the case of univariate data analysis, we discuss stochastic processes with auto-correlated increments and univariate distributions derived from specific stochastic processes, *i.e.* Lévy and Tsallis distributions. Inspired by the fact that there is an increasing interest in financial technology and computing, we use the Ising model applicable on the quantum computation on the D-Wave machine to discuss the stochastic process of real financial data generation and analysis.

A crucial observation is that stochastic processes with auto-correlated increments may lead to non-Gaussian distributed data that are relatively common among real-life data. One can consider here computer network traffic data, data generated for the machine learning purposes, audio signals, multiple sensors data, weather data, various medical data, and cosmological data, or finally financial data where the failure of a Gaussian predictive model may make a hazard in economy and lead in some cases to the bankruptcy. The motivation for this manuscript comes from the fact that it is expected from computer scientists to develop algorithms to handle real-life data such as non-Gaussian distributed ones. While analysing non-Gaussian distributed data, there may appear a temptation to assume a priori Gaussian distribution and disregard extreme data values that do not fit the assumption. Such a naive approach may worsen the outcome of the analysis of non-Gaussian distributed data, especially if simultaneous extreme values of many marginals are possible. Such extreme events are not predicted by a simple Gaussian model but rather by a non-Gaussian multivariate frequency distribution.

What is essential, in-depth investigation of multivariate non-Gaussian distributions requires the copula approach. A copula is a component of multivariate distribution (especially non-Gaussian one) that models the mutual interdependence between marginals. There are many copula families characterised by various measures of the dependence between marginals. Importantly, one of those is ‘tail’ dependencies that model the simultaneous appearance of extreme values in many marginals. Those extreme events may reflect a crisis given financial data, outliers in machine learning, or traffic congestion.

In this manuscript, we discuss copula-based data generation algorithms implemented in the Julia programming language that is an efficient open-source programming language suitable for scientific computation. The implementation is available on the GitHub repos-

itory, and the code is available for scientists for analysis and further development. We use a variety of copula families, especially those that can be applied in real-life data analysis (Gaussian, t -Student, Fréchet, Archimedean). Using those generators we perform experiments, demonstrating how different methods of features extraction or selection can distinguish between multivariate data distributed according to Gaussian or non-Gaussian copulas.

Having discussed non-Gaussian multivariate probabilistic models, we discuss higher order multivariate cumulants that are non-zero if the multivariate distribution is non-Gaussian. Nevertheless, the relation between those cumulants and copulas is not straight forward, but the d^{th} order multivariate cumulant encloses the natural measure of the d -variate cross-correlation between marginals. We discuss the application of those cumulants to extract information about non-Gaussian multivariate distributions, such that information about non-Gaussian copulas. The use of higher order multivariate cumulants in computer science is inspired by financial data analysis, especially by the safe investment portfolio evaluation. Apart from this, there are many other applications of higher order multivariate cumulants in data engineering, especially in: signal processing, non-linear system identification, blind sources separation, and direction finding algorithms of multi-source signals.

Another promising computer science discipline, where higher order multivariate cumulants are used, involves analysis of data obtained from hyper-spectral imaging. In this book, we discuss the small target detection scenario where the analysis of the non-Gaussian distribution of features is beneficial. We show on the real-life data example, from a forensic analysis, a need for non-Gaussian algorithms using copulas and higher order multivariate cumulants. Given those, we evolve algorithms based on higher order cumulants applicable for features selection and features extraction. We show by experiments the application of those methods in detecting subsets of marginals with non-Gaussian copulas, including copulas with ‘tail’ dependencies reflecting the appearance of simultaneous high values in many marginals being extreme events. For further real-life examples, we discuss through the manuscript applications of mentioned methods to analyse real-life biomedical data as well.

Contents

Foreword	3
List of symbols	6
1 Introduction	9
2 Univariate data models	15
2.1 Random variable and its increments	15
2.1.1 Central Limit Theorem	15
2.1.2 Scaling approach	18
2.1.3 Practical applications of auto-correlation analysis	21
2.2 Probabilistic non-Gaussian models	22
2.2.1 Lévy distribution	22
2.2.2 Tsallis q-Gauss distribution	24
2.3 Ising model of data	27
2.3.1 The Ising model	27
2.3.2 Simulated annealing on the D-Wave machine	28
3 Multivariate Gaussian models	31
3.1 Multivariate Gaussian Distribution	31
3.2 Gaussian copula	33
4 Copulas	37
4.1 Elliptical copulas	39
4.2 Upper and lower limit, Fréchet families	42
4.2.1 Maximal copula	42
4.2.2 Minimal copula	43
4.2.3 Independent copula and a Fréchet family copula	43
4.3 Archimedean copulas	45
4.3.1 Archimedean copulas examples	47
4.3.2 Sampling Archimedean copulas	48
4.3.3 Nested Archimedean copula	50
4.4 Data generation for features detection	54
4.4.1 t -Student copula case	56

4.4.2	Fréchet copula case	56
4.4.3	Archimedean copula case	57
4.5	Implementation and experiments	59
4.5.1	Implementation	59
4.5.2	Experiments	61
5	Higher order statistics of multivariate data	69
5.1	Cumulants of multivariate Gaussian distribution	72
5.2	Tensors and tensor networks - quantum mechanics inspired tools	72
5.2.1	Moments tensors	73
5.2.2	Cumulants tensors	75
5.2.3	Calculation and programming implementation	81
5.3	Cumulants of copulas	81
5.3.1	Archimedean copulas	83
5.3.2	Fréchet copula	83
5.3.3	<i>t</i> -Student copula	84
5.4	Auto-correlation function and cumulants	85
6	Cumulants in machine learning	89
6.1	Features selection	96
6.1.1	Classical method MEV	97
6.1.2	Cumulant based features selection	98
6.1.3	Experiments	103
6.2	Features extraction	104
6.2.1	High Order Singular Value Decomposition	106
6.2.2	Multi-cumulant higher order singular value decomposition	108
6.2.3	Experiments	110
7	Discussion	113

Symbol	Description/explanation
\mathfrak{X}	univariate random variable
$X = [x_1, \dots, x_t]^\top$	vector of its realisations
$\mathbb{E}(\mathfrak{X}), \mathbb{E}(\mathfrak{X}^2), \dots$	expectation value operators
$f(x), F(x)$	univariate PDF and CDF functions
$\mathcal{N}(\mu, \sigma^2)$	normal univariate distribution with mean μ and variance σ^2
Uniform($[0, 1]$)	uniform univariate distribution on segment $[0, 1]$
$(1 : n)$	a vector $[1, 2, \dots, n]$
$\mathfrak{X}^{(n)}, \mathfrak{X}_i$	n -variate random vector and its the i^{th} marginal
$\mathbf{X} \in \mathbb{R}^{t \times n}$	matrix of t realisations of n -variate random vector, with elements $x_{j,i}$
$\mathbf{x}_j = [x_{j,1}, \dots, x_{j,n}]$	the single j^{th} realisation of n -variate random vector
$\mathfrak{Z}_i, \mathfrak{Z}_i^{(n)}$	the i^{th} increment of an univariate or a multivariate random variable.
$\mathbf{f}(\mathbf{x}), \mathbf{F}(\mathbf{x})$	multivariate PDF and CDF functions
$\mathfrak{U}^{(n)}$	n -variate random vector with all marginals uniformly distributed on $[0, 1]$ segment
$\mathbf{c}(\mathbf{u}), \mathbf{C}(\mathbf{u})$	copula density and copula function
$\mathbf{A} \in \mathbb{R}^{n_1 \times n_2}$	matrix with elements a_{i_1, i_2}
$\mathbf{\Sigma} \in \mathbb{R}^{[n, 2]}$	covariance matrix with elements s_{i_1, i_2}
$\mathcal{N}(\mu, \mathbf{\Sigma})$	normal multivariate distribution parametrised by the mean vector μ and the covariance matrix $\mathbf{\Sigma}$
$\mathcal{T} \in \mathbb{R}^{n_1 \times \dots \times n_d}$	d mode tensor of size $n_1 \times \dots \times n_d$, with elements t_{i_1, \dots, i_d}
$\mathcal{T} \in \mathbb{R}^{[n, d]}$	d mode super-symmetric tensor of size $n \times \dots \times n$, with elements t_{i_1, \dots, i_d}
$\mathcal{C}_d \in \mathbb{R}^{[n, d]} \quad \mathcal{M}_d \in \mathbb{R}^{[n, d]}$	d^{th} cumulant, moment tensor with elements $c_{i_1, \dots, i_d}, m_{i_1, \dots, i_d}$

Table 1: Symbols used in the book.

Chapter 1

Introduction

The basic goal of computer engineering is the analysis of data. Such data are often large data sets distributed according to various distribution models. In this manuscript we focus on the analysis of non-Gaussian distributed data. To show that such data are rather common among real-life data, we can mention data with auto-correlated increments that may lead to non-Gaussian distributions both in an univariate (see Chapter 2) and in a multivariate data case. For comparison with multivariate Gaussian models see Chapter 3. Deep investigation of non-Gaussian multivariate distributions requires the copula approach [1], see Chapter 4. A copula is an component of multivariate distribution (especially non-Gaussian one) that models the mutual interdependence between marginals. To extract probabilistic information about non-Gaussian multivariate distributions we use multivariate higher order cumulants, see Chapter 5 that are non-zero if data are non-Gaussian distributed [2, 3]. Having introduced higher order multivariate cumulants we use them in Chapter 6 to discuss and develop some machine learning algorithms that can detect non-Gaussian features. For the programming implementation we use the Julia programming language [4, 5], that is modern, efficient, open source and high level programming language suitable for scientific computations.

The motivation for this book comes from the fact that there are many types of non-Gaussian distributed real life data, and it is expected from computer scientists to develop algorithms to analyse such data. While handling non-Gaussian distributed data, there may appear a temptation to assume a priory Gaussian distribution and disregard extreme data, that do not fit such Gaussian distribution and are out of priory assumed model. Gaussian models are discussed in Chapter 3. Such naive approach may worsen the outcome of the analysis of non-Gaussian distributed data. For a meaningful example consider financial data. Here simultaneously extreme values of many marginals, that are not expected by a simple Gaussian model, may appear especially during a crisis [6]. Such extremes results being the failure of a Gaussian predictive model, may lead in some cases to the bankruptcy [7].

To show wider application of non-Gaussian models, one can observe that computer network traffic data do not follow the Gaussian distribution [8]. This is due to the fact that computer network data may possess long range auto-correlations [9, 10, 11]

of increases, or may be modelled by the Lévy process [12]. The same is true for financial data [7]. To see more analogies between those two types of data, observe that to model both multivariate computer network traffic data [13, 14] and multivariate financial data [6] one uses non-Gaussian copulas. Beside those distinct examples, there are many other example of non-Gaussian distributed real-life data that are expected to be handled by computer scientists. One of them are audio signals [15, 16] (see also [17, 18, 19, 20]), or multiple sensors data [21]. The other are weather data [22, 23, 24], various medical data [25, 26], and cosmological data [27]. It is also worth to mention data generated for machine learning purposes using non-Gaussian copulas [28].

The probabilistic model for multivariate non-Gaussian distributed data, includes the copula that model interdependency between marginals this is discussed in Chapter 4. There are many copula families, all imposing different measures of the interdependence between marginals. One of such measures are ‘tail’ dependencies that model the simultaneous appearance of extreme values in many marginals. Such extreme events may reflect: a crisis while analysing financial data, outliers data in machine learning, or a traffic congestion. In this book we discuss widely copulas and copula-based data generation algorithms. We have implemented those algorithms in the Julia programming language that is an efficient open source programming language suitable for scientific computation. The implementation is available in the GitHub repository [29] and the code is available for scientists for analysis and further development. In the implementation we use variety of copula families (such as Gaussian, t -Student, Archimedean, Fréchet and Marshal-Olkin), that can be found in real life data analysis. For the application of copulas in decision making algorithms [30] or the machine learning, see copulas application in the remotely sensed images [31, 32] analysis.

Unfortunately, higher order multivariate cumulants are hard to calculate, especially for large multivariate data sets. This is due to high computational complexity of cumulants calculation while using straight forward algorithms. See [33] for discussion and the multivariate cumulants calculation algorithm implemented in the R programming language. To overcome this problem in [34] a fast parallel algorithm for multivariate high order cumulants calculation was introduced. Here multivariate cumulants were represented in the tensor form structured in the form of blocks to take advantage of their super-symmetry and reduce to minimum redundant operations. In this book we discuss algorithms implemented in Julia programming language [35]. Our approach makes the multivariate cumulants analysis more tractable and practical.

To understand the meaning of multivariate cumulants, one should observe that an univariate frequency distribution can be characterised by the series of scalar cumulants: the first is a mean, the second a variance, the third is proportional to an asymmetry, the fourth to a kurtosis, etc. The multivariate frequency distribution can be characterised by a series of cumulants as well, but those cumulants are no more scalars. If we consider multivariate data with n marginals (or features using the machine learning terminology) the first multivariate cumulant is a mean vector of size \mathbb{R}^n , the second one is a covariance matrix of size $\mathbb{R}^{n \times n}$. Multivariate cumulants of order d , where $d \geq 3$ are called higher order cumulants, and as discussed further in this book, they carry information about the

non-Gaussian multivariate distribution of data. Those higher order cumulants can be represented in the form of d -dimensional array of size n^d [34], called the d -mode tensor. Hence if computing or storing them, a computer memory requirement and a processor time requirement rises rapidly with d , especially for high n as in many real life data cases. This requires more sophisticated algorithms, as those introduced in [34] to reduce computational power and memory requirements.

Having overcome computational difficulties in calculating higher order multivariate cumulants, we can move to their practical application in non-Gaussian data analysis. In general, the use of higher order multivariate cumulants in computer science is inspired on financial data analysis. See [36, 37, 38, 39], where the practical use of such cumulants for safe investment portfolio determination is discussed. For the computer science application of those cumulants, consider for example signal processing [40, 16, 41, 42], non-linear system identification [43, 44], blind sources separation [45, 46], and direction finding algorithms of multi-source signals [17]. Another promising computer science discipline, where higher order multivariate cumulants are used, involves data analysis from hyper-spectral imaging. In [47] new higher order cumulant based algorithm of features selection for the small target detection of hyper-spectral data is discussed. This type of algorithms is discussed and developed in this manuscript. Finally, consider the analysis of computer network traffic data. There are some recent results concerning the use of higher order univariate cumulants [48, 49, 50] to analyse such data. For the discussion on the potential application of higher order multivariate cumulants, for such data scenario, see the introduction of [51]. Hence, one can hope for new results the use of higher order multivariate cumulants to model computer network traffic data.

Let us use the example of financial data, to discuss why data may be non-Gaussian distributed, despite the fact, that in many cases data records are sums on many increases and the Central Limit Theorem should hold leading to the Gaussian distribution of such data. In this case we consider financial data being a share prices traded on the stock exchange. The current share price is the price of last transaction. Such transactions may occur frequently. For major companies shares traded on major stock exchanges we have many transactions per second. The transaction price is derived from buy and sell orders on the stock exchange. However, as discussed in [52], the relation is not straight forward. In general, as time pass new orders are recorded, and new transactions are executed. Let $x_0 \in \mathbb{R}^+$ be an initial price and $x_1 \in \mathbb{R}^+$ a price after the transaction is recorded. In this case the increment is:

$$z_1 = x_1 - x_0. \quad (1.1)$$

The price after k transactions is given by the following sum of increments,

$$x = x_0 + \sum_{i=1}^k z_i \quad (1.2)$$

If increments z_1, \dots, z_k were independent, sampled from identical distribution with finite variance, than according to the Central Limit Theorem [53] x would be a sample from the Gaussian distribution. In practice for financial data, conditions of the Central Limit Theorem may not be fulfilled due to:

1. long range auto-correlations of increments, see [54],
2. increments from distribution without finite variance, see [55],
3. varying distributions of increments [56].

Hence, financial data may not be Gaussian distributed.

As discussed in Chapter 2, to demonstrate that it is true not only for financial data analysis, we can refer to some computer science data models inspired on financial data models. For this end consider that autoregressive models [56, 57, 58] rewarded by the Nobel Price in 2003 for financial data modelling. Analogically such models are used for computer network traffic [11]. Further [59] there are sophisticated financial data models concerning games theory, or analogies with complex physical systems [60]. Such analogies explains financial crisis using stochastic auto-correlated processes, fractals and multi-fractals, and non-Gaussian distributions. What more, there are hierarchical models of investors behaviour [61], and we have hierarchical models of the computer network traffic as well [62]. In Section 2.3 we discuss the Ising model of financial data [63] concerning a hierarchical relation between investors and we propose the quantum computing scheme applicable on the D-Wave machine to implement this model. Such approach is based on the discussion of features and limitations of the Chimera graph, being a scheme of a processor unit of the D-Wave machine. By analogy such model may be applicable to analyse other types of computer science data.

After introducing stochastic models leading do non-Gaussian distributions, we can discuss now real life applications of multivariate probabilistic models of non-Gaussian distributed data. One should note that, there is a vital real life issue of multivariate financial data analysis. It is an evaluation of a risk of investment portfolio composed of many assets. In the portfolio management practice one either minimise risk, given expected revenue, or maximise revenue given acceptable risk [64]. This can be generalised to the computer science multi-parameter optimisation problem. The classical financial engineering method [64] identifies risk with the variance of the portfolio value and assumes that financial data are multivariate Gaussian distributed. Next, it uses eigenvalue/eigenvector decomposition of the covariance matrix. However, as discussed before, financial data are often non-Gaussian distributed, hence the covariance matrix and a mean vector does not carry all information about their frequency distribution. It is why the classical financial engineering method fails to anticipate cross-correlated extreme events [37], especially during the crash, imposing the bankruptcy risk.

Such failure of the Gaussian distribution in financial engineering, gives the motivation to investigate machine learning methods applicable for non-Gaussian distributed financial data at first and other types of data as well. In machine learning, there are many feature extraction and features selection methods, based on the multivariate Gaussian distribution assumption [65]. There exists a temptation to use such methods without testing if data are Gaussian or non-Gaussian distributed. Examples of Gaussian distribution based machine learning methods are Singular Value Decomposition (SVD) of the covariance matrix or the Principle Component Analysis (PCA) [66, 67].

To discuss features selection, let us consider hyper-spectral camera data. We can consider spectral channels of such camera as n marginals of a random vector and light intensities recorded at each pixel as t realisations of such random vector. In practice $n \sim 100$, and $t \sim 10^5$. In the spectral approach [68], we analyse multivariate statistics of such data, hence we ignore spatial information due to pixel's relative positions. Due to the presence of phenomena such as spectral mixing and feature redundancy [69], we are often interested in selecting the subset of features (spectral canals) that carries information relevant for further processing. There are classical methods of features selection, that use only information stored in a covariance matrix, see for example the Maximum Ellipsoid Volume (MEV) [70].

Alternatively to the features selection scenario we may be interested in linear combinations of features that carries meaningful information. The classical method of such features extraction is the Principle Component Analysis (PCA) [67]. This method uses the Gaussian distribution assumption of data as well. Obviously there are methods of features extraction or features selection that does not require the Gaussian distribution assumption of data, see introduction in [47]. Those methods in general are either supervised or analyse only marginal frequency distributions of data. Supervised methods are dependent on the training samples what may lead to instability of the solution, therefore unsupervised methods may be more robust [71]. On the other hand, methods that analyses only marginal frequency distributions are not sensitive on copulas [1], what may decrease their predictive power for non-Gaussian copula of data. Besides those methods, consider the Independent Component Analysis [72] (ICA) that is useful for features extraction [73] and selection [74] of non-Gaussian distributed data. Unfortunately, ICA results are probabilistic and do not analyse standard correlations of data, what makes the ICA less robust.

There are few machine learning methods using higher order multivariate cumulants, despite the fact that such cumulants carry meaningful information about non-Gaussian joint frequency distribution of data. Hence, analogically to the financial engineering case, higher order multivariate cumulants should give better machine learning algorithms dedicated to non-Gaussian distributed data. In this book we discuss and improve some features selection and features extraction methods that use mentioned higher order multivariate cumulants. Furthermore we show by experiments the application of those methods in detecting subsets of marginals modelled by non-Gaussian copulas, including copulas with 'tail' dependencies reflecting the appearance of simultaneous high values of many marginals *i.e.* extreme events.

The implementation described in this book utilises tensors [75] to store high order multivariate cumulants. We use tensor operations presented in the form of tensor networks to increase the clarity of the formulas. Observe that such tensor network presentation is inspired by the quantum mechanics, see [37] where the method of even order cumulants calculation has been developed by analogy to Feynman diagrams used in the particle quantum physics. Such approach is used for financial data analysis, however priory Weibull class distribution of data is assumed. In this book we provide a general algorithm of any order multivariate cumulants calculation, regardless of the data distri-

bution. Concluding the analogy between tensor networks of higher order cumulants and Feynman diagrams is worth to notice.

Chapter 2

Univariate data models

In this chapter, we discuss univariate models of data employing stochastic processes. For this purpose, we assume that data are generated by the random process and we consider both random processes with independent or correlated increments.

2.1 Random variable and its increments

We start with the standard approach of independent increments and the Central Limit Theorem.

2.1.1 Central Limit Theorem

Let us start with a simple random process. Suppose that we start with initial value $x_0 = 0$. Next in a unit time we increment it by $z_i = \pm\delta$. The sign of an increment is chosen each time randomly, hence all increments are independent. The probability of being in position x after k steps is binomial

$$f_k(x) = \left(\frac{1}{2}\right)^k \binom{k}{\frac{(x/\delta)+k}{2}}. \quad (2.1)$$

Here $f_k(x)$ is the discrete function since $\frac{(x/\delta)+k}{2}$ must be an integer. One can show that $f_k(x)$ is normalised: $\sum_x f_k(x) = 1$ and positive valued. The discrete function fulfilling those conditions is called in literature the probability mass function. If increments are independent, $f_k(x)$ for relatively high k can be approximated by means of the continuous Gaussian PDF (Probability Distribution Function), see Figure 2.1(a).

Switching to a random variable notation, x is a single realisation of the following random variable

$$\mathfrak{X}_k = \sum_{i=1}^k \mathfrak{Z}_i, \quad (2.2)$$

where $\mathfrak{Z}_1, \dots, \mathfrak{Z}_k$ are independent random variables (increments). The random variable \mathfrak{Z}_i has two possible realisations $z_i = \delta$ with probability $\frac{1}{2}$, or $z_i = -\delta$ with probability $\frac{1}{2}$.

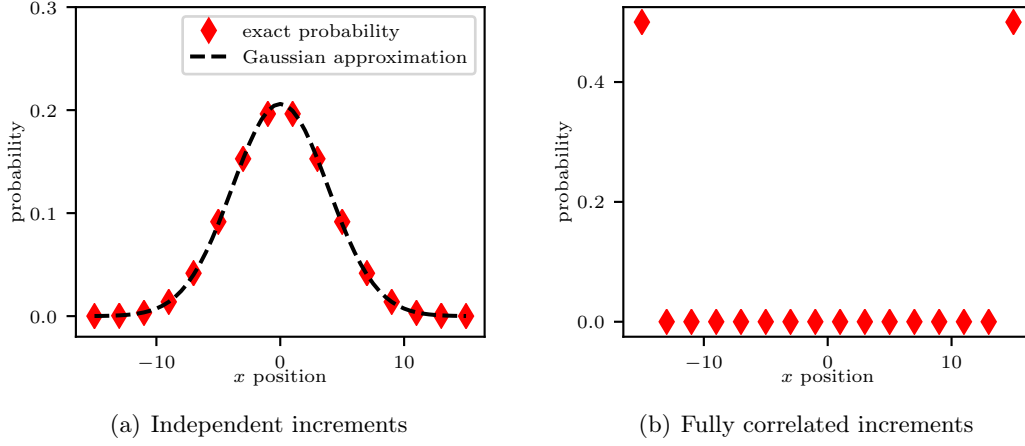


Figure 2.1: Probabilities of simple random process after $k = 15$ steps, $\delta = 1$

It is easy to show that the expecting value of \mathfrak{X}_k is $\mathbb{E}(\mathfrak{X}_k) = 0$. Following [76], the variance of \mathfrak{X}_k is

$$\begin{aligned} \sigma^2(\mathfrak{X}_k) &= \mathbb{E}\left((\mathfrak{X}_k - \mathbb{E}(\mathfrak{X}_k))^2\right) = \mathbb{E}\left(\sum_{i=1}^k \mathfrak{Z}_i\right)^2 = \mathbb{E}\left(\sum_{i=0}^k \mathfrak{Z}_i^2\right) + 2\mathbb{E}\left(\sum_{i>j}^k \mathfrak{Z}_i \mathfrak{Z}_j\right) \\ &= \delta^2 k + 0 = \delta^2 k, \end{aligned} \quad (2.3)$$

and the standard deviation is $\sigma = \delta\sqrt{k}$, hence $\sigma \propto \sqrt{k}$.

Remark 2.1.1. For the random variable \mathfrak{X} with realisations x_1, \dots, x_t occurring with probabilities p_1, \dots, p_t such that $p_i \geq 0 \wedge \sum p_i = 1$ the expecting value fulfils

$$\mathbb{E}(\mathfrak{X}) = \sum_{i=1}^t p_i x_i. \quad (2.4)$$

While estimating the expected value we can assume that each realisation is equally probable, hence the estimator would be

$$\mathbb{E}(\mathfrak{X}) = \frac{1}{t} \sum_{i=1}^t x_i. \quad (2.5)$$

According to Central Limit Theorem (Theorem 2.1.1) the distribution of \mathfrak{X}_k can be approximated by the Gaussian one. The higher the k , the better the approximation.

The Gaussian distribution has the following Probability Distribution Function (PDF)

$$f(x) = \frac{1}{\sqrt{2\pi}\sigma} \exp\left(-\frac{x^2}{2\sigma^2}\right), \quad (2.6)$$

and the following Cumulative Distribution Function (CDF)

$$F(x) = p(\mathfrak{X} \leq x) = \int_{-\infty}^x \frac{1}{\sqrt{2\pi}\sigma} \exp\left(-\frac{u^2}{2\sigma^2}\right) du. \quad (2.7)$$

Let us move to the formal definition of the Central Limit Theorem [53].

Theorem 2.1.1. *Let $\mathfrak{Z}_1, \mathfrak{Z}_2, \dots, \mathfrak{Z}_k$ be univariate random variables which*

1. *are independent,*
2. *are identically distributed,*
3. *have defined finite variance $\delta^2 = \sigma^2(\mathfrak{Z}_i)$ and the mean value μ_z .*

The random variable

$$\mathfrak{X}'_k = \frac{1}{\sqrt{k}} \sum_{i=1}^k (\mathfrak{Z}_i - \mu_z) \quad (2.8)$$

has the frequency distribution that converges to $\mathcal{N}(0, \delta^2)$ as $k \rightarrow \infty$.

Remark 2.1.2. One of the important features of a Gaussian distribution is a fact that it is stable in the following sense. Suppose we have two independent random variables $\mathfrak{Z}_1 \sim \mathcal{N}(\mu_1, \sigma_1^2)$ and $\mathfrak{Z}_2 \sim \mathcal{N}(\mu_2, \sigma_2^2)$, their sum is Gaussian distributed as well,

$$\mathfrak{Z}_1 + \mathfrak{Z}_2 \sim \mathcal{N}(\mu_1 + \mu_2, \sigma_1^2 + \sigma_2^2). \quad (2.9)$$

If \mathfrak{Z}_1 and \mathfrak{Z}_2 are Gaussian distributed increments their sum would be Gaussian distributed as well.

Let us now discuss a few examples where the Central Limit Theorem holds or does not hold.

Example 2.1.1. *Suppose that $\mathfrak{Z}_1, \mathfrak{Z}_2, \dots, \mathfrak{Z}_k$ are identically distributed with mean μ and variance δ^2 , but not independent. The distribution of \mathfrak{X} will be Gaussian (but with changed parameters) if the auto-correlation between $\mathfrak{Z}_i, \mathfrak{Z}_j$ is short range i.e. the auto-correlation function $acf_{i,j}$ falls rapidly with $|i-j|$, see [77] for details. The auto-correlation function [78] is defined by:*

$$acf_{i,j} = \mathbb{E}((\mathfrak{Z}_i - \mu)(\mathfrak{Z}_j - \mu)) \quad (2.10)$$

i.e. without normalisation. For the auto-correlation coefficient [78] one introduces the following normalisation:

$$acc_{i,j} = \frac{acf_{i,j}}{\delta^2} \quad (2.11)$$

Example 2.1.2. *Suppose now, that $\mathfrak{Z}_1, \mathfrak{Z}_2, \dots, \mathfrak{Z}_k$ are fully dependent. Assume that $z_1 = \pm\delta$ with equal probability, but: If $z_1 = \delta$ than $z_2 = \dots = z_k = \delta$, and oppositely if $z_1 = -\delta$ than $z_2 = \dots = z_k = -\delta$. It follows that:*

$$\sigma^2(\mathfrak{X}) = \mathbb{E}(\mathfrak{X}^2) = \mathbb{E}\left(\sum_{i=1}^k \mathfrak{Z}_i\right)^2 = k^2 E(\mathfrak{Z}_1)^2 = k^2 \delta^2. \quad (2.12)$$

The standard deviation would be: $\sigma = k\delta$ i.e. $\sigma \propto k$, and the PDF would be:

$$f_k(x) = \begin{cases} \frac{1}{2} & \text{if } x = k\delta \\ \frac{1}{2} & \text{if } x = -k\delta \\ 0 & \text{elsewhere} \end{cases}, \quad (2.13)$$

that do not converge to a Gaussian distribution, see Figure 2.1(b). Importantly in this case we have $\sigma \propto k$ in contrary to the independent increments case, where $\sigma \propto \sqrt{k}$ see Eq. (2.3). This observation will be used further in an auto-correlation analysis.

Example 2.1.3. Consider the following Auto-Regressive Conditional Heteroskedasticity (ARCH, GARCH) models [56, 79, 80]. We have a random process defined by increments $\mathfrak{Z}_1, \dots, \mathfrak{Z}_k$ with realisations z_1, \dots, z_k , where

$$\mathfrak{Z}_i \sim \mathcal{N}(0, \delta_i^2). \quad (2.14)$$

The variance is a function of past realisations of increments, in the ARCH model it is:

$$\delta_i^2 = \alpha_0 + \sum_{j=1}^p \alpha_j (z_{(i-j)})^2. \quad (2.15)$$

In the Generalised ARCH model, called GARCH [81, 82] the variance is:

$$\delta_i^2 = \alpha_0 + \sum_{j=1}^p \alpha_j (z_{(i-j)})^2 + \sum_{j=1}^p \beta_j \delta_{(i-j)}^2 \quad (2.16)$$

where $\alpha_0 > 0, \alpha_j, \beta_j \geq 0$ and p is the length of the auto-correlation. Such models break conditions 1 and 2 of the Central Limit Theorem, Theorem 2.1.1, hence a sum of increments

$$\mathfrak{X} = \sum_{i=1}^k \mathfrak{Z}_i \quad (2.17)$$

may not be Gaussian distributed. Such autoregressive models were developed to analyse financial data [56, 79, 82] and rewarded by the Nobel prize in 2003. Moreover, similar auto-regressive models appear in modelling computer network traffic data [11, 83, 84]. Beside this non-linear GARCH/ARCH models are recently used to analyse various data such as weather data [85], EEG signal analysis [86], brain activity analysis [87], EMG (electromyography) data analysis [88], speech signal analysis [89], and sonar imaging [90].

2.1.2 Scaling approach

In this subsection we concentrate on the specific ceases of auto-correlation of increments. For the need of this and the following subsections we introduce random variables as a

sum of zero mean increments

$$\begin{aligned}\mathfrak{X}(k) &= \sum_{i=1}^k \mathfrak{Z}_i, \\ \Delta\mathfrak{X}(k, \Delta k) &= \sum_{i=k+1}^{k+\Delta k} \mathfrak{Z}_i.\end{aligned}\tag{2.18}$$

Suppose now that increments are independent and, for the sake of clarity of, all distributed according to $\mathfrak{Z}_i \sim \mathcal{N}(0, 1)$. It is easy to show that

$$\mathbb{E}(\mathfrak{X}(k)\mathfrak{X}(k+h)) = \mathbb{E}(\mathfrak{X}(k)\mathfrak{X}(k)) + \mathbb{E}(\mathfrak{X}(k)\Delta\mathfrak{X}(k, \Delta k)) = k.\tag{2.19}$$

Analogously the following auto-correlation is zero

$$\mathbb{E}(\Delta\mathfrak{X}(k, \Delta k)\Delta\mathfrak{X}(k+h, \Delta k)) = 0.\tag{2.20}$$

Following [7], consider now a random variable being a sum of not independent but zero mean increments \mathfrak{Z}_i . Such random variable is assumed to fulfil

$$\mathbb{E}(\mathfrak{X}(k)\mathfrak{X}(k+h)) = \frac{1}{2} \left(k^{2H} + (k+h)^{2H} - h^{2H} \right),\tag{2.21}$$

where we have the scaling exponent $0 < H < 1$. Here we do not require explicitly \mathfrak{Z}_i to be Gaussian distributed. Given these, it can be shown from Eq. (2.21) that

$$\mathbb{E}(\mathfrak{X}^2(k)) = k^{2H},\tag{2.22}$$

and for $H = \frac{1}{2}$ we reproduce independent case in Eq. (2.19).

Following Eq. (2.21) and taking $h \gg \Delta k$ we measure the long-range auto-correlation. Using the expansion

$$(h \pm \Delta k)^{2H} = h^{2H} \pm 2Hh^{2H-1}\Delta k + 2H(2H-1)h^{2H-2}\frac{(\Delta k)^2}{2} \pm \dots + \dots\tag{2.23}$$

we obtain the following long range auto-correlation function of $\Delta\mathfrak{X}$:

$$\begin{aligned}\mathbb{E}(\Delta\mathfrak{X}(k, \Delta k)\Delta\mathfrak{X}(k+h, \Delta k)) &= \mathbb{E}((\mathfrak{X}(k+\Delta k) - \mathfrak{X}(k))(\mathfrak{X}(k+h+\Delta k) - \mathfrak{X}(k+h))) \\ &= \frac{1}{2} \left((h+\Delta k)^{2H} + (h-\Delta k)^{2H} \right) - h^{2H} \\ &\approx H(2H-1)h^{2H-2}(\Delta k)^2.\end{aligned}\tag{2.24}$$

Now, from Eq. (2.21) we can show that

$$\mathbb{E}(\Delta\mathfrak{X}^2(k, \Delta k)) = (\Delta k)^{2H}\tag{2.25}$$

Importantly, Eq. (2.25) or its modification can be used to determine the scaling exponent. The auto-correlation coefficient (normalised auto-correlation function [78]) of $\Delta\mathfrak{X}$ given the time lag $h \gg \Delta k$ is:

$$\text{acc}_{\Delta k, h} \approx \frac{H(2H-1)h^{2H-2}(\Delta k)^2}{(\Delta k)^{2H}}, \quad (2.26)$$

which depends on Δk . However, we are rather interested in the sign of the auto-correlation function for large h that is:

$$\text{sign}(\text{acc}_{\Delta k, h}) = \begin{cases} +1 & \text{if } \frac{1}{2} < H < 1 \\ 0 & \text{if } H = \frac{1}{2} \\ -1 & \text{if } H < \frac{1}{2} \end{cases}. \quad (2.27)$$

Suppose now that despite the auto-correlation of elementary increments, $\Delta\mathfrak{X}$ are Gaussian distributed, at least for some range of Δk . Then for $2q \in \mathbb{N}$ we have

$$\mathbb{E}(|\Delta\mathfrak{X}(k, \Delta k)|^{2q}) = (\Delta k)^{2qH} \left(\frac{2^q \Gamma\left(\frac{2q+1}{2}\right)}{\sqrt{\pi}} \right) \quad (2.28)$$

that are moments of a Gaussian distribution with covariance $\sigma^2 = (\Delta t)^{2H}$. Hence:

$${}^{2q}\sqrt{\mathbb{E}(|\Delta\mathfrak{X}(k, \Delta k)|^{2q})} \propto (\Delta k)^H, \quad (2.29)$$

at least for $2q \in \mathbb{N}$. We have the same scaling exponent regardless which moment we analyse.

On the other hand, if $\Delta\mathfrak{X}$ is not Gaussian distributed due to auto-correlation or non-Gaussian distributions of elementary increments, we have the multi-fractal scaling [7]

$${}^{2q}\sqrt{\mathbb{E}(|\Delta\mathfrak{X}(k, \Delta k)|^{2q})} \propto (\Delta k)^{H(q)}, \quad (2.30)$$

where each $H(q)$ belongs to the spectrum of scaling exponents. In practice such multi-fractal analysis is extended as well on non-integer $2q$, negative q and zero q . For such multi-fractal scaling in financial data see [7], in computer network traffic data see [91, 92], in image analysis see [93] while in biomedical data see [94].

Remark 2.1.3. Consider that the auto-correlation coefficient (normalised auto-correlation function [78]) is a Pearson's correlation coefficient between $\Delta\mathfrak{X}(k, \Delta k)$ and $\Delta\mathfrak{X}(k+h, \Delta k)$. As discussed further in Chapter 4 and Section 5.1 such Pearson's correlation carry a whole information about the auto-correlation given a Gaussian distribution of $\Delta\mathfrak{X}$. Otherwise, complementary to the multi-fractal approach, we may use higher order cumulant's approach, as discussed in [95, 40], see also Section 5.4. Exemplary tri-variate auto-correlation would be

$$\mathbb{E}(\Delta\mathfrak{X}(k+h_1, \Delta k)\Delta\mathfrak{X}(k+h_2, \Delta k)\Delta\mathfrak{X}(k, \Delta k)). \quad (2.31)$$

Given $\Delta k = 1$ we can use elementary increments. If the random process is stationary, this tri-variate auto-correlation is k independent. Given those it is only parametrised by two lags parameters h_1 and h_2 .

Algorithm 1 Compute a Hurst Exponent using multifractal DFA.

```

1: Input:  $Y \in \mathbb{R}^t$  - univariate time series,  $q \in \mathbb{R}$ , a multi-fractal parameter,  $N \ll t$  -
   Int, the algorithm parameter.
2: Output:  $H(q) \in \mathbb{R}$  a Hurst exponent value.
3: function DFA( $Y, q$ )
4:   for  $i \leftarrow 1$  to  $N$  do
5:      $\tau = \lceil \frac{t}{i} \rceil$ 
6:     for  $k \leftarrow 1$  to  $i$  do
7:        $\mathbb{R}^\tau \ni Y' = [y_{(\tau-1)k+1}, y_{(\tau-1)k+2}, \dots, y_{((\tau-1)k+k)}]^\top$ 
8:       fit model  $Y' \rightarrow M$   $\triangleright$  model predictions  $M = [m_1, \dots, m_\tau]$ 
9:        $\Delta_k = \frac{1}{\tau} \sum_{j=1}^{\tau} \left( (y'_j - m_j)^2 \right)^q$   $\triangleright Y' = [y'_1, \dots, y'_\tau]$ 
10:    end for
11:     $\Delta_{(2q)}(\tau) = \frac{1}{i} \sum_{k=1}^i \Delta_k$ ,
12:  end for
13:  find  $H_q$  using linear regression of:  $\log(\Delta_{(2q)}(\tau)) \propto 2q \cdot H(q) \log(\tau)$ 
14:  return  $H_q$ 
15: end function

```

2.1.3 Practical applications of auto-correlation analysis

Let us state the following practical problem. We have a series of realisation of an univariate random variable \mathfrak{Y} , and want to analyse auto-correlation. Such analysis may be helpful to predict potential statistics of \mathfrak{Y} . Further real data are often a joint result of the deterministic and random process, for example

$$\Delta \mathfrak{Y}(k, \Delta k) = f(k, \Delta k) + \Delta \mathfrak{X}(k, \Delta k), \quad (2.32)$$

were $f(k, \Delta k)$ is the deterministic term. To analyse the auto-correlation of $\Delta \mathfrak{X}$, than can reveal a dynamics of interesting us system, one can use the Detrended Fluctuation Analysis (DFA), where the scaling of the divergence from the local trend is analysed [96, 97]. In practice linear trend models are often used here, but other non-linear models are also possible. In the multi-fractal DFA, one can determine spectrum of scaling exponents $H(q)$ [98]. By taking $q = 1$ we reproduce a mono-fractal approach.

The DFA is presented in Algorithm 1. Given data series $\mathbb{R}^t \ni Y = [y_1, \dots, y_t]^\top$, we divide it into i non-overlapping sub-series of length $\tau = \lceil t/i \rceil$ each. In practice last two sub-series may overlap but this does not affect results. For each sub-series we determine data model, usually by performing the linear regression from data in the sub-series. Values predicted by the model $M \in \mathbb{R}^\tau$. Given the sub-series and the model we determine the measure of the noise divergence Δ_k - see line 9 of Algorithm 1. Next we average this measure over sub-series. Finally we investigate its scaling versus the length of a sub-series.

Remark 2.1.4. Mention that the DFA is only one of the methods of determining the scaling (Hurst) exponent or exponents. One can mention here an original as R/S method

[99], wavelet methods [100, 101, 102], multi-fractal wavelet methods [103, 104], or the Detrended Cross Correlation Analysis [105] applicable to the auto-correlation analysis in the multivariate data domain.

Hurst exponent analysis has many applications. Let us mention here the analysis of financial data, since it reveals log periodic oscillations that are present before the crash [7, 53, 106, 107, 108] or change in trend see [109] and bibliography within. In [39], the Hurst exponent was used to predict the crash on the Warsaw Stock Exchange, while applying higher order multivariate cumulants to determine safe investment portfolios for this crash, see Section 6.2.2. Furthermore, the Hurst exponent can be used to analyse different types of auto-correlated data in signal analysis [104], biomedical data analysis [102, 110], computer network traffic analysis [103, 111, 112], or as initially introduced weather analysis [99, 113]. Those analysis examples give evidence of long range auto-correlations of increments of many types of data. Hence such data may not be Gaussian distributed and more advanced methods are necessary for their statistical analysis. Such methods (copulas, higher order cumulants tensors and relative methods) will be discussed in further part of this manuscript.

2.2 Probabilistic non-Gaussian models

Having discussed stochastic processes suggesting non-Gaussian probabilistic models of data, we can discuss some of such non-Gaussian models resulting from particular types of stochastic processes.

2.2.1 Lévy distribution

Lévy distribution family contains stable distributions. If increments are Lévy distributed the sum is Lévy distributed as well. Given those the Gaussian distribution belong to the Lévy distribution family as well.

Definition 2.2.1. Let $\mathfrak{Z}_1, \dots, \mathfrak{Z}_i, \dots, \mathfrak{Z}_k$ be independent random variables with identical frequency distributions $f'(z)$. The frequency distribution $f'(z)$ is stable if

$$\forall_{k \geq 2} \exists_{a'_k, b'_k} : \mathfrak{Z}_1 + \dots + \mathfrak{Z}_k = \mathfrak{X} \sim f(x), \quad (2.33)$$

where

$$f(x) = \frac{1}{a_k} f' \left(\frac{z - b_k}{a_k} \right). \quad (2.34)$$

Example 2.2.1. If f and f' are zero mean Gaussian distribution

$$f(x) = \frac{1}{\sqrt{k}} f' \left(\frac{z}{\sqrt{k}} \right), \quad (2.35)$$

then we have $a_k = \sqrt{k}$.

It was shown by Paul Lévy [114] that there exists a family containing all stable distributions, the Lévy distributions family. For simplicity we will discuss here a symmetric Lévy distributions with zero location parameter, defined by a following characteristic function

$$\varphi_{\alpha,\gamma}(v) = \exp(-|\gamma v|^\alpha), \quad (2.36)$$

where $0 < \alpha \leq 2$ and $\gamma > 0$. Characteristic function is a Fourier transform of the PDF function, hence:

$$f_{S_{\alpha,\gamma}}(x) = \frac{1}{2\pi} \int_{-\infty}^{\infty} \varphi_{\alpha,\gamma}(v) e^{-ixv} dv, \quad (2.37)$$

here S is a notation for the stable distribution. The analytical calculation of the integral in Eq. (2.37) can be performed in a simple way only for $\alpha = 1, 2$ yielding

1. Lorentz / Cauchy distribution $f_{S_{\alpha=1,\gamma}}(x) = \frac{1}{\pi} \frac{\gamma}{x^2 + \gamma^2}$,
2. Gaussian distribution with standard deviation $\sigma = \gamma\sqrt{2}$:

$$f_{S_{\alpha=2,\gamma}}(x) = \frac{1}{\sqrt{4\pi\gamma^2}} e^{-\frac{x^2}{4\gamma^2}}. \quad (2.38)$$

Remark 2.2.1. Given a zero mean symmetric Lévy distribution we have the following scaling [115]

$$f_{S_{\alpha,\gamma}}(x) = f'_{S_{\alpha,\gamma'}}(z), \quad (2.39)$$

where $\gamma = \gamma' k^{\frac{1}{\alpha}}$, and other notation is as in Definition 2.2.1.

Remark 2.2.2. Importantly it can be shown that for $\alpha < 2$ the Lévy distribution does not have defined variance as well as higher moments and cumulants. Hence if $\alpha < 2$ the sum of Lévy distributed random variables with infinite variance gives a Lévy distributed random variable, that is not a Gaussian distribution. In the following two remarks we would take $\gamma = 1$ for simplicity.

Remark 2.2.3. For $0 < \alpha < 2$, asymptotic behaviour of Lévy PDF $f_{S_\alpha}(x)$ can be approximated by [7]

$$f_{S_\alpha}(x) \approx \frac{C_\alpha}{|x|^{1+\alpha}} \text{ for } |x| \rightarrow \infty, \quad (2.40)$$

where

$$C_\alpha = \frac{\alpha}{\pi} \Gamma(1 + \alpha) \sin\left(\frac{\alpha\pi}{2}\right), \quad (2.41)$$

and Γ is the Euler Gamma function [116].

Remark 2.2.4. There is a generalisation of the Central Limit Theorem for increments modelled by the distribution with infinite variance [117]. For $0 < \alpha < 2$ the sum of identically distributed random variables modelled by the distribution with a power law asymptotic behaviour

$$f_{S_\alpha}(x) \propto \frac{1}{|x|^{1+\alpha}} \text{ for } |x| \rightarrow \infty, \quad (2.42)$$

converges to the Lévy distribution.

Algorithm 2 Sample general Lévy distribution.

```

1: Input:  $0 < \alpha \leq 2$  - parameter,  $-1 \leq \beta \leq 1$  - parameter.
2: Output:  $x \in \mathbb{R}$  a sample of the general Lévy distribution.
3: function LEVYGEN( $\alpha, \beta$ )
4:   sample  $\theta \sim \text{Uniform}(-\frac{\pi}{2}, \frac{\pi}{2})$ 
5:   sample  $w \sim F_{ex_1}$  ▷ exponential with scale 1:  $f_{ex_1}(x) = e^{-x}$ 
6:   if  $\alpha = 1$  then
7:     return  $\frac{2}{\pi} \left( \left( \frac{\pi}{2} + \beta\theta \right) \tan(\theta) - \beta \log \left( \frac{\frac{\pi}{2} w \cos(\theta)}{\frac{\pi}{2} + \beta\theta} \right) \right)$ 
8:   else
9:      $\theta_0 = \frac{\arctan(\beta \tan(\frac{\pi\alpha}{2}))}{\alpha}$ 
10:    return  $\frac{\sin(\alpha(\theta_0 + \theta))}{(\cos(\alpha\theta_0) \cos(\theta))^{\frac{1}{\alpha}}} \left( \frac{\cos(\alpha\theta_0 + (\alpha-1)\theta)}{w} \right)^{\frac{1-\alpha}{\alpha}}$ 
11:  end if
12: end function

```

Remark 2.2.5. The general ‘asymmetric’ Lévy distribution [118] characteristic function is given by

$$\varphi_{\alpha,\beta,\gamma,\delta}(v) = \exp(it\delta - |\gamma v|^\alpha (1 - i\beta \text{sign}(v)\Phi)), \quad (2.43)$$

where

$$\Phi = \begin{cases} \tan\left(\frac{\pi\alpha}{2}\right) & \text{for } \alpha \neq 1 \\ -\frac{2}{\pi} \log(|v|) & \text{otherwise} \end{cases}, \quad (2.44)$$

and i is an imaginary unit. Here $-1 \leq \beta \leq 1$, and in case of $\beta \neq 0$ the Lévy distribution is not symmetric. Further $c \in (0, \infty)$ and $\mu \in (-\infty, \infty)$ are scale and location parameters. This general case of Lévy distribution will be used further in Section 4.3.2 and Section 4.3.3 while sampling Lévy distribution in sampling algorithms of some copulas. Remind that in most cases its PDF $f_{S(\alpha,\beta,c,\mu)}$ and CDF $F_{S(\alpha,\beta,c,\mu)}$ do not have an analytical form, however they can be sampled, as presented in Algorithm 2 [119]. Histograms of exemplary Lévy stable distributions are presented in Figure 2.2(a).

Analogically to the Wiener process case, increments from distribution with asymptotic behaviour as in Eq. (2.42), would lead to another random process called the Lévy Flight [120]. Such process models different types of data such as a network (internet) traffic [12], biological data [121, 122, 123] and is applicable in computer science optimisation and a global maximum search [124, 125]. Unfortunately the non-trivial Lévy distribution do not have defined variance and higher order cumulants as well, hence it imposes the limitation for the use of higher order cumulants analysis of data that is discussed further in this book.

2.2.2 Tsallis q-Gauss distribution

While discussing models of data generated from a random process it is worth to mention the Tsallis q-Gauss distribution that is a generalisation of a Gaussian distribution in a same sense as the Tsallis entropy is a generalization of the standard Shannon entropy

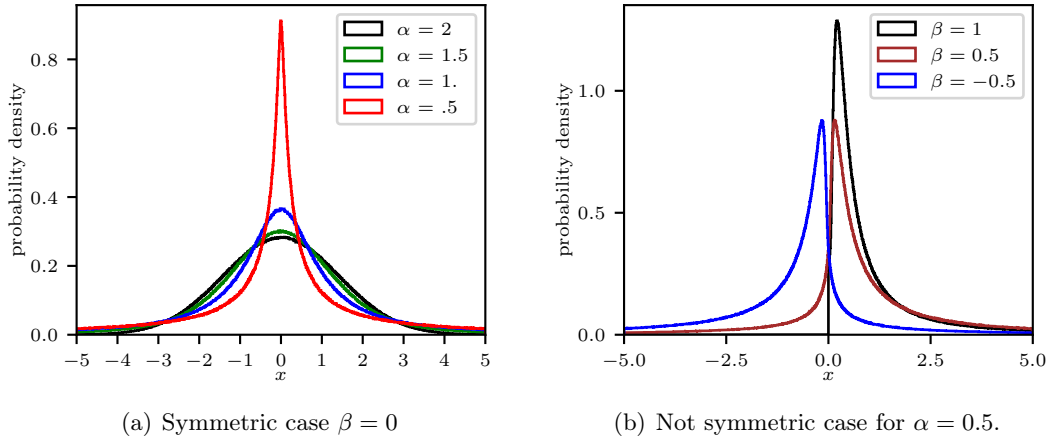


Figure 2.2: Histograms of data generated by the Lévy stable distribution for $\gamma = 1$ and $\delta = 0$.

[126, 127]. Sampling of the Tsallis q -Gauss distribution [128] has an application in Generalised Simulated Annealing in computer science, where instead of standard Boltzman distribution [129]

$$p_i = \frac{\exp(-\beta H_i)}{\sum_j \exp(-\beta H_j)} \quad (2.45)$$

in standard simulated annealing algorithm [130], we sample [131]

$$p_i = \frac{(1 - \beta(1 - q)H_i)^{\left(\frac{1}{1-q}\right)}}{\sum_j (1 - \beta(1 - q)H_j)^{\left(\frac{1}{1-q}\right)}}. \quad (2.46)$$

Here H_i is the generalised energy of the i^{th} configuration. If we have a continuous energy spectrum given by $H(x) = x^2$ and we replace sums in Eq. (2.45) by an integral over dx , we reproduce the Gaussian distribution. Analogously from Eq. (2.46) we reproduce the Tsallis q -Gauss distribution [132]

$$f_q(x) = \frac{\sqrt{\beta}}{C_q} (1 - (1 - q)\beta x^2)^{\left(\frac{1}{1-q}\right)}, \quad (2.47)$$

where the normalisation constant is

$$C_q = \begin{cases} \frac{2\Gamma\left(\frac{1}{1-q}\right)\sqrt{\pi}}{(3-q)\Gamma\left(\frac{3-q}{3(1-q)}\right)\sqrt{1-q}} & \text{if } -\infty < q < 1 \\ \sqrt{\pi} & \text{if } q = 1 \\ \frac{\Gamma\left(\frac{3-q}{2(q-1)}\right)\sqrt{\pi}}{\Gamma\left(\frac{1}{q-1}\right)\sqrt{q-1}} & \text{if } 1 < q \leq 3 \end{cases}. \quad (2.48)$$

Parameter β , in physics denoting the inverse of the temperature [129], controls the spread of samples and is decreased during the simulated annealing as we are moving toward a global solution. Recall that this β here not comply with the β parameter for a Lévy distribution, where the scale parameter in literature is rather γ [119], but they are not equivalent.

Remark 2.2.6. What is important here, Tsallis q -Gauss distribution parametrised by $1 \leq q < 3$ is an outcome of the generalisation of the Central Limit Theorem, called the q -Central Limit Theorem, where the independence condition is lifted and increments are allowed to be long-range correlated in some specific manner [132]. Here we require the existence of the generalised q -mean and the generalised $(2q - 1)$ -variance [132] or the distribution of increments. Recall that since we use some generalised for of the mean and variance a standard scaling stability as in the Lévy distribution case may not hold.

The Tsallis q -Gauss distribution models better than a Gaussian distribution and many types of non-Gaussian distributed data e.g. the financial data [133, 134, 135]. In a case of $q < 1$ the q -Gauss distributed random variable is limited to $x \in \left[-\frac{1}{\sqrt{(1-q)\beta}} : \frac{1}{\sqrt{(1-q)\beta}} \right]$ and can be applicable to analyse some biological systems [136].

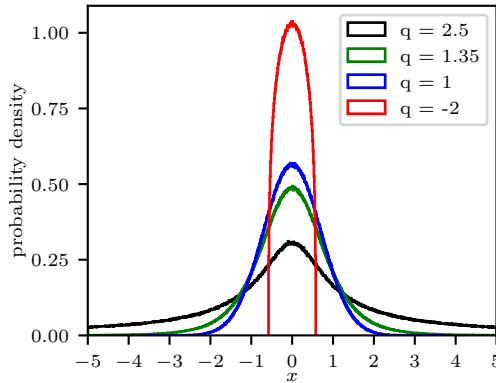


Figure 2.3: Zero mean q -Gaussian histograms for different q values, $\beta = 1$. In a case of $q = 1$ we have a Gaussian distribution with standard deviation $\sigma = \sqrt{\frac{1}{2}}$.

Since the CDF of the q -Gauss distribution, given in Eq. (2.47), is rather complicated we use in general algorithm introduced in [128] to sample univariate q -Gaussian distribution. We present this procedure in Algorithm 3.

The correspondence between the q -Gaussian distribution and other distributions is as follow. For $q = 1$ case we reproduce the Gaussian distribution, for $q = \frac{\nu+3}{\nu+1}$ we reproduce the t -Student distribution with ν degrees of freedom [137], while for $q = 2$ we reproduce the Cauchy distribution [138, 139]. The relation to the t -Student distribution gives the motivation to the discussion of the t -Student multivariate distribution and the t -Student copula further in this book. Observe finally, that for $q < \frac{d+3}{d+1}$ the q -Gauss distribution

Algorithm 3 Generate data from q-Gauss distribution.

1: **Input:** $-\infty < q < 3$ - parameter.
2: **Output:** $x \in \mathbb{R}$ a sample of q-Gauss distribution.
3: **function** Q-GAUSSGEN(q)
4: sample independently $u_1 \sim \text{Uniform}(0, 1), u_2 \sim \text{Uniform}(0, 1)$
5: $q' = \frac{q+1}{3-q}$
6: $u_1 = \frac{u_1^{1-q'} - 1}{1-q'}$ \triangleright q' -logarithm as defined in [128]
7: $\beta = 3 - q$
8: **return** $\frac{\sqrt{-2u_1} \cos(2\pi u_2)}{\sqrt{\beta}}$
9: **end function**

has defined d^{th} moment and the d^{th} cumulant as well. Given certain q values it can be analysed by means of higher order cumulants.

2.3 Ising model of data

The portfolio management problem discussed in further part of this book is computationally complex, especially if the number of assets in the portfolio is large. Hence, the quantum annealing on the D-Wave machine that uses the Ising model is promising due to potential computational time gain in comparison with classical computing in [140, Chapter 4], [141, Section 6.1] and [142, 143]. In general, the problem of solving the Ising model is NP-hard. However, there are attempts to reduce the computational complexity of such problem by means of the quantum computing [144].

The classical approach to the portfolio optimisation takes the Markovitz model [145] that uses the Gaussian distribution of financial data. As discussed in previous sections, real-life financial data are in most cases non-Gaussian distributed. It is why, to utilise quantum computing for financial data analysis, we focus rather on a stochastic model of investors behaviour as discussed in [63]. Such Ising model is applicable to analyse investors driven complex dynamic of financial data. We hope, that one can use quantum annealing while searching for investors optimal behaviour given both their potential for aggregate or individual behaviours.

2.3.1 The Ising model

In this subsection, we discuss an example of a model of investors interactions that can be used to model financial data employing the Ising model. Following [63], let us observe that the crash on the stock market occurs if a large group of investors simultaneously decide to sell their assets. In most cases, those agents do not know each other, do not arrange their actions, and do not follow any leader. For most of the trading time, they aggregately give a similar amount of buy and sell orders and hence the price of an asset is rather stable. However, sometimes they simultaneously sell stocks causing a crash.

Let us model investor's interaction by means of the regular network of N nodes (investors) with γ neighbours each. Let us now assume, that each investor's action is influenced both by its nearest surrounding and its individual preference. Investors are rather following each other. It is why the neighbour interaction will introduce order. Oppositely the individual preference will introduce disorder [63].

Following [63], to model investor's mutual interaction, we assign a number $s_i = \pm 1$ (+1 means sell, -1 means buy) to the i^{th} investor, and use the following 'classical' Ising Hamiltonian

$$H(\mathbf{s}) = - \sum_{i < j} \varepsilon_{ij} s_i s_j, \quad (2.49)$$

where the sum goes over the nearest neighbours set given the particular graph of investors interrelationship. Here $\mathbf{s} = [s_1, \dots, s_N]$ is a configuration showing actions of each investor, and ε_{ij} is an interaction strength. Suppose for simplicity that the interaction is constant $\varepsilon_{ij} = \varepsilon > 0$ over the graph. Given a regular graph of N nodes (investors), and γ neighbours for each node there are $\frac{\gamma N}{2}$ elements of the sum in Eq. (2.50),

$$H(\mathbf{s}) = -\varepsilon \sum_{\{ij\}} s_i s_j. \quad (2.50)$$

Here $H(\mathbf{s})$ is a discrete function and we use the discrete form of the Boltzman distribution, as in Eq. (2.45),

$$f_{\beta}(\mathbf{s}) = \frac{e^{-\beta H(\mathbf{s})}}{Z(\beta)}. \quad (2.51)$$

The normalisation constant is called the partition function

$$Z(\beta) = \sum_{\mathbf{s}} e^{-\beta H(\mathbf{s})}, \quad (2.52)$$

where the sum goes over the set of all possible configurations of \mathbf{s} (all possible actions of investors). The constant β , which in physics refers to the inverse of the temperature of the system, reflects the strength of the statistical noise *i.e.* there is no noise if $\beta \rightarrow \infty$. In our model the noise correspond to the disorder imposed by personal preferences of investors. Hence, as such disorder falls, investors organise, and a crash occurs [63]. Observe, however that presented in this subsection model is very simple, hence it can be exactly solved.

2.3.2 Simulated annealing on the D-Wave machine

To make the model more realistic, we assume that the network of investors is not a regular lattice, but rather it reveals some hierarchical structure [61]. Furthermore, we can introduce varying interaction strengths, ε_{ij} , since different investors may be affected by others in different way. Finally, we can introduce h_i representing interaction with some sort of the 'external field', that we can model some external factors affecting agents

or their particular group. This leads to more general Ising Hamiltonian

$$H(\mathbf{s}) = - \sum_{i < j} \varepsilon_{ij} s_i s_j - \sum_i h_i s_i. \quad (2.53)$$

Unfortunately, such model becomes more complicated, and hard to simulate. To handle it, we can refer to the potentially fast quantum computation on the D-Wave machine [146, 147]. The D-Wave machine is designed to solve a specific problem of finding a ground state of the following Hamiltonian

$$H = - \sum_{i < j} \varepsilon_{ij} \sigma_z^{(i)} \sigma_z^{(j)} - \sum_i h_i \sigma_z^{(i)}. \quad (2.54)$$

Here $\sigma_z^{(i)}$ is a z-Pauli matrix acting on the q-bit [148] located in the i^{th} node, in other words, on the quantum state of the i^{th} node. Formally,

$$\sigma_z^{(i)} = \underbrace{\mathbb{1} \otimes \dots \otimes \mathbb{1}}_{i-1} \otimes \sigma_z \otimes \underbrace{\mathbb{1} \otimes \dots \otimes \mathbb{1}}_{N-i}. \quad (2.55)$$

The quantum propagation on a D-Wave machine gives a minimal energy state of the Hamiltonian model presented in Eq. (2.54). This would correspond to the minimal energy solution of classical Hamiltonian presented in Eq. (2.53).

The Hamiltonian in Eq. (2.54) has some limitation due to the hardware graph of the D-Wave computer chip which is full graph nor a regular lattice as in [63]. This processor chip is an intermediate case between two types of mentioned graphs, see Figure 2.4 [149, 150, 151], and it is called a Chimera graph χ_{ij} . Such graph imposes a hierarchical relation similar to this observed among investors [61]. In our case, investors may be organised in groups, that correspond to Chimera cells and 1st degree of the organisation. Those groups are organised in the network yielding the 2nd degree of the organisation. Its hierarchical layout may be of advantage while modelling investors behaviour.

Let us now discuss to some extent how the D-Wave machine works [146]. It starts with the ground state of the H_0 Hamiltonian given by

$$H_0 = - \sum_i h_i \sigma_x^{(i)}. \quad (2.56)$$

Next, it performs the adiabatic evolution of the time dependent Hamiltonian $H(t)$ given by

$$H(t) = \left(1 - \frac{t}{\tau}\right) H_0 + \frac{t}{\tau} H, \quad (2.57)$$

where $0 \leq t \leq \tau$ and τ is an annealing time parameter. In results we should obtain a ground state eigenvector $|\psi^{(\tau)}\rangle_0$ of the following eigen-equation

$$H(t) |\psi^{(t)}\rangle_n = E_n(t) |\psi^{(t)}\rangle_n, \quad (2.58)$$

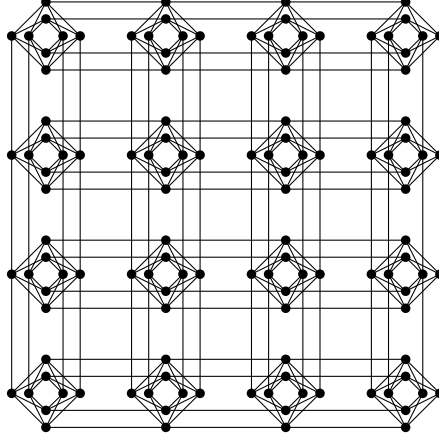


Figure 2.4: The Chimera graph used actually by the D-Wave machine [152].

where $E_n \in \mathbb{R}$ is the n^{th} eigenvalue (energy) and $|\psi\rangle_n$ corresponding eigenvector. The following order is fulfilled $E_0 \leq E_1 \leq \dots \leq E_n$. The output configuration that is supposed to represent the ground state can be represented in the form of the vector

$$\mathbf{s} = [s_1, \dots, s_N], \quad (2.59)$$

where $s_i = \pm 1$. The D-Wave propagation is performed many times, and the result is probabilistic [146]. As the result we obtain have a series $\mathbf{s}_1, \mathbf{s}_2, \dots, \mathbf{s}_M$ all corresponding (in theory) to the ground state *i.e.* the minimum of Eq. (2.53), since the D-Wave propagation [146] is performed in (almost) 0 Kelvin environment.

In our case, each \mathbf{s} models the optimal state of investors for the given parameters of the network of, their mutual interaction and other external parameters. This minimal energy Boltzmann distribution with (almost) no thermal noise. In the case of the financial data modelling, however, we can still be interested in a zero temperature solution to maximally ‘ordered’ behaviour of investors to answer a question if a crisis is possible given initial settings of the model. To introduce a thermal noise, we can set the annealing time parameter τ very short [146] resulting in the not full annealing yielding sometimes the ground state and sometimes one of the excited states with higher energy. In another approach, given an input Ising model see Eq. (2.53) we can introduce a noise via a random factor in parameter h_i . Hence we can observe how the choice of statistics of the noise incorporated in h_i would affect statistics of investors behaviour. Finally, statistics of investor behaviour can be retranslated on statistics of financial data. One can analyse how the initial set of parameters affects the financial data, and answer when they are Gaussian distributed and when not.

Chapter 3

Multivariate Gaussian models

Gaussian models are widely used to analyse various types of real life data [65]. Unfortunately often Gaussian models are assumed a priori without testing normal distribution on data. To test multivariate Gaussian distribution one can use the Marida's test [153], or the BHEP test [154]. In this book we will focus on higher order multivariate cumulants that are zero for multivariate Gaussian distributed data and hence can be used to test their distribution. The advantage of the last comes from the fast programming implementation [34] especially applicable for large data sets.

Henceforth in this book we understand n -variate data as a collection of realisations of the n -dimensional random vector $\mathfrak{X}^{(n)} = (\mathfrak{X}_1, \dots, \mathfrak{X}_n)$. Such random vector consists of n interdependent univariate random variables \mathfrak{X}_i . Given those, t realisations of n -dimensional random vector can be presented in the form of matrix:

$$\mathbb{R}^{t \times n} \ni \mathbf{X} = \begin{bmatrix} x_{1,1} & \dots & x_{1,n} \\ \vdots & x_{j,i} & \vdots \\ x_{t,1} & \dots & x_{t,n} \end{bmatrix}. \quad (3.1)$$

The i^{th} column \mathfrak{X}_i of such matrix is the column vector of all realisations of the i^{th} marginal

$$\mathbb{R}^t \ni X_i = [x_{1,i}, \dots, x_{j,i}, \dots, x_{t,i}]^{\text{T}}, \quad (3.2)$$

and the single realisation of the random vector $\mathfrak{X}^{(n)}$ is the row vector

$$\mathbb{R}^n \ni \mathbf{x}_j = [x_{j,1}, \dots, x_{j,n}]. \quad (3.3)$$

3.1 Multivariate Gaussian Distribution

The Multivariate Gaussian Distribution is widely used to analyse multivariate data. The main argument for such probabilistic model comes from the results Multivariate Central Limit Theorem (MCLT) [155].

Theorem 3.1.1. Let $\mathfrak{Z}^{(n)}_1, \dots, \mathfrak{Z}^{(n)}_k$ be k independent random vectors with identical distributions having a mean vector $\mu \in \mathbb{R}^n$ and a positive definite symmetric covariance matrix $\Sigma \in \mathbb{R}^{n \times n}$. The random vector

$$\mathfrak{X}^{(n)} = \frac{1}{\sqrt{k}} \sum_{i=1}^k \left(\mathfrak{Z}^{(n)}_i - \mu \right) \quad (3.4)$$

has distribution that converges as $k \rightarrow \infty$ to the multivariate Gaussian distribution with zero mean vector and a covariance matrix Σ .

The multivariate Gaussian Probability Density Function (PDF) reads

$$\mathbf{f}_{\mathcal{N}(\mu, \Sigma)}(\mathbf{x}) = \frac{1}{(2\pi)^{\frac{n}{2}} \det(\Sigma)^{\frac{1}{2}}} \exp\left(-\frac{1}{2}(\mathbf{x} - \mu)^T \Sigma^{-1}(\mathbf{x} - \mu)\right), \quad (3.5)$$

and the corresponding multivariate Gaussian Cumulative Distribution Function (CDF) is given by

$$\mathbf{F}_{\mathcal{N}(\mu, \Sigma)}(\mathbf{x}) = P(\mathfrak{X}_1 \leq x_1 \wedge \dots \wedge \mathfrak{X}_n \leq x_n) = \int_{-\infty}^{x_1} \dots \int_{-\infty}^{x_n} \mathbf{f}_{\mathcal{N}(\mu, \Sigma)}(y_1, \dots, y_n) dy_1 \dots dy_n. \quad (3.6)$$

Gaussian distributed random vector is: $\mathfrak{X}^{(n)} \sim \mathcal{N}(\mu, \Sigma)$. The covariance matrix parameter $\Sigma \in \mathbb{R}^{n \times n}$ is symmetric and positive definite. Its elements s_{i_1, i_2} are either diagonal $s_{i, i} = \sigma_i^2$, being a variance of the i^{th} marginal, or off-diagonal $s_{i_1 \neq i_2}$, being a covariance between i_1 and i_2 marginals. These elements yield the Pearson cross-correlation coefficient [156]

$$\text{cor}(\mathfrak{X}_{i_1}, \mathfrak{X}_{i_2}) = r_{i_1, i_2} = \frac{s_{i_1, i_2}}{\sqrt{s_{i_1, i_1} s_{i_2, i_2}}}. \quad (3.7)$$

The Pearson correlation matrix (or simply the correlation matrix) $\mathbf{R} \in \mathbb{R}^{n \times n}$ is positive definite, and symmetric matrix with ones on a diagonal $r_{i, i} = 1$. Since \mathbf{R} is positive definite we get $-1 < r_{i_1, i_2} < 1$.

If we have data distributed according to multivariate Gaussian model, there are some statistical features important in analysing such data. Let us mention a few that may not be fulfilled if data are non-Gaussian distributed as discussed in the further part of this book.

Remark 3.1.1. Given $\mathfrak{X}^{(n)} \sim \mathcal{N}(\mu, \Sigma)$ the cross-correlation between marginals is included in \mathbf{R} matrix with elements r_{i_1, i_2} . Hence the pairwise analysis of the cross-correlation of Gaussian distributed data would extract all information about marginals interdependence. The observation presented in Remark 3.1.1 is not true in general. In Chapter 5, we discuss higher order cumulants of multivariate data that carries information about the simultaneous interdependence of more than 2 marginals, and are zero for Gaussian distributed multivariate data.

Remark 3.1.2. Given $\mathfrak{X}^{(n)} \sim \mathcal{N}(\mu, \Sigma)$ we can use the Singular Value Decomposition (SVD) of the covariance matrix to obtain project data on independent directions. The new random vector

$$\mathfrak{Y}^{(n)} = \mathfrak{X}^{(n)} \mathbf{A} \quad (3.8)$$

consists of independent marginals, that can be ordered with respect to information significance [65].

The symmetric and positive definite covariance matrix Σ can be decomposed as

$$\Sigma = \mathbf{A}\Sigma_{(d)}\mathbf{A}^\top, \quad (3.9)$$

where $\Sigma_{(d)}$ is a diagonal matrix real and positive eigenvalues of Σ notes by $s_{(d)_{i,i}}$, and $\mathbf{A} \in \mathbb{R}^{n \times n}$ is an unitary matrix of eigenvectors. We assume eigenvectors are normalised to 1. The ordering $s_{(d)_{i_1,i_1}} \geq s_{(d)_{i_2,i_2}}$ if $i_1 > i_2$ results in ordering of \mathfrak{Y}_i with respect to their variability and hence information they are carrying.

Such approach is the core of the Principal Component Analysis (PCA) [67] used to extract information from data. If $\mathfrak{X}^{(n)}$ is not multivariate Gaussian distributed, here information may be tied to higher order cross-correlation between marginals. Hence, Eq. (3.8) gives marginals $\mathfrak{Y}_1, \dots, \mathfrak{Y}_n$ that are not independent and their informative hierarchy is not straightforward.

To show non-Gaussian distribution of data that are modelled as a sum of many increments consider financial data, where conditions of the MCLT may not hold. Take as example multivariate ARCH and GARCH models [157, 158, 159] that break increments independence and identical distributions conditions. To discuss the practical application of the SVD in financial data analysis observe the following example.

Example 3.1.1. *In classical financial engineering one uses the SVD of the covariance matrix in the classical Value at Risk (VaR) procedure [64], determining eigenvectors that correspond to low eigenvalues. These eigenvectors are supposed to give linear combinations of marginals with low variance corresponding to safe portfolio of risky assets, if one tie the variance with the variability and risk. Negative weights correspond to so called ‘short sale’. In practice, financial data are often non-Gaussian distributed and the covariance analysis may fails to anticipate cross-correlated extreme events, appearing for many assets simultaneously [6, 160]. This typically happens during the crisis, and as non-predicted by the Gaussian model is potentially dangerous for equity holders.*

In next section we are going to discuss a family of non-Gaussian multivariate distributions that can be easily transformed to the Gaussian one.

3.2 Gaussian copula

By the Sklar’s theorem [161] each multivariate distribution can be split onto marginal distributions and the copula, being a ‘core’ of the distribution, responsible for the interdependence of marginals. Formally the Sklar’s theorem is following.

Theorem 3.2.1. *Every multivariate CDF $\mathbf{F}(x_1, \dots, x_n)$ of a random vector $\mathfrak{X}^{(n)} = (\mathfrak{X}_1, \dots, \mathfrak{X}_n)$ can be expressed in terms of its marginal univariate CDFs $F_i(x_i)$ and the copula $\mathbf{C} : [0, 1]^n \rightarrow [0, 1]$. The relation reads*

$$\mathbf{F}(x_1, \dots, x_n) = \mathbf{C}(F_1(x_1), \dots, F_n(x_n)). \quad (3.10)$$

The Sklar's theorem also implies that if $F_1(x_1), \dots, F_n(x_n)$ are continuous, the copula function \mathbf{C} is uniquely defined by \mathbf{F} .

Henceforth we will discuss the case of continuous univariate PDFs. To construct Gaussian multivariate distribution we need the Gaussian copula and the Gaussian marginals. Consider multivariate random vector $\mathfrak{X}^{(n)} \sim \mathcal{N}(\mu, \Sigma)$. Its marginals are univariate Gaussian distributions $\mathfrak{X}_i \sim \mathcal{N}(\mu_i, \sigma_i^2)$, where $\sigma_i^2 = s_{i,i}$ which is the i^{th} diagonal element of Σ . Let $F_{\mathcal{N}(\mu_i, \sigma_i^2)}(x_i)$ be marginal univariate Cumulative Distribution Function (CDF) of those marginals. Now define a new n -variate random vector $\mathfrak{U}^{(n)} = (\mathfrak{U}_1, \dots, \mathfrak{U}_n)$ fulfilling

$$\mathfrak{U}_i = F_{\mathcal{N}(\mu_i, \sigma_i^2)}(\mathfrak{X}_i) \text{ or } \mathfrak{X}_i = F_{\mathcal{N}(\mu_i, \sigma_i^2)}^{-1}(\mathfrak{U}_i). \quad (3.11)$$

Each marginal \mathfrak{U}_i is uniformly distributed on a line segment $[0, 1]$, *i.e.* $\mathfrak{U}_i \sim \text{Uniform}([0, 1])$, see Table 1. A realisations matrix and the single realisation vector of $\mathfrak{U}^{(n)}$ random vector are

$$\mathbf{U} \in [0, 1]^{t \times n} \text{ and } \mathbf{u} \in [0, 1]^n, \quad (3.12)$$

where t is a number of realisations. We can introduce the Gaussian copula.

Definition 3.2.1. A Gaussian copula [1] $\mathbf{C}_{\mathbf{R}} : [0, 1]^n \rightarrow [0, 1]$ is the multivariate CDF of $\mathfrak{U}^{(n)}$ with uniform marginals on $[0, 1]$ segment, such that

$$\begin{aligned} [0, 1] \ni \mathbf{C}_{\mathbf{R}}(\mathbf{u}) &= \mathbf{F}_{\mathcal{N}(\mu, \Sigma)} \left(F_{\mathcal{N}(\mu_1, \sigma_1^2)}^{-1}(u_1), \dots, F_{\mathcal{N}(\mu_n, \sigma_n^2)}^{-1}(u_n) \right) \\ &= \mathbf{F}_{\mathcal{N}(0, \mathbf{R})} \left(F_{\mathcal{N}(0,1)}^{-1}(u_1), \dots, F_{\mathcal{N}(0,1)}^{-1}(u_n) \right). \end{aligned} \quad (3.13)$$

The Gaussian copula models interdependency between marginals of $\mathfrak{U}^{(n)}$ by means of multivariate Gaussian distribution. Following Eq. (3.7) $\mathbf{R} \in \mathbb{R}^{n \times n}$ is the correlation matrix, and $F_{\mathcal{N}(0,1)}(x)$ is the standard Gaussian univariate CDF (with zero mean and 1 variance). Suppose, we have univariate continuous CDFs F_1, \dots, F_n . The multivariate distribution

$$\mathbf{F}(\mathbf{y}) = \mathbf{C}_{\mathbf{R}}(F_1(y_1), \dots, F_n(y_n)) \quad (3.14)$$

has Gaussian copula and F_1, \dots, F_n marginals. To show the importance of the Gaussian copula consider the following theorem.

Theorem 3.2.2. *Let us consider a random vector $\mathfrak{Y}^{(n)}$ distributed according to \mathbf{F} , that is certain multivariate CDF, with continuous univariate marginal CDFs F_1, \dots, F_n , such that $F_i : (-\infty, \infty) \rightarrow [0, 1]$. There exist a transformation of marginals changing $\mathfrak{Y}^{(n)}$ to a multivariate Gaussian distributed $\mathfrak{X}^{(n)}$ iff \mathbf{F} (if and only if) has the Gaussian copula.*

Proof. We transform the random vector $\mathfrak{Y}^{(n)} \rightarrow \mathfrak{U}^{(n)}$, by the following transformation of all marginals

$$\mathfrak{U}_i = F_i(\mathfrak{Y}_i). \quad (3.15)$$

Since F_i is continuous, \mathfrak{U}_i is continuous and uniformity distributed on $[0, 1]$. Now we can use the inverse univariate Gaussian CDFs (quantile function) $F_{\mathcal{N}(\mu_i, \sigma_i^2)}^{-1}$ and transform each marginal further as

$$\mathfrak{X}_i = F_{\mathcal{N}(\mu_i, \sigma_i^2)}^{-1}(\mathfrak{U}_i). \quad (3.16)$$

Parameters μ_i and σ_i^2 are arbitrary parameter of an univariate Gaussian distribution. The transformation $\mathfrak{Y}^{(n)} \rightarrow \mathfrak{U}^{(n)} \rightarrow \mathfrak{X}^{(n)}$ affects only marginals. Hence it requires Gaussian copula of $\mathfrak{U}^{(n)}$ to produce multivariate Gaussian distribution of $\mathfrak{X}^{(n)}$. Finally Gaussian copula of $\mathfrak{U}^{(n)}$ yields a Gaussian copula of $\mathfrak{Y}^{(n)}$. \square

Remark 3.2.1. Observe that such transformation $\mathfrak{Y}^{(n)} \rightarrow \mathfrak{X}^{(n)}$ preserves rank cross-correlation between marginals. As previously, F_i is univariate continuous CDFs, hence it is increasing. The probability of y being a sample of F_i equals $f_i(y) = \frac{dF_i(y)}{dy}$, hence we can exclude such ranges of y where $F_i(y)$ is constant. Based on these two observations the relation $u = F_i(y)$ is order preserving. Observe as well, that $F_{\mathcal{N}(\mu_i, \sigma_i^2)}^{-1}$ is strictly increasing and hence order preserving. Finally the relation

$$x = F_{\mathcal{N}(\mu_i, \sigma_i^2)}^{-1}(F_i(y)) \quad (3.17)$$

is order preserving as well. Referring to Theorem 3.2.2, if data have Gaussian copula, they may be transformed to multivariate Gaussian distribution in a rank cross-correlation preserving method. Then methods of Gaussian data analysis such as PCA can be applied. Nevertheless, the Gaussian copula assumption is necessary here.

Referring to Remark 3.1.1 a Gaussian multivariate distribution introduces the cross-correlation between pairs of marginals by means of the correlation matrix \mathbf{R} . The same is the case for a Gaussian copula. Hence it is convenient to use bivariate Gaussian sub-copula while discuss interdependencies between marginals. The sub-copula notation is not often used in the copula literature, however we used it here to distinguish between bivariate and d -variate (as $d > 2$) interdependency measures. The later are included in d^{th} order multivariate cumulants discussed further in this book.

Definition 3.2.2. Suppose we have the Gaussian copula $\mathbf{C}_{\mathbf{R}}(\mathbf{u})$, where $\mathbf{u} = [u_1, \dots, u_n]$ is single realisation of the random vector $\mathfrak{U}_{(n)}$ with following marginals $\mathfrak{U}_i \sim \text{Uniform}([0, 1])$, the probability of $\mathfrak{U}_i \leq 1$ equals one. The bivariate Gaussian sub-copula for marginals i_1 and i_2 is defined as

$$\begin{aligned} \mathbf{C}_{\mathbf{R}'}(u_{i_1}, u_{i_2}) &= P(\mathfrak{U}_{i_1} \leq u_{i_1} \wedge \mathfrak{U}_{i_2} \leq u_{i_2}) \\ &= P(\mathfrak{U}_{i_1} \leq u_{i_1} \wedge \mathfrak{U}_{i_2} \leq u_{i_2} \wedge_{k \neq i_1, i_2} \mathfrak{U}_k \leq 1) \\ &= \mathbf{C}_{\mathbf{R}}(1, \dots, 1, u_{i_1}, 1, \dots, 1, u_{i_2}, 1, \dots, 1), \end{aligned} \quad (3.18)$$

where $\mathbf{R}' = \begin{bmatrix} 1 & r_{i_1, i_2} \\ r_{i_2, i_1} & 1 \end{bmatrix}$, and $r_{i_1, i_2} = r_{i_2, i_1}$ are corresponding elements of the original correlation matrix \mathbf{R} .

It is easy to conclude that bivariate sub-copula $\mathbf{C}_{\mathbf{R}'}$ models bivariate measures of interdependency between marginals i_1 and i_2 . Besides standard Pearson cross-correlation (equal to r_{i_1, i_2} given Gaussian marginals) another bivariate interdependency measures are bivariate ‘tail’ dependencies.

Definition 3.2.3. The lower ‘tail’ dependency [1] is defined as

$$\lambda_l = \lim_{u \rightarrow 0^+} P(\mathfrak{Y}_1 \leq u | \mathfrak{Y}_2 \leq u) = \lim_{u \rightarrow 0^+} \frac{P(\mathfrak{Y}_1 \leq u, \mathfrak{Y}_2 \leq u)}{P(\mathfrak{Y}_2 \leq u)} = \lim_{u \rightarrow 0^+} \frac{\mathbf{C}(u, u)}{u}, \quad (3.19)$$

the last equality results from the fact, that $P(\mathfrak{Y} \leq u) = u$ since $\mathfrak{Y} \sim \text{Uniform}([0, 1])$. Here $u_i \rightarrow 0$ corresponds to very low value of $x_i = F_i^{-1}(u_i)$, and $\mathbf{C}(u, u)$ is a copula function, for this Chapter it is bivariate Gaussian copula $\mathbf{C}_{\mathbf{R}'}$.

Definition 3.2.4. Analogically to definition 3.2.3, the upper ‘tail’ dependency [1] is defined as

$$\begin{aligned} \lambda_u &= \lim_{u \rightarrow 1^-} P(\mathfrak{Y}_1 > u | \mathfrak{Y}_2 > u) \\ &= \lim_{u \rightarrow 1^-} \frac{P(\mathfrak{Y}_1 > u, \mathfrak{Y}_2 > u)}{P(\mathfrak{Y}_2 > u)} \\ &= \lim_{u \rightarrow 1^-} \frac{1 - P(\mathfrak{Y}_1 \leq u) - P(\mathfrak{Y}_2 \leq u) + P(\mathfrak{Y}_1 \leq u, \mathfrak{Y}_2 \leq u)}{P(\mathfrak{Y}_2 > u)} \\ &= \lim_{u \rightarrow 1^-} \frac{1 - 2u + \mathbf{C}(u, u)}{1 - u}. \end{aligned} \quad (3.20)$$

The lower ‘tail’ dependency gives a probability of the appearance of an extreme low value of one marginal given an extreme low value of another marginal. Analogically upper ‘tail’ dependency gives a probability of the extreme high value of one marginal given an extreme high value of an another. Importantly, it is easy to show, that for Gaussian copula $\lambda_l = \lambda_u = 0$ [1]. To model data where simultaneous extreme values of many marginals are possible, we need other non-Gaussian copula. Some of them are introduced in the next Chapter.

Chapter 4

Copulas

In the previous chapter we introduced the Gaussian copula that is a specific case of the wide family of copulas discussed in this chapter. For many real-life data non-Gaussian copulas are better models than Gaussian one. This is the case especially if simultaneous extreme event in many marginals are recorded. Such copulas are used in financial data analysis [6], reliability analysis [162, 163], Civil Engineering [164, 165], time series analysis [28], neuroscience [166], hydrology [167], climate research [23, 168] and random data generation [169, 170], to mention a few.

In this chapter we discuss multivariate models of data constructed from the non-Gaussian copula and continuous univariate marginals. The formal definition of the copula function [1, 161] states as follows.

Definition 4.0.1. The function $\mathbf{C} : [0, 1]^n \rightarrow [0, 1]$ is the n -dimensional copula if

1. $\mathbf{C}(u_1, \dots, u_{k-1}, 0, u_{k+1}, \dots, u_n) = 0$,
2. $\mathbf{C}(1, \dots, 1, u_k, 1, \dots, 1) = u_k$,
3. $\mathbf{C}(\mathbf{u})$ is n non-decreasing in the following manner

$$\forall B \subseteq [0, 1]^n \int_B d\mathbf{C}(\mathbf{u}) \geq 0, \quad (4.1)$$

given $\mathbf{u} = [u_1, \dots, u_n] \in [0, 1]^n$, and $B = \prod_{i=1}^n [u_i, v_i] \subseteq [0, 1]^n$, where $0 \leq u_i \leq v_i \leq 1$.

It can be easily shown that the Gaussian copula, from Definition 3.2.1 fulfils those conditions.

Remark 4.0.1. Following Definition 4.0.1 copula is a multivariate CDF of the random vector $\mathfrak{U}^{(n)} = (\mathfrak{U}_1, \dots, \mathfrak{U}_n)$ with uniform marginals *i.e.* $\mathfrak{U}_i \sim \text{Uniform}([0, 1])$

$$[0, 1] \ni \mathbf{C}(u_1, \dots, u_n) = P(\mathfrak{U}_1 \leq u_1 \wedge \dots \wedge \mathfrak{U}_n \leq u_n). \quad (4.2)$$

The corresponding multivariate PDF of $\mathfrak{U}^{(n)}$ is called the copula density

$$\mathbf{c}(\mathbf{u}) = \frac{\partial^n}{\partial u_1 \dots \partial u_n} C(\mathbf{u}). \quad (4.3)$$

Analogically to the Gaussian copula case in Eq. (3.14), each copula \mathbf{C} can be used to construct variety of multivariate distributions. The multivariate CDF of the n -variate random vector $\mathfrak{X}^{(n)}$ modelled by a copula \mathbf{C} and marginal CDFs F_i is

$$\mathbf{F}(\mathbf{x}) = P(\mathfrak{X}_1 \leq x_1 \wedge \dots \wedge \mathfrak{X}_n \leq x_n) = \mathbf{C}(F_1(x_1), \dots, F_n(x_n)). \quad (4.4)$$

As $u_i = F_i(x_i)$ and $\frac{du_i}{dx_i} = \frac{d}{dx_i}F_i(x_i) = f_i(x_i)$, corresponding multivariate PDF is

$$\mathbf{f}(\mathbf{x}) = \mathbf{c}(F_1(x_1), \dots, F_n(x_n)) \prod_{i=1}^n f_i(x_i). \quad (4.5)$$

We will use here the sub-copula notation in order to discuss various measures of the interdependency between marginals. This includes both bivariate measures and d -variate measures imposed by d^{th} order multivariate cumulants discussed in following chapters. For the significance of bivariate sub-copulas let us refer to [171], where the measures of dependencies between pairs of marginals of a given multivariate random vector are discussed by means of such bivariate sub-copulas. However, such approach is limited, as discussed further in Chapter 5.

Definition 4.0.2. Let $\mathbf{r} = (r_1, \dots, r_k) \subset (1, 2, \dots, n)$, $k < n$, and let $\mathbf{C} : [0, 1]^n \rightarrow [0, 1]$ be the n -variate copula. The multivariate CDF of the marginal's subset indexed by \mathbf{r} is a sub-copula $\mathbf{C}^{(s)} : [0, 1]^k \rightarrow [0, 1]$, where

$$\mathbf{C}^{(s)}(u_{r_1}, \dots, u_{r_k}) = \mathbf{C}(w_1, \dots, w_n), \text{ where } w_i = \begin{cases} u_i & \text{if } i \in \mathbf{r} \\ 1 & \text{otherwise} \end{cases}. \quad (4.6)$$

It can be shown, that such k -dimensional sub-copula fulfils conditions from Definition 4.0.1 and is a copula itself [6]. Recall that in Definition 3.2.2 we have introduced a Gaussian bivariate sub-copula in similar manner.

Suppose we have a bivariate random vector $\mathfrak{U}^{(2)}$ with marginals $\mathfrak{U}_i \sim \text{Uniform}(0, 1)$ modelled by a bivariate copula $\mathbf{C}(u_1, u_2)$. The covariance between marginals is

$$\text{cov}(\mathfrak{U}_1, \mathfrak{U}_2) = \int_0^1 \int_0^1 \left(u_1 - \frac{1}{2}\right) \left(u_2 - \frac{1}{2}\right) d\mathbf{C}(u_1, u_2), \quad (4.7)$$

or equivalently [172] for continuous copulas

$$\text{cov}(\mathfrak{U}_1, \mathfrak{U}_2) = \int_0^1 \int_0^1 (\mathbf{C}(u_1, u_2) - u_1 u_2) du_1 du_2 = \int_0^1 \int_0^1 \mathbf{C}(u_1, u_2) du_1 du_2 - 3. \quad (4.8)$$

The variance of an uniform distribution on $[0, 1]$ is $\frac{1}{12}$, hence the Pearson cross-correlation between marginals is

$$\text{cor}(\mathfrak{U}_1, \mathfrak{U}_2) = 12\text{cov}(\mathfrak{U}_1, \mathfrak{U}_2). \quad (4.9)$$

The Spearman's rank cross-correlation coefficient [172] is

$$\rho(\mathfrak{U}_1, \mathfrak{U}_2) := \text{cor}(\text{rank}(\mathfrak{U}_1), \text{rank}(\mathfrak{U}_2)) = \text{cor}(\mathfrak{U}_1, \mathfrak{U}_2). \quad (4.10)$$

The second equity results from the fact, that univariate marginals are uniformly distributed on $[0, 1]$. Kendall's rank cross-correlation coefficient $-1 \leq \tau \leq 1$ equals to [173]

$$\tau(\mathfrak{U}_1, \mathfrak{U}_2) = 4 \int_0^1 \int_0^1 \mathbf{C}(u_1, u_2) d\mathbf{C}(u_1, u_2) - 1. \quad (4.11)$$

Remark 4.0.2. Suppose we have random vectors $\mathfrak{X}^{(n)}$ and $\mathfrak{U}^{(n)}$ with the same copula. $\mathfrak{U}^{(n)}$ have all uniform marginals on $[0, 1]$, and $\mathfrak{X}^{(n)}$ has continuous univariate marginal CDFs F_i , hence $\mathfrak{U}_i = F_i(\mathfrak{X}_i)$. Following Remark 3.2.1 such transformations does not change the rank of the given realisation of the given marginal. Hence it does not change Spearman's and Kendall's rank cross-correlation sa well. We have

$$\rho(\mathfrak{X}_1, \mathfrak{X}_2) = \rho(\mathfrak{U}_1, \mathfrak{U}_2), \quad \tau(\mathfrak{X}_1, \mathfrak{X}_2) = \tau(\mathfrak{U}_1, \mathfrak{U}_2). \quad (4.12)$$

On the other hand, this does not hold for Pearson's cross-correlation [172]

$$\text{cov}(\mathfrak{X}_1, \mathfrak{X}_2) = \int_0^1 \int_0^1 (\mathbf{C}(u_1, u_2) - u_1 u_2) dF_1^{-1}(u_1) dF_2^{-1}(u_2), \quad (4.13)$$

and in general

$$\text{cor}(\mathfrak{X}_1, \mathfrak{X}_2) \neq \text{cor}(\mathfrak{U}_1, \mathfrak{U}_2). \quad (4.14)$$

Another important bivariate measures of interdependency between marginals are bivariate 'tail' dependencies defined as [1]

$$\lambda_l = \lim_{u \rightarrow 0^+} \frac{\mathbf{C}(u, u)}{u}, \quad (4.15)$$

and

$$\lambda_u = \lim_{u \rightarrow 1^-} \frac{1 - 2u + \mathbf{C}(u, u)}{1 - u}. \quad (4.16)$$

In the Gaussian copula case those would correspond to Definitions 3.2.3, and 3.2.4. As discussed further, many non-Gaussian copulas have non-zero 'tail' dependencies and hence can be used to model simultaneous extreme events appearing in two (or many in general case) marginals.

4.1 Elliptical copulas

The Gaussian copula mentioned in Chapter 3 is a member of wider family of elliptical copulas derived from elliptical multivariate distributions, see Definition 5.1 in [174].

Definition 4.1.1. The random vector $\mathfrak{X}^{(n)} \sim \mathbf{E}(\mu, \Sigma, \psi)$ is modelled by an elliptical distribution if the probability distribution function of $\mathfrak{Y}^{(n)} = \mathfrak{X}^{(n)} - \mu$ has the following characteristic function

$$\phi_{\mathfrak{Y}^{(n)}}(\tau) = \psi(\tau^\top \Sigma \tau). \quad (4.17)$$

Here $\mu \in \mathbb{R}^n$, and ψ is some scalar function [175], and $\Sigma \in \mathbb{R}^{n \times n}$ is positive semi-definite symmetric matrix.

Gaussian multivariate distribution is an elliptical one with $\psi(t) = e^{-\frac{t}{2}}$ [174].

Definition 4.1.2. The elliptical copula $\mathbf{C}_{\mathbf{E}}$ is given by

$$\mathbf{C}_{\mathbf{E}}(u_1, \dots, u_n) = \mathbf{E}_{\mu, \Sigma, \psi}(E_1^{-1}(u_1), \dots, E_n^{-1}(u_n)). \quad (4.18)$$

Here $\mathbf{E}_{\mu, \Sigma, \psi}$ is the multivariate Cumulative Distribution Function (CDF) of the elliptical distribution, and E_i are corresponding univariate marginal CDFs. For simplicity, we can use $\mu = 0$ both in $\mathbf{E}_{\mu, \Sigma, \psi}$ and all E_i .

Remark 4.1.1. Suppose we want to generate t realisations of n -variate elliptical copula, derived from $\mathbf{E}(\Sigma, \psi)$, we can perform it using the following steps:

1. Sample $\mathbf{X} \in \mathbb{R}^{t \times n}$ with elements $x_{j,i}$ from $\mathbf{E}(\Sigma, \psi)$.
2. Transform $\mathbf{X} \rightarrow \mathbf{U} \in [0, 1]^{t \times n}$ by means of $u_{j,i} = E_i(x_{j,i})$.

For the special case of t -Student distribution see Algorithms 5.2 in [174].

It can be shown, that a t -Student multivariate distribution is an elliptical one [176], its multivariate PDF reads

$$\mathbf{t}_{\mathbf{R}, \nu}(\mathbf{x}) = \frac{\Gamma(\frac{\nu+n}{2})}{\Gamma(\frac{\nu}{2}) \sqrt{\nu^n \pi^n \det(\mathbf{R})}} \left(1 + \frac{\mathbf{x} \mathbf{R}^{-1} \mathbf{x}^\top}{\nu} \right)^{-\frac{\nu+n}{2}}. \quad (4.19)$$

In this case, the function ψ has complicated analytical form, and is parametrised by an integer parameter $\nu \in \mathbb{N}^+$ [176]. Further $\mathbf{R} \in \mathbb{R}^{n \times n}$ is symmetric positive definite matrix with ones on a diagonal. The integer parameter $\nu \in \mathbb{N}^+$ is an number of degrees of freedom parameter. Obviously, the multivariate t -Student CDF would be

$$[0, 1] \ni \mathbf{T}_{\nu, \mathbf{R}}(\mathbf{x}) = \int_{-\infty}^{x_1} \dots \int_{-\infty}^{x_n} \mathbf{t}_{\nu, \mathbf{R}}(y_1, \dots, y_n) dy_1 \dots dy_n. \quad (4.20)$$

The marginal univariate t -Student PDF is

$$t_\nu(x) = \frac{\Gamma(\frac{\nu+n}{2})}{\Gamma(\frac{\nu}{2}) \sqrt{\nu \pi}} \left(1 + \frac{x^2}{\nu} \right)^{-\frac{\nu+n}{2}}, \quad (4.21)$$

which can be integrated to marginal CDF $T_\nu(x) \in [0, 1]$. Following Definition 4.1.2, the t -Student copula $\mathbf{C}_{\mathbf{R}, \nu} : [0, 1]^n \rightarrow [0, 1]$ is

$$\mathbf{C}_{\mathbf{R}, \nu}(\mathbf{u}) = \mathbf{T}_{\mathbf{R}, \nu}(T_\nu^{-1}(u_1), \dots, T_\nu^{-1}(u_n)). \quad (4.22)$$

It is used mainly to model financial data [177, 178, 179]. However it is applied also in a machine learning, for example in colour texture classification [180] or as a kernel function of the Support Vector Data Description [181].

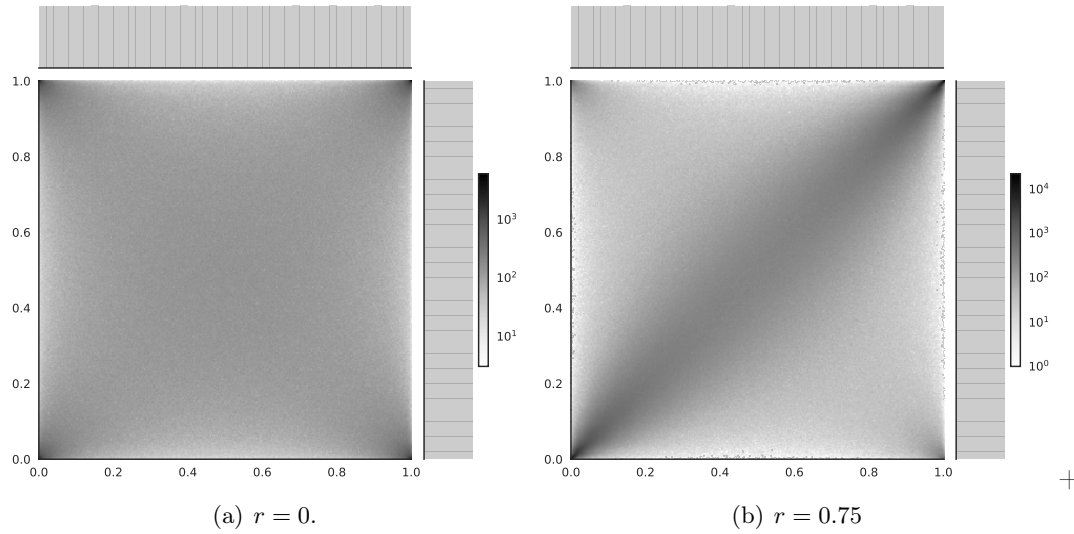


Figure 4.1: A scatter plot and histograms of data sampled from a bivariate t -Student copula with $\nu = 1$.

Remark 4.1.2. Take bivariate t -Student copula parametrised by $\mathbf{R} = \begin{bmatrix} 1 & r \\ r & 1 \end{bmatrix}$ where $-1 < r < 1$ and $\nu \in \mathbb{N}^+$, Kendall's rank cross-correlation [182] equals

$$\tau = \frac{2}{\pi} \arcsin(r), \quad (4.23)$$

and both 'tail' dependencies [1] are

$$\lambda_l = \lambda_u = 2t_{\nu+1} \left(-\sqrt{\nu+1} \left(\frac{\sqrt{1-r}}{\sqrt{1+r}} \right) \right), \quad (4.24)$$

where t_ν is introduced in Eq. (4.21).

As discussed in [183], Eq. (4.23) holds in general for elliptical copulas, including the Gaussian one. To see the Gaussian copula case take $\nu \rightarrow \infty$. Below we present some interesting example of the t -Student copula.

Example 4.1.1. In Figure 4.1 we present a scatter-plot and univariate histograms of data sampled from the t -Student bivariate copula parametrised by $\nu = 1$ and $\mathbf{R} = \begin{bmatrix} 1 & 0.75 \\ 0.75 & 1 \end{bmatrix}$ - left panel, and $\nu = 1$ and $\mathbf{R} = \begin{bmatrix} 1 & 0 \\ 0 & 1 \end{bmatrix}$ - right panel. Figure 4.1(a) refers to zero Kendall's, Spearman's and Pearson's cross-correlation between marginals, but a data pattern is not simple uniform, but with higher concentration on corners.

Example 4.1.2. Consider bivariate random vector $\mathfrak{U}^{(2)}$ modelled by a t -Student copula with $\mathbf{R} = \begin{bmatrix} 1 & 0 \\ 0 & 1 \end{bmatrix}$ and $\nu = 1$, see Figure 4.1(a). Referring to Eq. (4.24), for this model we have $\lambda_l = \lambda_u = \frac{1}{4}$. The covariance matrix for such data model would be

$$\Sigma = \begin{bmatrix} \frac{1}{12} & 0 \\ 0 & \frac{1}{12} \end{bmatrix}, \quad (4.25)$$

which is diagonal. Hence, the columns of $\mathbb{1} = \begin{bmatrix} 1 & 0 \\ 0 & 1 \end{bmatrix}$ are its eigenvectors. From this point of view marginal variables \mathfrak{U}_1 and \mathfrak{U}_2 should be independent. Despite the fact, that Pearson's, Spearman's and Kendall's cross-correlation measures are zero their 'tail' dependencies, modelling simultaneous extreme events, are not. Hence the Singular Value Decomposition of the covariance matrix Σ do not reduce risk of simultaneous extreme events.

For further discussion on elliptical distributions and elliptical copulas see Chapter 4 in [183], where elliptical distributions are discussed in Section 4.2, while elliptical copulas in Section 4.5.

4.2 Upper and lower limit, Fréchet families

The Fréchet copula's family is derived from limits imposed on copulas functions. The n -dimensional copula function can be limited from above and from below by following Fréchet-Hoeffding copula bounds [1],

$$\max \left(1 - n + \sum_{i=1}^n u_i, 0 \right) \leq \mathbf{C}(u_1, \dots, u_n) \leq \min(u_1, \dots, u_n). \quad (4.26)$$

4.2.1 Maximal copula

The upper limit,

$$\mathbf{C}_{\max}(u_1, \dots, u_n) = \min(u_1, \dots, u_n), \quad (4.27)$$

is a copula (fulfils conditions in Definition 4.0.1) for each n . It corresponds to perfectly positively correlated marginal variables. It is easy to show that if $\mathfrak{U}^{(n)}$ is a random vector modelled by the maximal copula for each pair of marginals all bivariate measures of the cross-correlation, Kendall's, Spearman's or Pearson's ones equal to 1. Given bivariate maximal copula its tail dependencies are $\lambda_l = \lambda_r = 1$. Finally observe, that since $0 \leq u_i, u_j \leq 1$, a bivariate maximal sub-copula is given by

$$\mathbf{C}_{\max}^{(s)}(u_i, u_j) = \min(\{1, \dots, u_i, \dots, 1, \dots, u_j, \dots, 1\}) = \min(u_i, u_j). \quad (4.28)$$

4.2.2 Minimal copula

The lower limit form Eq. (4.26),

$$\max \left(1 - n + \sum_{i=1}^n u_i, 0 \right) = \mathbf{L}(u_1, \dots, u_n), \quad (4.29)$$

in only a copula in the bivariate case, this is called the minimal copula

$$\mathbf{C}_{\min}(u_1, u_2) = \max(u_1 + u_2 - 1, 0). \quad (4.30)$$

For $n > 2$, the condition (3) from Definition 4.0.1 is not fulfilled [1]. To show it intuitively, observe that in bivariate case $\mathbf{C}_{\min}(u_1, u_2)$ corresponds to perfectly negative cross-correlated marginals with elements $u_{t,1}$ and $u_{t,2} = 1 - u_{t,1}$. Obviously, it is not possible to have more than 2 univariate real valued marginals that are all pairwise perfectly negatively cross-correlated. As such, it is easy to show, that given a bivariate minimal copula Kendall's, Spearman's and Pearson's cross-correlation coefficients equal to -1 . Finally, both 'tail' dependencies of the minimal copula are $\lambda_u = \lambda_l = 0$. Both maximal and minimal copulas are examples of the wider Fréchet family of copulas.

4.2.3 Independent copula and a Fréchet family copula

The last component to the Fréchet family of copulas is the independent copula.

Definition 4.2.1. Independent copula of the n -variate random vector $\mathfrak{U}^{(n)}$ is simply a product of arguments,

$$\mathbf{C}_{\perp}(u_1, \dots, u_n) = \prod_{i=1}^n u_i. \quad (4.31)$$

The independent copula correspond to the random vector with all independent marginals. It is easy to show that \mathbf{C}_{\perp} fulfils all conditions from Definition 4.0.1.

Obviously, a bivariate sub-copula would be

$$\mathbf{C}_{\perp}^{(s)}(u_i, u_j) = 1 \cdot \dots \cdot 1 \cdot u_i \cdot 1 \cdot \dots \cdot 1 \cdot u_j \cdot 1 \dots = u_i \cdot u_j. \quad (4.32)$$

Given a independent copula all measures of the cross-correlation (e.g. Kendall's, Spearman's, Pearson's or 'tail' dependencies) equal to 0.

Given maximal, minimal and independent copulas we can integrate them into the Fréchet copulas. In the case of $n = 2$ we can use \mathbf{C}_{\max} , \mathbf{C}_{\perp} and \mathbf{C}_{\min} , while in the case of $n > 2$ we can use \mathbf{C}_{\max} and \mathbf{C}_{\perp} , since \mathbf{C}_{\min} is not a copula any-more.

Definition 4.2.2. The 2-parameters Fréchet copula [1] of a bivariate random vector $\mathfrak{U}^{(2)}$ is given by

$$\mathbf{C}_{\alpha,\beta}(u_1, u_2) = \alpha \mathbf{C}_{\max}(u_1, u_2) + \beta \mathbf{C}_{\min}(u_1, u_2) + (1 - \alpha - \beta) \mathbf{C}_{\perp}(u_1, u_2), \quad (4.33)$$

where $0 \leq \alpha \leq 1$, $0 \leq \beta \leq 1$ and $\alpha + \beta \leq 1$. These parameters indicate portions of maximal, minimal and independent copula accordingly. It is easy to show that $\mathbf{C}_{\alpha,\beta}$ is a copula by Definition 4.0.1.

Algorithm 4 Sample bivariate Fréchet copula

```

1: Input:  $t$  – Int, number of samples:  $0 \leq \alpha, \beta \leq 1$  - parameters:  $\alpha + \beta \leq 1$ .
2: Output:  $\mathbf{U} \in [0, 1]^{t \times 2}$  – samples.
3: function FRECHETCOPULAGEN( $t, \alpha, \beta$ )
4:   for  $j \leftarrow 1$  to  $t$  do
5:     sample  $v \sim \text{Uniform}([0, 1])$ 
6:     if  $v \leq \alpha$  then
7:       sample  $u_{j,1} \sim \text{Uniform}([0, 1])$ 
8:        $u_{j,2} = u_{j,1}$ 
9:     else if  $\alpha < v \leq \alpha + \beta$  then
10:      sample  $u_{j,1} \sim \text{Uniform}([0, 1])$ 
11:       $u_{j,2} = 1 - u_{j,1}$ 
12:     else
13:       Sample independently  $u_{j,1} \sim \text{Uniform}([0, 1]), u_{j,2} \sim \text{Uniform}([0, 1])$ 
14:     end if
15:   end for
16:   return  $\mathbf{U}$ 
17: end function

```

The impact to ‘tail’ dependencies of $\mathbf{C}_{\alpha,\beta}$ will come from the maximal copula only, and thus

$$\lambda_l = \lambda_u = \alpha. \quad (4.34)$$

Analogically, one can show that the Spearman’s cross-correlation of the 2-parameters Fréchet copula is

$$\rho = \alpha - \beta. \quad (4.35)$$

Referring to Eq. (4.34) and Eq. (4.35) there may appear a suggestion that by varying parameters α and β we can easily fit bivariate Fréchet copula to given Spearman cross-correlation and ‘tail’ dependencies, if lower and upper ‘tail’ dependencies are expected to be similar. However formally, a 2-parameters Fréchet copula refers to the simple stochastic process where two elements of a bivariate realisation are either fully correlated, or uncorrelated (independent), or fully anti-correlated. Based on these, the simple procedure of sampling 2-parameters Fréchet copula is presented in Algorithm 4. However, stochastic processes of real life data modelling are more complex in most cases, hence we will discuss other families of copulas in next section. Now we will discuss the n -variate generalisation of the Fréchet copula, where its flexibility is reduced, since we have to drop the minimal copula. Hence, the n -variate Fréchet copula refers to even simpler stochastic process where all elements of a realisation are either fully correlated, or uncorrelated (independent), we present a sampling procedure in Algorithm 5.

Definition 4.2.3. The 1-parameter Fréchet copula is given by

$$\mathbf{C}_\alpha(u_1, \dots, u_n) = \alpha \mathbf{C}_{\max}(u_1, \dots, u_n) + (1 - \alpha) \mathbf{C}_\perp(u_1, \dots, u_n), \quad (4.36)$$

Algorithm 5 Sample n -variate Fréchet copula

```

1: Input:  $t$  – Int, number of samples,  $n$  – Int, number of marginals,  $0 \leq \alpha \leq 1$  –
   parameter.
2: Output:  $\mathbf{U} \in [0, 1]^{t \times n}$  – samples.
3: function FRECHETCOPULAGEN( $t, n, \alpha$ )
4:   for  $j \leftarrow 1$  to  $t$  do
5:     sample  $v \sim \text{Uniform}([0, 1])$ 
6:     if  $v \leq \alpha$  then
7:       sample  $u_{j,1} \sim \text{Uniform}([0, 1])$ 
8:        $u_{j,n} = u_{j,n-1} = \dots = u_{j,2} = u_{j,1}$ 
9:     else
10:      Sample indep.  $u_{j,1} \sim \text{Uniform}([0, 1]), \dots, u_{j,n} \sim \text{Uniform}([0, 1])$ 
11:    end if
12:  end for
13:  return  $\mathbf{U}$ 
14: end function

```

where $0 \leq \alpha \leq 1$. Here α is a portion of the maximal copula, while $1 - \alpha$ is a portion of the independent copula.

It is easy to show, that both Spearman's cross-correlation and 'tail' dependencies for each pair of marginals modelled by the 1-parameter Fréchet copula are

$$\rho = \lambda_l = \lambda_u = \alpha. \quad (4.37)$$

Example 4.2.1. *Let us take a 2-parameter bivariate Fréchet copula with $\alpha = \beta$, fulfilling $\alpha + \beta \leq 1$. Referring to Eq. (4.35) the Spearman's cross-correlation between marginals will be 0. Analogically to Example 4.1.2 the correlation matrix will be*

$$\Sigma = \begin{bmatrix} \frac{1}{12} & 0 \\ 0 & \frac{1}{12} \end{bmatrix}, \quad (4.38)$$

which eigenvectors being $[1 \ 0]^\top$, $[0 \ 1]^\top$. Hence, analogically to Example 4.1.2 the Singular Value Decomposition of the covariance matrix Σ would not reduce the risk of simultaneous extreme events.

4.3 Archimedean copulas

The motivation for introducing Archimedean copulas family comes from their wide application in real data analysis concerning: modelling financial data (shares prices, credit assets and risk analysis) [174, 184, 185, 186], modelling computer networks traffic [13, 14], wireless communication analysis [187], hydrological research [188, 189, 22, 23, 24], signal processing [190], and neuroimage data analysis [191]. Following [192] let us move to the following definition.

Definition 4.3.1. The Archimedean copula generator $\psi_\theta : [0, \infty) \rightarrow [0, 1]$ is the continuous function parametrised by θ such that

1. $\psi_\theta(0) = 1$,
2. $\psi_\theta(\infty) = 0$,
3. ψ_θ is strictly decreasing on $[0, \inf\{v : \psi_\theta(v) = 0\}]$.

We can define an inverse ψ_θ^{-1} on $(0, 1]$. Following [192] we take $\psi_\theta^{-1}(0) = \inf\{v : \psi_\theta(v) = 0\}$ introducing a pseudo-inverse defined on $[0, 1]$. Further one can show that $\psi_\theta^{-1}(1) = 0$.

Definition 4.3.2. Given the convex Archimedean copula generator as in Definition 4.3.1, the bivariate Archimedean copula is given by [192]

$$[0, 1] \ni \mathbf{C}_{\psi_\theta}(u_1, u_2) = \psi_\theta(\psi_\theta^{-1}(u_1) + \psi_\theta^{-1}(u_2)). \quad (4.39)$$

It can be shown, that such function fulfils conditions of a copula from Definition 4.0.1.

The n -variate generalisation needs further conditions to be fulfilled by the generator function [192].

Definition 4.3.3. If the Archimedean copula generator $\psi_\theta : [0, \infty) \rightarrow [0, 1]$ fulfils conditions in Definition 4.3.1, and additionally is n -monotone on $[0, \infty)$ in a sense of Definition 2.3 in [192], *i.e.*

$$\forall_{v \in [0, \infty)} (-1)^k \frac{d^k}{dv^k} \psi(v) \geq 0 \text{ where } k = 0, 1, \dots, n-2, \quad (4.40)$$

and

$$(-1)^{n-2} \frac{d^{n-2}}{dv^{n-2}} \psi(v) \text{ is nonincreasing and convex on } [0, \infty), \quad (4.41)$$

it defines the n -variate Archimedean copula

$$[0, 1] \ni \mathbf{C}_{\psi_\theta}(\mathbf{u}) = \psi_\theta \left(\sum_{i=1}^n \psi_\theta^{-1}(u_i) \right). \quad (4.42)$$

In a case of $n = 2$ the n -monotone condition from Definition 4.3.3 gives convexity conditions in Definition 4.3.2. Furthermore, it can be shown that if the function is n -monotone, it is $(n-1)$ -monotone as well, however the opposite may not be true. Hence if ψ_θ is the generator of the n -variate copula is a generator of the $(n-1)$ -variate copula [192], while the opposite may not be true.

Remark 4.3.1. To show a necessity of the d -monotone condition, following [192] let us take a generator

$$\psi(v) = \max(1 - v, 0), \quad (4.43)$$

fulfilling all conditions in Definition 4.3.2 but is not n -monotone and $n > 2$. Its pseudo-inverse is $\psi^{-1}(x) = 1 - x$. From Eq. (4.42) we have Eq. (4.29), that represents the minimal copula that is well defined only in the bivariate case.

Remark 4.3.2. Following Definition 4.0.2, using $\psi_\theta^{-1}(1) = 0$, and taking n -variate Archimedean copula, we can introduce a sub-copula, by setting to 1 those u_i arguments we are not interested in. Such sub-copula would be a copula as well.

For bivariate Archimedean copula the Kendall's cross-correlation can be computed in the following manner [193]

$$\tau = 1 - 4 \int_0^{\psi_\theta^{-1}(0)} v \left(\frac{d\psi_\theta(v)}{dv} \right)^2 dv. \quad (4.44)$$

4.3.1 Archimedean copulas examples

In this subsection we discuss well known one parameter Archimedean copulas, defined by following generator functions [194, 195].

1. Gumbel copula with generator

$$\psi_\theta(v) = \exp\left(-t^{\frac{1}{\theta}}\right) \quad \text{and} \quad \psi_\theta^{-1}(x) = (-\log(x))^\theta. \quad (4.45)$$

2. Clayton copula [196] with generator

$$\psi_\theta(v) = \max\left((1 + \theta v)^{-1/\theta}, 0\right) \quad \text{and} \quad \psi_\theta^{-1}(x) = \frac{x^{-\theta} - 1}{\theta}. \quad (4.46)$$

3. Frank copula with generator

$$\psi_\theta(v) = -\frac{1}{\theta} \log\left(1 + e^{-v} (e^{-\theta} - 1)\right) \quad \text{and} \quad \psi_\theta^{-1}(x) = -\log\left(\frac{e^{-\theta x} - 1}{e^{-\theta} - 1}\right). \quad (4.47)$$

4. Ali-Mikhail-Haq (AMH) copula [197] with generator

$$\psi_\theta(v) = \frac{1 - \theta}{\exp(v) - \theta} \quad \text{and} \quad \psi_\theta^{-1}(x) = \log\left(\frac{1 - \theta(1 - x)}{x}\right). \quad (4.48)$$

There are some limitations on copula parameter θ value necessary to fulfil conditions in Definition 4.3.2 in bivariate case, or in Definition 4.3.3 in n -variate case, where $n > 2$. In the bivariate case these limitations are presented in Table 4.1, see [1] or [198] for the AMH copula. For some measures of cross-correlations between marginals given these copulas, see Table 4.2.

	Gumbel	Clayton	Frank	AMH
$\theta \in$	$[1, \infty)$	$[-1, 0) \cup (0, \infty)$	$(-\infty, 0) \cup (0, \infty)$	$[-1, 1]$

Table 4.1: Parameters limitations for bivariate Archimedean copulas.

In n -variate case θ limitations are stronger and n dependent. In Table 4.3 we present limitations on θ sufficient for arbitrary n [195]. It was shown, that if these limitations are fulfilled we can sample arbitrary n -variate copula using the Marshall-Olkin algorithm [199], we require here the Archimedean copula generator to be completely monotone, *i.e.* to be n -monotone according to Definition 4.3.3 for each n [195].

	Gumbel	Clayton	Frank	AMH
τ	$1 - \frac{1}{\theta}$	$\frac{\theta}{\theta+2}$	$1 - \frac{4}{\theta} \left(1 - \frac{1}{\theta} \int_0^\theta \frac{t}{e^t-1} dt\right)$	$\frac{3\theta-2}{3\theta} - \frac{2(1-\theta)^2 \log(1-\theta)}{3\theta^2}$
λ_u	$2 - 2^{\frac{1}{\theta}}$	0	0	0
λ_l	0	$2^{-\frac{1}{\theta}}$	0	$= \begin{cases} 0.5 & \text{for } \theta = 1 \\ 0 & \text{for } \theta < 1 \end{cases}$

Table 4.2: Kendall’s cross-correlation and ‘tail’ dependencies for bivariate Archimedean copulas.

Example 4.3.1. *Limitations on θ parameter presented in Table 4.3 may be weakened in some cases, still leading to properly defined Archimedean copula. For example for n -variate Clayton copula to fulfil conditions of Definition 4.3.3 we require $\theta \in \left[\frac{-1}{n-1}, 0\right) \cup (0, \infty)$ [192]. However in this case we can not use the Marshall-Olkin sampling algorithm.*

	Gumbel	Clayton	Frank	AMH
$\theta \in$	$[1, \infty)$	$(0, \infty)$	$(0, \infty)$	$[0, 1)$

Table 4.3: Parameters limitations for multivariate Archimedean copulas.

4.3.2 Sampling Archimedean copulas

A basic method of sampling data from n -variate Archimedean copula is to use the Marshall-Olkin algorithm [199, 195]. It assumes, that Archimedean copula generator ψ_θ is the Laplace–Stieltjes transform of certain continuous univariate CDF function $F_T(v)$ or discrete probability mass function f_{T_k} . It was shown, that this assumption holds, if ψ_θ is completely monotone according to Definition 4.3.3, and $\psi_\theta(0) = 1$, see [200]. For Gumbel or Clayton copula we have the continuous case

$$\psi_\theta(s) = \int_{-\infty}^{\infty} e^{-sv} dF_T(v) = \mathbb{E} \left(e^{-s\mathfrak{V}} \right) \text{ for } s \in [0, \infty), \quad (4.49)$$

where \mathbb{E} is the expecting value operator and \mathfrak{V} the corresponding random variable. In the Clayton copula case, $F_T(v)$ is the CDF of the Gamma distribution $\Gamma_{(\frac{1}{\theta}, 1)}$, while in the Gumbel copula case $F_T(v)$ is the CDF of the Lévy general distribution $FS_{(\frac{1}{\theta}, 1, (\cos(\frac{\pi}{2\theta}))^\theta, 0)}$, see Remark 2.2.5 and Table 1 in [195]. For the Frank or AMH copulas we have a discrete case,

$$\psi_\theta(s) = \sum_{k=0}^{\infty} f_{T_k} e^{-v_k s} \text{ where } 0 < v_0 < v_1 < \dots \text{ and } s \in [0, \infty). \quad (4.50)$$

The probability mass function f_{T_k} is the geometric series expansion for AMH copula, and the logarithmic series expansion for Frank copula, see Table 1 in [195]. After performing the difficult step of sampling the inverse Laplace–Stieltjes transform of the Archimedean

Algorithm 6 Sampling an n -variate Archimedean copula.

```

1: Input:  $t$  – Int, number of samples,  $n$  – Int, number of marginals,  $\psi_\theta$  – completely
   monotone [195] Archimedean generator function.
2: Output:  $\mathbf{U} \in [0, 1]^{t \times n}$  – samples.
3: function ARCHCOPULAGEN( $t, n, \psi_\theta$ )
4:   for  $j = 1, \dots, t$  do
5:     sample  $v \sim F_T$  fulfilling  $\psi_\theta(s) = \begin{cases} \int_{-\infty}^{\infty} e^{-sv} dF_T(v) \\ \sum_{k=0}^{\infty} f_{T,k} e^{-x_k s} \end{cases}$ 
6:     Sample independently  $x_1 \sim \text{Uniform}([0, 1]), \dots, x_n \sim \text{Uniform}([0, 1])$ .
7:     for  $i = 1, \dots, n$  do
8:        $u_{j,i} \leftarrow \psi_\theta\left(\frac{-\log(x_i)}{v}\right)$ 
9:     end for
10:  end for
11:  return  $\mathbf{U}$ 
12: end function

```

copula generator, the Marshall-Olkin algorithm [199, 195] is straightforward, see Algorithm 6. For the proof see Algorithm 2.1 and its discussion see [183]. In [183] the Marshall-Olkin algorithm is presented in slightly different way and compared with the analogical algorithm that uses the Williamson n -transform instead of the inverse Laplace-Stieltjes transform, see Algorithm 2.3 therein.

As mentioned before, for valid ranges of copulas parameters for the Marshall-Olkin algorithm, see Table 4.3. This may limit the vast part of the parameters range, specially in the bivariate case of the Clayton, Frank and AMH copulas, see Table 4.1. To overcome this problem one can use more straightforward sampling method that is relatively simple for bivariate copulas [1], that can be represented as

$$\mathbf{C}(u_1, u_2) = P(\mathfrak{U}_1 \leq u_1 \wedge \mathfrak{U}_2 \leq u_2) = P(\mathfrak{U}_2 \leq u_2 | \mathfrak{U}_1 \leq u_1) P(\mathfrak{U}_1 \leq u_1) = \mathbf{C}(u_2 | u_1) u_1 \quad (4.51)$$

since u_1 is uniformly distributed on $[0, 1]$ and one can write $P(\mathfrak{U}_1 \leq u_1) = u_1$. Thanks to the conditional copula

$$\mathbf{C}(u_2 | u_1) = \frac{\partial \mathbf{C}(u_1, u_2)}{\partial u_1}, \quad (4.52)$$

and given a product in Eq. (4.51) we can now sample u_1 from $\text{Unirom}([0, 1])$ and u_2 from $\mathbf{C}(u_2 | u_1)$. This algorithm was introduced in practice in [1] for Clayton and Frank copulas, and in [198] for the AMH copula, see also Algorithms 2.5 and 2.6 in [183]. It is presented in the book as Algorithm 7.

Example 4.3.2. *Suppose we want to sample the bivariate Frank copula*

$$\mathbf{C}_F(u_1, u_2) = -\frac{1}{\theta} \log \left(1 + \frac{(e^{-u_1 \theta} - 1)(e^{-u_2 \theta} - 1)}{e^{-\theta} - 1} \right). \quad (4.53)$$

Algorithm 7 Sampling bivariate Archimedean copula for $n = 2$.

```

1: Input:  $t - \text{Int}$ ,  $\psi_\theta - \text{convex Archimedean copula generator}$ .
2: Output:  $\mathbf{U} \in [0, 1]^{t \times 2} - \text{samples}$ .
3: function ARCHCOPULAGEN( $t, \psi_\theta$ )
4:   for  $j = 1, \dots, t$  do
5:     sample  $u_{j,1} \sim \text{Uniform}([0, 1])$ 
6:     sample  $u_{j,2} \sim \mathbf{C}_{\psi_\theta}(u_2|u_1)$ 
7:   end for
8:   return  $\mathbf{U}$ 
9: end function

```

We sample $u_1 \sim \text{Uniform}(0, 1)$ in the first step. We use u_1 to determine $\mathbf{C}(u_2|u_1)$ and sample it in the second step. We can treat $\mathbf{C}(u_2|u_1)$ as an univariate CDF of u_2 parametrised by u_1 . Its inverse (a quantile function) would be

$$Q(w) \Big|_{u_1} = -\frac{1}{\theta} \log \left(\frac{1 + w(1 - e^{-\theta})}{w(e^{-\theta u_1} - 1) - e^{-\theta u_1}} \right). \quad (4.54)$$

Now we can sample $w \sim \text{Uniform}([0, 1])$, and use $u_2 = Q(w) \Big|_{u_1}$.

Remark 4.3.3. Analogically one can sample the 3-variate Archimedean copula using rule [1]

$$\mathbf{C}(u_1, u_2, u_3) = \mathbf{C}(u_3|u_2, u_1) \mathbf{C}(u_2|u_1)u_1 \quad (4.55)$$

however the computation of such chain especially if n is large is computationally complicated in comparison with the bivariate case. Further the larger the n , the parameter range gain would be smaller. For the copula to be correctly defined the generator ψ_θ has to be n -monotone, see Definition 4.3.3. For the Algorithm 6 to be applicable the generator has to be completely monotone, *i.e.* n -monotone, as $n \rightarrow \infty$. To demonstrate how the n -monotone condition reflect the parameter range of the Clayton copula see example 4.3.1, and compare it with Table 4.3 where the parameter range is given for the completely monotone ψ_θ .

Example 4.3.3. In Figure 4.2 we present a scatter-plot and univariate histograms sampled from the Archimedean copula with the Kendall's τ cross-correlation equal to ± 0.6 . Compare the positive τ and θ case in Figure 4.2(a) that can be sampled either by Algorithm 6 or by Algorithm 7, with the negative τ and θ case in Figure 4.2(b) sampled by Algorithm 7. One can observe completely different patterns, especially in the low tail region.

4.3.3 Nested Archimedean copula

It is easy to observe, that one parameters Archimedean copulas such as the Gumbel, Clayton, Frank or AMH ones have the same cross-correlation between all pairs of marginals,

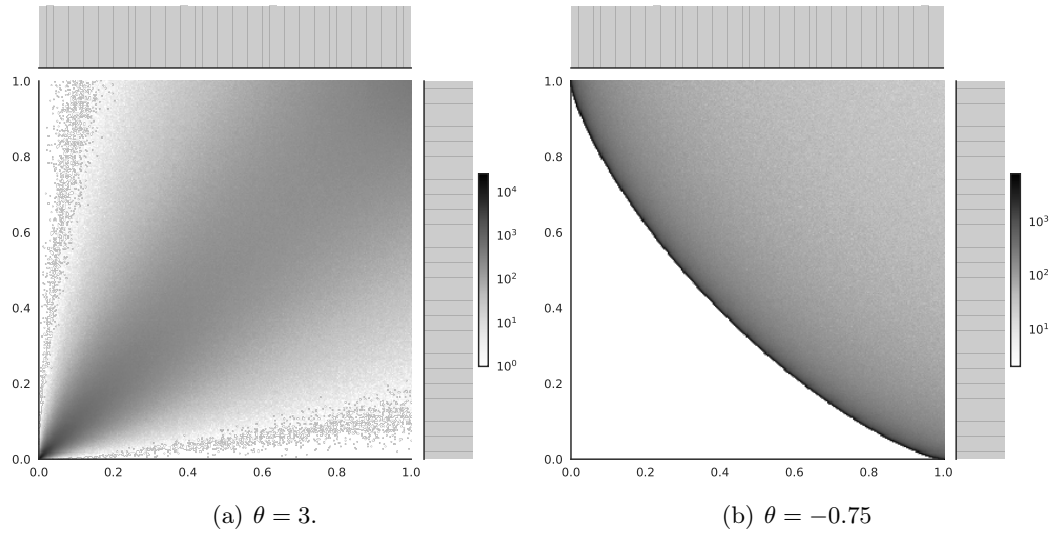


Figure 4.2: A scatter plot and histograms of the Clayton copula for positive and negative Kendall's cross-correlation $\tau = \pm 0.6$.

derived from their scalar θ parameter. Unfortunately, this is far from modelling the real live data, especially if we deal with large number of marginals- n . To overcome this problem, one can use nested Archimedean copulas [201] that model data in such a way, that chosen subsets of marginals may have higher cross-correlations in comparison with an overall cross-correlation between marginals.

Definition 4.3.4. Nested copula [201] is defined as follows

$$\mathbf{C}(\mathbf{u}) = \mathbf{C}_0(\mathbf{C}_1(\mathbf{u}_{\mathbf{r}_1}), \dots, \mathbf{C}_\ell(\mathbf{u}_{\mathbf{r}_\ell}), \dots, \mathbf{C}_s(\mathbf{u}_{\mathbf{r}_s}), \mathbf{u}_{\mathbf{r}'}) \quad (4.56)$$

where $\mathbf{u} = (u_1, \dots, u_n)$ is a vector of arguments of the copula, and $\mathbf{u}_{\mathbf{r}_\ell} = (u_{r_{\ell 1}}, u_{r_{\ell 2}}, \dots)$ is the sub-vector of \mathbf{r} indexed by \mathbf{r}_ℓ , that correspond to the ℓ^{th} child copula \mathbf{C}_ℓ . Here $\{\mathbf{r}_1, \dots, \mathbf{r}_\ell, \dots, \mathbf{r}_s, \mathbf{r}'\}$ is the set partition of $(1 : n)$ that is a vector $[1, 2, \dots, n]$. In this notation \mathbf{C}_0 is the parent copula. Obviously, we can have such set partition, that $\mathbf{r}' = \emptyset$ and each marginal is modelled both by the parent copula and some child copula.

Interestingly, nested copula leads to different sub-copulas given by Definition 4.0.2, depending on a subset of marginals we are interested in, it will be shown in following examples.

Example 4.3.4. Suppose we have nested copula as in Definition 4.3.4. Suppose we are interested in the subset $\mathbf{u}_{\mathbf{r}''}$ whole belonging the single child copula, say \mathbf{C}_ℓ , i.e. $\mathbf{r}'' \subseteq \mathbf{r}_\ell$. We set $u_i = 1$ if $i \notin \mathbf{r}''$ and we have the following sub-copula

$$\mathbf{C}^{(s)}(\mathbf{u}_{\mathbf{r}''}) = \mathbf{C}_0(1, \dots, 1, \mathbf{C}_\ell(\mathbf{u}_{\mathbf{r}''}), 1, \dots, 1), \quad (4.57)$$

since $\mathbf{C}_{i \neq i}(1, \dots, 1) = 1$. The i^{th} child copula will return some $v \in [0, 1]$. By Definition 4.0.1 the outcome is a i^{th} child copula if $\mathbf{r}_i = \mathbf{r}''$ or its sub-copula if $\mathbf{r}_i \subset \mathbf{r}''$

$$\mathbf{C}^{(s)}(\mathbf{u}_{\mathbf{r}''}) = \mathbf{C}_0(1, \dots, 1, v, 1, \dots, 1) = v = \mathbf{C}_i^{(s)}(\mathbf{u}_{\mathbf{r}''}). \quad (4.58)$$

Example 4.3.5. Suppose we have $\mathbf{r}'' \subset (1 : n)$, obtained by taking one marginal from each child copula

$$\forall_i \#(\mathbf{r}'' \cap \mathbf{r}_i) = 1, \quad (4.59)$$

and all marginals modelled only by a parent copula

$$\mathbf{r}'' \setminus (\cup_i \mathbf{r}_i) = \mathbf{r}'. \quad (4.60)$$

As in the previous example, we set $u_i \neq 1$ only if $i \in \mathbf{r}''$. Each child copula will return

$$\mathbf{C}_i(\mathbf{u}_i) = \mathbf{C}_i(1, \dots, 1, u_i, 1, \dots, 1) = u_i. \quad (4.61)$$

Given these we have only the parent copula

$$\mathbf{C}^{(s)}(\mathbf{u}_{\mathbf{r}''}) = \mathbf{C}_0(\mathbf{u}_{\mathbf{r}''}). \quad (4.62)$$

Remark 4.3.4. In an intermediate case, there will remain some nesting structure. The use of the sub-copula notation allows making a simple observation, that given the bivariate sub-copula, the intermediate case is not possible. The sub-copula would refer either one child copula or to the parent copula. Given nested copula, any bivariate dependency measures of marginals would refer either to the parent copula or to the child one. A more interesting intermediate case may be recorded while measuring interdependency of d marginals simultaneously, where $d > 2$.

Although an Archimedean copula is introduced by the single copula generator, nested Archimedean copula can be introduced by the series of generators.

Definition 4.3.5. The nested Archimedean copula [201], is defined as

$$\mathbf{C}_{\psi_{\theta_0}, \psi^1, \dots, \psi^s}(u_1, \dots, u_n) = \mathbf{C}_{\psi_{\theta_0}}(\mathbf{C}_{\psi^1}(\mathbf{u}_{\mathbf{r}_1}), \dots, \mathbf{C}_{\psi^s}(\mathbf{u}_{\mathbf{r}_s}), \mathbf{u}_{\mathbf{r}'}), \quad (4.63)$$

we use notation as in Definition 4.3.4. The $\mathbf{C}_{\psi_{\theta_0}}$ is the parents copula with generator ψ_{θ_0} parametrised by θ_0 and \mathbf{C}_{ψ^t} are children copula with generators ψ^t .

There are some further generalisations of nested Archimedean copulas discussed for example in [201], however not included in this book for the simplicity of presentation. One of those is the use of a higher degree of nesting by using the parent copula, children copulas, grandchildren copulas etc. Another generalisation comes from the fact that parents and children copulas may be from different copulas families, as long as they fulfil some conditions called sufficient nesting conditions [202, 201]. Nevertheless, for the clarity of presentation, we will concentrate in this book on the case where a parent and children copulas are from the same Archimedean family.

To sample nested Archimedean copulas one can use the advanced version of the Marshall-Olkin algorithm. We start with the parent copula generator ψ_{θ_0} parametrised by θ_0 and sample v_0 as in Algorithm 6 (where it is called v). Given v_0 we have following children copulas generators each, parametrised by global θ_0 and v_0 and individual θ_l [202, 194],

$$\psi_{v_0, \theta_0, \theta_l}(t) = \exp(-v_0 \psi_{\theta_0}^{-1}(\psi_{\theta_l}(t))) = (\exp(-\psi_{\theta_0}^{-1}(\psi_{\theta_l}(t))))^{v_0}. \quad (4.64)$$

Such child copula generator must have completely monotone derivative [194] in a sense of Definition 2.3 in [192]. This condition is called the sufficient nesting condition.

In our case it is equivalent to

$$\forall_l \theta_0 \leq \theta_l, \quad (4.65)$$

see [202, 194] for justification. Further parameter θ_0 has to fulfil conditions in Table 4.3, in a particular case of the AMH nested copula $\theta_l < 1$ condition is required [202] for each l .

Following [202], next step concern sampling an inverse of the Laplace–Stieltjes transform of the child copula generator given in Eq. (4.64), analogically to the Archimedean copula generator in Eq. (4.49). In the continuous case, for Clayton and Gumbel nested copula we have

$$\psi_{v_0, \theta_0, \theta_l}(s) = \int_{-\infty}^{\infty} e^{-sv} dF_{T_{v_0, \theta_0, \theta_l}}(v). \quad (4.66)$$

In the discrete case, for Frank and AMH nested copula we have

$$\psi_{v_0, \theta_0, \theta_l}(s) = \sum_{k=0}^{\infty} (f_{T_{v_0, \theta_0, \theta_l}})_k e^{-v_k s}, \quad (4.67)$$

where $0 < v_0 < v_1 < \dots$ and $s \in [0, \infty)$.

Given these, sampling of nested Archimedean copulas is summarised in Algorithm 8. Generators of children copulas are as follows.

1. Gumbel copula (continuous case) we sample the Lévy general distribution parametrised by $\alpha = \frac{\theta_0}{\theta_l}$, $\beta = 1$, $\gamma = \left(\cos\left(\frac{\pi\theta_0}{2\theta_l}\right)v_0\right)^{\frac{\theta_l}{\theta_0}}$ and $\delta = v_0$, the $F_{S(\alpha, \beta, \gamma, \delta)}$, see Remark 2.2.5. To simplify we can change parameter $\gamma \rightarrow \gamma' = \left(\cos\left(\frac{\pi\theta_0}{2\theta_l}\right)\right)^{\frac{\theta_l}{\theta_0}}$ and $\delta \rightarrow \delta' = 0$, and sample $F_{S(\alpha, \beta, \gamma', \delta')}$, and use in next step $\tilde{\psi}_{\theta_0, \theta_l}(t) = \exp\left(-t^{\frac{\theta_0}{\theta_l}}\right)$, instead of $\psi_{v_0, \theta_0, \theta_l}(t) = \exp\left(-v_0 t^{\frac{\theta_0}{\theta_l}}\right)$. Given such approach discussed in [194] the v_0 will cancel out.
2. Clayton copula (continuous case) we sample the exponentially tilted Lévy general distribution [194] with the PDF

$$f_{(v_0, \frac{\theta_0}{\theta_l})}(x) = \frac{f_{S(\alpha, \beta, \gamma', \delta')}(x)}{e^{-v_0}} e^{-x v_0^{\frac{\theta_0}{\theta_l}}}. \quad (4.68)$$

Algorithm 8 Generate data using nested Archimedean copula [194].

```

1: Input:  $t$  - Int, samples number;  $n_1, \dots, n_\ell, \dots, n_s$  - Ints marginals' numbers for each
   child copula,  $\theta_1, \dots, \theta_\ell, \dots, \theta_s$  - Floats children copulas parameters,  $\theta_0$  - Float parent
   copula parameter.
2: Output:  $\mathbf{U} \in [0, 1]^{t \times k}$  - samples. ▷ where  $k = \sum_\ell n_\ell$ 
3: function NESTEDARCHCOPULAGEN( $t, n_1, \dots, n_s, \theta_1, \dots, \theta_s, \theta_0$ )
4:   for  $j \leftarrow 1$  to  $t$  do
5:     sample  $v_0 \sim F_T$  ▷ see line 5 in Algorithm 6
6:     sample indep.  $x_1 \sim \text{Uniform}([0, 1]), \dots, x_k \sim \text{Uniform}([0, 1])$ 
7:     for  $\ell \leftarrow 1$  to  $s$  do ▷ over children
8:       Sample  $v_\ell \sim F_{T_{v_0, \theta_0, \theta_\ell}}$  or  $f_{T_{v_0, \theta_0, \theta_\ell}}$  ▷ see Eq. s (4.66) (4.67)
9:       for  $i \leftarrow \sum_{l=1}^{\ell-1} n_l + 1$  to  $\sum_{l=1}^{\ell} n_l$  do
10:         $x_{j,i} = \psi_{v_0, \theta_0, \theta_\ell} \left( \frac{-\log(x_{j,i})}{v_\ell} \right)$ 
11:      end for
12:    end for
13:    for  $i \leftarrow 1$  to  $k$  do
14:       $u_{j,i} = \psi_\theta \left( \frac{-\log(x_{j,i})}{v_0} \right)$ 
15:    end for
16:  end for
17:  return  $\mathbf{U}$ 
18: end function

```

3. AMH copula (discrete case): we sample y from negative binomial distribution with parameters $\left(v_0, \frac{1-\theta_\ell}{1-\theta_0}\right)$ and return $v_0 + y$.
4. Frank copula (discrete case): there is a complicated representation of $\psi_{v_0, \theta_0, \theta_\ell}$ and its Laplace-Stieltjes transform, hence we use a sampling scheme described step by step in [202].

4.4 Data generation for features detection

We use introduced copulas, to prepare artificial data in analysing cumulants based features selection and features extraction methods discussed in Chapter 6. Given tests on artificially generated data for which statistical features are known, discussed further features selection and features extraction methods can be applicable for the real life non-Gaussian distributed data analysis.

Since we are interested in information tied to non-Gaussian joint distribution of features, we transform multivariate Gaussian distributed data by introducing higher order cross-correlations into chosen subset of marginals using copula. Ideally the procedure should be performed in such a way that univariate statistics and standard cross-correlation measures are affected as little as possible. Given these, changed subset of

marginals should be hard to detect using simple methods. This section is the evaluation of [203] where such algorithm was introduced by means of Archimedean copulas and [204] for the t -Student copula case. To prepare data for further analysis, we start with multivariate data $\mathbf{X} \in \mathbb{R}^{t \times n}$ sampled from $\mathcal{N}(\mu, \Sigma)$, and we transform these data set $\mathbf{X} \rightarrow \mathbf{X}' \in \mathbb{R}^{t \times n}$, in such a way that univariate statistics, the covariance matrix and the rank cross-correlation between marginals are as little affected as possible.

Remark 4.4.1. Let us introduce the particular data transformation $\mathbf{X} \rightarrow \mathbf{X}'$, where $\mathbf{X}, \mathbf{X}' \in \mathbb{R}^{t \times n}$ and $\mathbf{X} \sim \mathcal{N}(\mu, \Sigma)$ by fulfilling.

1. All univariate marginal distributions are the same for \mathbf{X} and \mathbf{X}' .
2. The given subset of marginals $\mathbf{r} = (r_1, \dots, r_k) \subset (1 : n)$ of \mathbf{X}' is modelled by the non-Gaussian copula \mathbf{C}_{ng} .
3. Rank cross-correlations between marginals of \mathbf{X}' belonging to the \mathbf{r} subset are similar to rank cross-correlations of analogical marginals of \mathbf{X} ,

$$\rho(X_a, X_b) \approx \rho(X'_a, X'_b) \quad \forall a, b \in \mathbf{r}. \quad (4.69)$$

By point 1 the Pearson's cross-correlations would be similar as well.

4. For remaining marginals subset $(1 : n) \setminus \mathbf{r}$, we have the same Gaussian copula for both case, hence referring to point 1 we have

$$\text{cor}(X_a, X_b) = \text{cor}(X'_a, X'_b) \quad \forall a, b \in (1:n) \setminus \mathbf{r}. \quad (4.70)$$

5. Cross-correlation between subsets $(1 : n) \setminus \mathbf{r}$ and \mathbf{r} in \mathbf{X}' is similar to those in \mathbf{X}

$$\text{cor}(X_a, X_b) \approx \text{cor}(X'_a, X'_b) \quad \forall a \in \mathbf{r}, b \in (1:n) \setminus \mathbf{r}. \quad (4.71)$$

Finally, from points 3 and 4 we have

$$\text{cor}(\mathbf{X}) \approx \text{cor}(\mathbf{X}'). \quad (4.72)$$

From point 1 we have

$$\text{cov}(\mathbf{X}) \approx \text{cov}(\mathbf{X}'). \quad (4.73)$$

To fulfil point 1, we need to use the copula approach to separate off univariate marginal distributions. To fulfil point 2, the \mathbf{r} subset of marginals need to be modelled by the non-Gaussian copula. To fulfil point 3, we need to determine such copula parameter or parameters that would produce rank cross-correlations similar to those of the corresponding marginals of original data. To fulfil point 4, we simply leave unchanged marginals $(1 : n) \setminus \mathbf{r}$ while transforming $\mathbf{X} \rightarrow \mathbf{X}'$. Fulfilling point 5 is not simple. If we generate randomly marginals $X'_{r_1}, \dots, X'_{r_k}$ using the non-Gaussian copula fulfilling points 1 – 4 we would have little cross-correlation between the subset \mathbf{r} and remaining $(1 : n) \setminus \mathbf{r}$. We call such approach the naive one that fragments the covariance matrix of \mathbf{X}' into two blocks and gives the covariance matrix based algorithms advantage to find the subset \mathbf{r} . As discussed in [203], to maintain the correlation between changed and non-changed subsets on the other hand we have to transfer $X_{r_1}, \dots, X_{r_k} \rightarrow X'_{r_1}, \dots, X'_{r_k}$ in information preserving way.

4.4.1 t -Student copula case

Let us discuss the case, where we use the t -Student copula to modify the \mathbf{r} subset of marginals according to Remark 4.4.1 by means of the relatively simple approach discussed in [204]. This approach is based on the fact, that there is well known algorithm of transforming multivariate Gaussian distributed data into t -Student distributed ones [176]. Further we need only to transform back t -Student univariate marginals into the Gaussian ones.

To transform the \mathbf{r} subset of marginals of multivariate Gaussian distributed data, with zero means and variances one each, into t -Student multivariate distributed one we need to perform the following transformation for each realisation of multivariate data, see [176]. First, sample independently the scalar v_0 from $\chi^2(\nu)$ distribution, where the parameter ν is the scalar parameter of a t -Student copula. Next, for the \mathbf{r} subset of marginals multiple each element of the subset by $\sqrt{\frac{\nu}{v_0}}$. This transformation, as performed on the subset of marginals \mathbf{r} , affects slightly a cross-correlation between this subset and the reminding $(1:n) \setminus \mathbf{r}$ subset. This effect diminishes as ν rises, since the higher the ν value, the lower the spread of the distribution of $\sqrt{\frac{\nu}{v_0}}$. In next subsection we will discuss more complex cases where the subset is modelled by the Fréchet or the Archimedean copula.

4.4.2 Fréchet copula case

We can transform the \mathbf{r} subset of marginals of multivariate Gaussian distributed data with zero means and variances one into such modelled by a Fréchet copula according to Remark 4.4.1 where conditions 3 and 5 are fulfilled at least approximately. We can perform it by modifying Algorithm 5 to such that transform k independent vectors U_1, \dots, U_k all uniformly distributed on $[0, 1]$ to such that are still uniformly distributed on $[0, 1]$, but cross-correlated according to the Fréchet copula. This modification is presented in Algorithm 9, where last column of \mathbf{U} is distinguished especially for large α , see loop starting in line 8. Hence this column appear to be a candidate to carry an information about an overall correlation between the subset \mathbf{r} and the subset $(1:n) \setminus \mathbf{r}$. This observation will be used in data transformation.

Following [203] we observe, that it is easy to transform Gaussian distributed k -variate $\mathbf{X} \in \mathbb{R}^{t \times k}$ into $\mathbf{U} \in [0, 1]^{t \times k}$ where each columns $U_1, \dots, U_i, \dots, U_k$ are uniformly distributed on $[0, 1]$ independent on each other and carrying information about original \mathbf{X} in such a way that the higher i the more meaningful the information is. We make this transformation by performing the eigenvalue, eigenvector decomposition of the covariance matrix, sorting eigenvalues in increasing order, transforming data using corresponding eigenvectors and finally transforming univariate marginals to uniformly distributed on $[0, 1]$ see Algorithm 10. Despite the fact that columns of the output U_1, \dots, U_k are independent on each other they still carry the information, that in our case concerns the cross-correlation between the subset \mathbf{r} and the subset $(1:n) \setminus \mathbf{r}$.

Finally given the subset of multivariate Gaussian distributed marginals denoted by \mathbf{r} we can input them into Algorithm 10 to achieve independent uniformly distributed

Algorithm 9 Transform independent uniformly distributed on $[0, 1]$ data to such modelled by multivariate Fréchet copula parametrised by $0 \leq \alpha \leq 1$.

```

1: Input:  $\mathbf{U} \in [0, 1]^{t \times k}$  - uniformly distributed data with independent marginals,  $0 \leq \alpha \leq 1$  - parameter of Fréchet copula.
2: Output:  $\mathbf{U}' \in [0, 1]^{t \times k}$  - data modelled by a Fréchet copula.
3: function FRECHET( $\mathbf{U}$ ,  $\alpha$ )
4:    $\mathbf{U}' = \mathbf{U}$ 
5:   for  $j \leftarrow 1$  to  $t$  do
6:     sample  $v \sim \text{Uniform}([0, 1])$ 
7:     if  $v \leq \alpha$  then
8:       for  $i \leftarrow 1$  to  $k - 1$  do
9:          $u'_{j,i} = u'_{j,k}$ 
10:      end for
11:    end if
12:  end for
13:  return  $\mathbf{U}' \in [0, 1]^{t \times k}$ 
14: end function

```

marginals that are carrying interesting us information. Next we can input them into Algorithm 9 to achieve the subset of marginals modelled by the Fréchet copula and finally we can transform back their univariate distributions into the Gaussian one. Obviously the Fréchet copula gives the same cross-correlation between all marginals, hence the point 3 in Remark 4.4.1 will be fulfilled only approximately. This is due to the fact that the Spearman's cross-correlation inside the subset of marginals modelled by the Fréchet copula will be constant and equal to the copula's parameter α , see Eq. (4.37). Further, observe that due to the resampling scheme in Algorithm 9 some information about the cross-correlation between the subset \mathbf{r} and the subset $(1 : n) \setminus \mathbf{r}$ may be lost, especially for low α . In the case of the Archimedean copulas this two problems can be resolved at least to some extend, what is discussed in the next subsection.

4.4.3 Archimedean copula case

We can transform the \mathbf{r} subset of marginals of multivariate Gaussian distributed to such modelled by the Archimedean copula using an analogical approach as in the Fréchet copula case, see also [204]. The basic difference is that to obtain a sample of k -variate Archimedean copula, by means of the Algorithm 6, we need $k + 1$ independent samples from uniform distribution on $[0, 1]$ - one additional sample is required. In other words, following Algorithm 6, k samples will be used in line 6 while the additional can be transformed to v via the quantile function F_T^{-1} of the inverse Laplace-Stieltjes transform of the corresponding Archimedean copula generator in line 5. Following [203], recall that this generator ψ_θ is strictly decreasing by Definition 4.3.1. Hence the function

$$f_i(u, x_i) = \psi_\theta \left(\frac{-\log(x_i)}{F_T^{-1}(u)} \right), \quad (4.74)$$

Algorithm 10 Transform multivariate normally distributed data with 0 means and variance 1 into independent marginals uniformly distributed on $[0, 1]$

```

1: Input:  $\mathbf{X} \in \mathbb{R}^{t \times k}$  -  $t$  realization of  $k$ -variate  $\mathcal{N}(0, \mathbf{R})$ 
2: Output:  $\mathbf{U} \in [0, 1]^{t \times k}$  -  $t$  realisations of  $k$  independent  $\mathfrak{U}_i \sim \text{Uniform}(0, 1)$ .
3: function NORM2UNIF( $\mathbf{X}$ )
4:    $\mathbf{R}' = \text{COR}(\mathbf{X})$   $\triangleright \mathbf{R}' \approx \mathbf{R}$ 
5:    $\lambda, U = \text{EIGENVALS}(\mathbf{R}'), \text{EIGENVEC}(\mathbf{R}')$   $\triangleright \lambda_1 < \dots < \lambda_k$ 
6:   for  $j \leftarrow 1$  to  $t$  do
7:      $\mathbf{x}_j \leftarrow \mathbf{x}_j \cdot U$   $\triangleright \mathbf{x}_j = [x_{j,1}, \dots, x_{j,k}]$ 
8:     for  $i \leftarrow 1$  to  $k$  do
9:        $u_{j,i} = F_{\mathcal{N}(0, \lambda_i)}(x_{j,i})$   $\triangleright$  convert to uniform univ. marginals
10:    end for
11:  end for
12:  return  $\mathbf{U}$ 
13: end function

```

used in line 8 of Algorithm 6 will be strictly increasing in x_i for constant u . Moreover for constant $x_i \in (0, 1)$ it will be strictly increasing in u if $F_{\mathbf{T}}$ is continuous (the Gumbel and Clayton copula case), or non-decreasing if $F_{\mathbf{T}}$ is discrete (the AMH and Frank copula case). In data transformation scheme such u can be used to carry a general information into transformed data. Hence we will take it from the most informative (last) column of the output of Algorithm 10. On the other hand x_1, \dots, x_k can be used to carry individual informations. We will take them from other columns of the output of Algorithm 10. Due to the monotonicity of Eq. (4.74) the rank of u will affect the rank of the realisation of all marginals (general information), while the rank of x_i would affect the rank of the i^{th} marginal (individual information). Here the general information affects all realisations, not only part of them as in the Fréchet copula case. It is why the outcome given an Archimedean copula should be better than given the Fréchet copula. To produce $k + 1$ independent uniformly distributed data by means of the Algorithm 10, from $\mathbf{X} \in \mathbb{R}^{t \times k}$ we sample independently t samples from univariate $\mathcal{N}(0, 1)$ and add them as another marginal to \mathbf{X} before inputting data to Algorithm 10.

One can note that the same function as in Eq. (4.74) is used in the nested case - see line 14 of Algorithm 8. Hence the nested Archimedean copula generator can be used as well to transform data. Observe as well that sampling or data input to lines 5 and 6 in both Algorithm 6 and 8 is the same. Further in line 14 of Algorithm 8 we have the same monotone transformation as in line 8 of Algorithm 6. There are some differences as well. Data inputted to x_1, \dots, x_k in Algorithm 8 have to pass through line 10 of the algorithm, where we have a child copula generator $\psi_{v_0, \theta_0, \theta_i}$ parametrised by v_0 , see Eq. (4.64). Although this generator, in analogy to Eq. (4.74), gives the function $g_i(x_i) = \psi_{v_0, \theta_0, \theta_i} \left(\frac{-\log(x_i)}{v_i} \right)$ that is expected to be strictly increasing in x_i , we have there randomly generated v_i , see line 8 in Algorithm 8. Unfortunately, this random factor will worsen to some extent the cross-correlation between subsets \mathbf{r} and $(1 : n) \setminus \mathbf{r}$. On the

Algorithm 11 Determining subsets of marginals with higher cross-correlation

```

1: Input:  $\mathbf{C} \in \mathbb{R}^{k \times k}$  – "correlation" matrix
2: Output:  $\mathbf{r}_1, \dots, \mathbf{r}_s$  – such that  $\{\mathbf{r}_1, \dots, \mathbf{r}_s, \mathbf{r}''\}$  is the set partition of  $(1 : n)$ ,  $\rho_1, \dots, \rho_s$ 
   – correlations inside each subset,  $\rho_0$  – general correlation.
3: function GETCORS( $\mathbf{C}$ )
4:   for  $\mathbf{r}_1, \dots, \mathbf{r}_s \leftarrow$  set partitions  $(1 : k)$  do ▷ chose as  $\forall_l |\mathbf{r}_l| \geq 2$  and  $s > 1$ 
5:     for  $\iota \leftarrow 1 : s$  do
6:        $\rho_\iota = \text{mean}_{a,b}(c_{a,b})$  ▷ mean over  $a, b \in \mathbf{r}_\iota$  such that  $a \neq b$ 
7:     end for
8:      $\rho_0 = \text{mean}_{a_0, b_0}(c_{a_0, b_0})$  ▷  $a_0 \in \mathbf{r}_\iota, b_0 \in \mathbf{r}_{\iota'} : \iota \neq \iota' \wedge a_0 \neq b_0$ 
9:     test sufficient nesting  $\forall_l \rho_\iota > \rho_0$ 
10:     $(c_{\text{theor}})_{a,b} = \begin{cases} 1 & \text{if } a = b \\ \rho_\iota & \text{if } a, b \in \mathbf{r}_\iota \\ \rho_0 & \text{elsewhere.} \end{cases}$ 
11:    penalty =  $\|\mathbf{C} - \mathbf{C}_{\text{theor}}\|$  ▷ Frobenius norm
12:  end for
13:  return  $[\mathbf{r}_1, \dots, \mathbf{r}_s], [\rho_1, \dots, \rho_s], \rho_0$  such that penalty is minimal
14: end function

```

other hand, the advantage of the use of the nested Archimedean copula is the fact that we do not have a constant cross-correlation within \mathbf{r} subset but we can have subsets $\mathbf{r}_\iota \subset \mathbf{r}$ with higher cross-correlations ρ_ι in comparison with an overall cross-correlation ρ_0 within \mathbf{r} . Finally, we require $\rho_\iota > \rho_0$ to fulfil the sufficient nesting condition, see Eq. (4.65), since we assume that parents and children copulas are from the same Archimedean family.

The procedure of determination of $\{\mathbf{r}_1, \dots, \mathbf{r}_\iota, \dots, \mathbf{r}_s, \mathbf{r}''\}$, being a set partition of $(1 : n)$, is summarised in Algorithm 11. Here each \mathbf{r}_ι determines such subset of marginals, where a cross-correlation ρ_ι is higher than an overall cross-correlation ρ_0 . The input to the Algorithm 11 is the matrix of the Spearman's cross-correlations of size $n \times n$. The Algorithm 11 returns an overall cross correlation ρ_0 that is used to determine parameter θ_0 and cross-correlations ρ_ι corresponding to higher cross-correlations regions of children copulas parametrised by θ_ι and modelling marginals subsets denoted by \mathbf{r}_ι .

4.5 Implementation and experiments

4.5.1 Implementation

Discussed copula-based data generation algorithms were implemented in the Julia programming language [4, 5]. The Julia is a modern, open source and high-level programming language. As it is open source, the code can be accessed, reviewed and developed online by scientists, making Julia the proper tool for scientific computation. Apart from this, the main advantage of the language is its solid performance. Linear operations and random sampling operations implemented in this language require significantly less

processor time than similar operations implemented in other well-known programming languages, see [5]. Furthermore, Julia is specialised in multidimensional arrays (tensors) calculation [205], which is an advantage for cumulants tensors calculations.

Discussed here copula sampling algorithms are available on a GitHub repository [29] as the `DatagenCopulaBased.jl` module. Using implemented there functions one can sample Gaussian, t -Student, Fréchet and Archimedean (Gumbel, Frank, Clayton, AMH) copulas. In the case of the Fréchet and Archimedean copulas bivariate case is distinguished, since a wider range of parameters is available. The nested Archimedean copulas are supported as well. Instead of Archimedean copula parameter or parameters values, one can insert expected Spearman's or Kendall's cross-correlation coefficient or coefficients in a nested case.

Apart from these copulas, in module `DatagenCopulaBased.jl` the sampler for Marshall-Olkin copula is introduced. For definition and features of this copula see [206]. In the bivariate case, such copula is introduced by the stochastic process modelling exponentially distributed extinctions parametrised by three parameters λ_1 , λ_2 and $\lambda_{1,2}$. In the n variate case we have many parameters concerning single marginals, all combinations of two marginals, all combinations of three marginals etc., hence their number grows rapidly with n . The investigation of the relationship between higher order cumulants and parameters of the Marshall-Olkin copula seems to be interesting but complicated.

Module `DatagenCopulaBased.jl` provides functions that change a subset of marginals of multivariate Gaussian distributed data into those modelled by the t -Student, Fréchet or Archimedean copulas. This is important for future experiments. In the last case, both a nested and non-nested cases are supported. We have implemented as well the Marshall-Olkin copula case, but only for the subset of marginals of size 2, since for this copula, the number of free parameters rises rapidly with the size of the subset. Due to this observation, the Marshall-Olkin copula is rather not applicable for experiments discussed in the next part of this book. Finally, there are many methods of random correlation matrix generation for tests, see [203] for details. In experiments in the next subsection we use the following methods of the covariance matrix generation, all implemented in [29].

1. Constant $\mathbf{R}_{\text{const},\alpha} \in \mathbb{R}^{n \times n}$, we set simply each off-diagonal element to the constant value $0 < \alpha < 1$.

```
julia> cormatgen_constant(3, 0.5)
3×3 Array{Float64,2}:
 1.0  0.5  0.5
 0.5  1.0  0.5
 0.5  0.5  1.0
```

2. Constant noised $\mathbf{R}_{\text{const},\alpha,\epsilon} \in \mathbb{R}^{n \times n}$, to each element of the constant matrix we add the random value multiplied by the parameter ϵ . By default $\epsilon = \frac{1-\alpha}{2}$.

```
julia> Random.seed!(42);

julia> cormatgen_constant_noised(3, 0.5)
```

```

3×3 Array{Float64,2}:
 1.0      0.392423  0.515595
 0.392423  1.0      0.649938
 0.515595  0.649938  1.0

```

3. Random, we sample independently elements $\mathbf{A} \in \mathbb{R}^{n \times n}$ from the Uniform($[0, 1]$). Next for normalisation we use $\mathbf{D}_{\mathbf{A}} = \text{diag}(\mathbf{A}\mathbf{A}^\top)$ and return

$$\mathbb{R}^{n \times n} \ni \mathbf{R}_{\text{rand}} = \mathbf{D}_{\mathbf{A}}^{-\frac{1}{2}} \mathbf{A}\mathbf{A}^\top \mathbf{D}_{\mathbf{A}}^{-\frac{1}{2}}. \quad (4.75)$$

This method returns rather high positive correlations.

```

julia > Random.seed!(42);

julia > cormatgen_rand(3)
3×3 Array{Float64,2}:
 1.0      0.673166  0.538302
 0.673166  1.0      0.756497
 0.538302  0.756497  1.0

```

4. Toeplitz, given a parameter $0 < \rho < 1$, we return $\mathbf{R}_{\text{T},\rho} \in \mathbb{R}^{n \times n}$ with off diagonal elements $r_{i_1, i_2} = \rho^{|i_1 - i_2|}$

```

julia > cormatgen_toeplitz(3, 0.5)
3×3 Array{Float64,2}:
 1.0  0.5  0.25
 0.5  1.0  0.5
 0.25 0.5  1.0

```

4.5.2 Experiments

In this subsection we analyse the following experiment. We generate at random element-wise positive symmetric and positive definite covariance matrix \mathbf{R} with ones on a diagonal. The generation methods are discussed in [203]. In this book, we use following methods, *i.e.* random, constant noised, and Toeplitz. In noised examples we use the default noise parameter $\epsilon = \frac{1-\alpha}{2}$. In Figure 4.3 we present chosen elements of the \mathbf{R} matrix generated by different methods. Obviously $r_{i_1, i_2} = 1$ if $i_1 = i_2$ and $r_{i_1, i_2} < 1$ otherwise. For random method correlations are rather high, for Toeplitz method we have a specific correlation pattern, while for constant noised matrix the mean correlation is determined by the α parameter.

Given the correlation matrix, we sample $\mathbb{R}^{t \times n} \ni \mathbf{X} \sim \mathcal{N}(0, \mathbf{R})$ (with standard normal marginals) and perform the transformation $\mathbf{X} \rightarrow \mathbf{X}'$ *i.e.* we change randomly chosen subsets of marginals \mathbf{r} of given length $|\mathbf{r}| = k$ by means of t -Student, Fréchet and

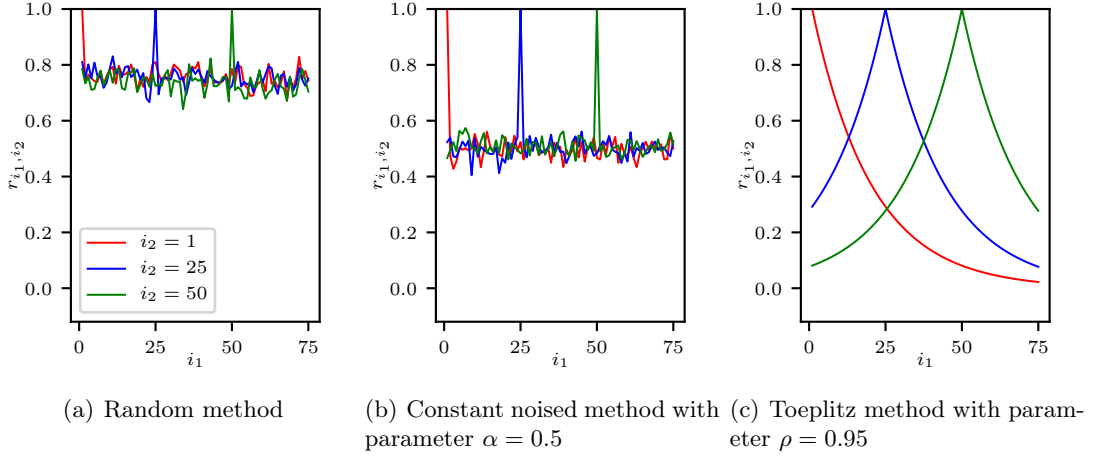


Figure 4.3: Values of chosen elements of the correlation matrix given different methods of generation, $n = 75$. We chose such methods and parametrisations to have different patterns of the cross-correlation between marginals.

Archimedean copulas. We use following parameters, number of marginals $n = 75$, number of changed marginals $k = 10$. For each experiment we compute the measure of the change of the covariance matrix due to the transformation of data.

$$\delta(\mathbf{X}, \mathbf{X}') = \frac{\|\text{cov}(\mathbf{X}) - \text{cov}(\mathbf{X}')\|}{\|\text{cov}(\mathbf{X})\|}, \quad (4.76)$$

where we use the Frobenius norm of the difference between covariance matrices of \mathbf{X} and \mathbf{X}' . The lower the $\delta(\mathbf{X}, \mathbf{X}')$ the better the transformation is.

In Figures 4.4(a)-(c) we present $\delta(\mathbf{X}, \mathbf{X}')$ values for the t -Student copula, different ν parameters and different correlation matrices. As proposed in Subsection 4.4.1 the higher the ν parameter value the lower $\delta(\mathbf{X}, \mathbf{X}')$. What is important the $\delta(\mathbf{X}, \mathbf{X}')$ is low in comparison with the naive approach regardless the correlation matrix.

In Figures 4.4(d)-(f) we present $\delta(\mathbf{X}, \mathbf{X}')$ values for the Fréchet copula and different correlation matrices. Results are much worse than in the t -Student copula. They are still on the comparable level in the random case, see Figure 4.4(d), where the correlation between marginals is high. Here the little information about the correlation between changed and unchanged subset of marginals is lost during the sampling procedure in Algorithm 9. For the Toeplitz case, see Figure 4.4(f), we have poor results almost as bad as the naive algorithm outcome.

In Figures 4.4(g)-(i) we present $\delta(\mathbf{X}, \mathbf{X}')$ values for Archimedean not-nested copulas. In the case of high correlations the outcome of the AMH copula is rather poor since this copula has a limit for the Persons coefficient equal to 0.5. Further the sampling of the Frank and AMH copula included discrete inverse Laplace-Stieltjes transform of the copula generator. Hence the function from Eq. (4.74) is not strictly increasing and may

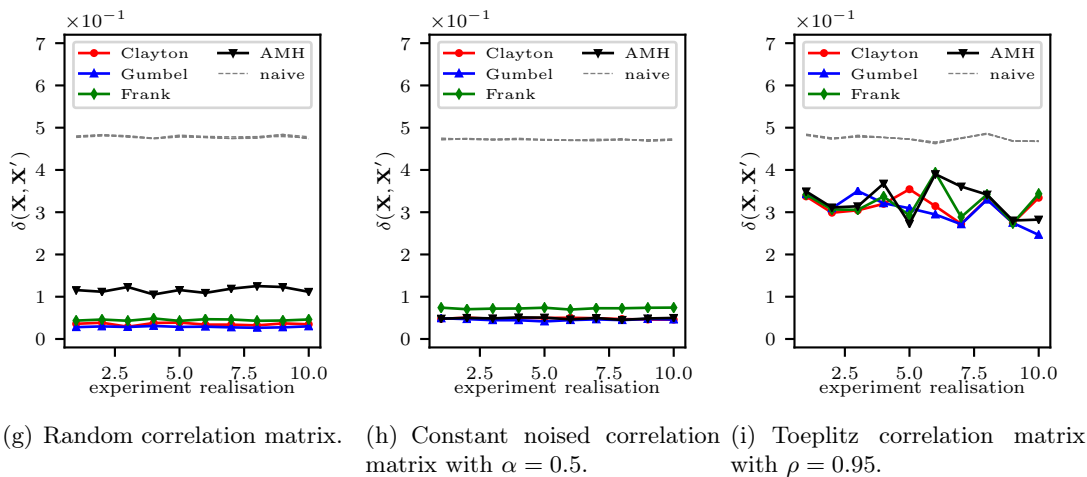
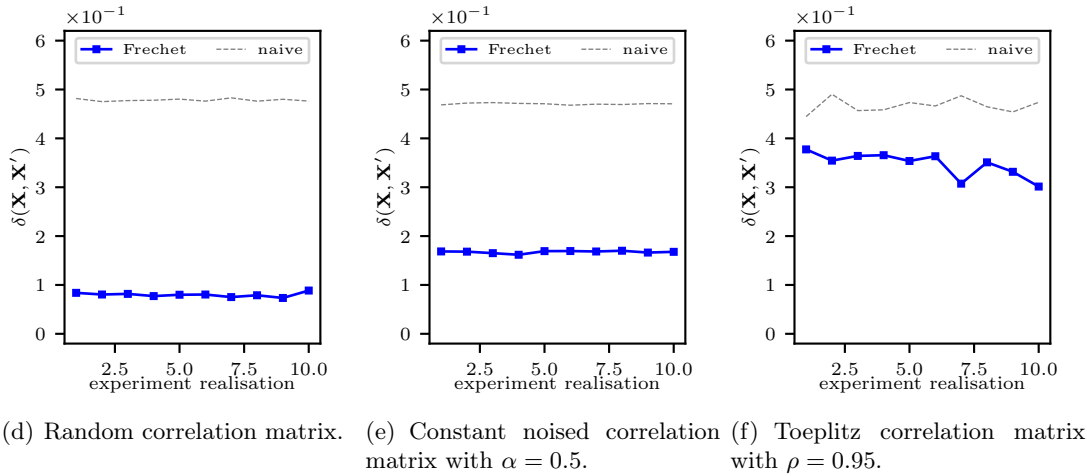
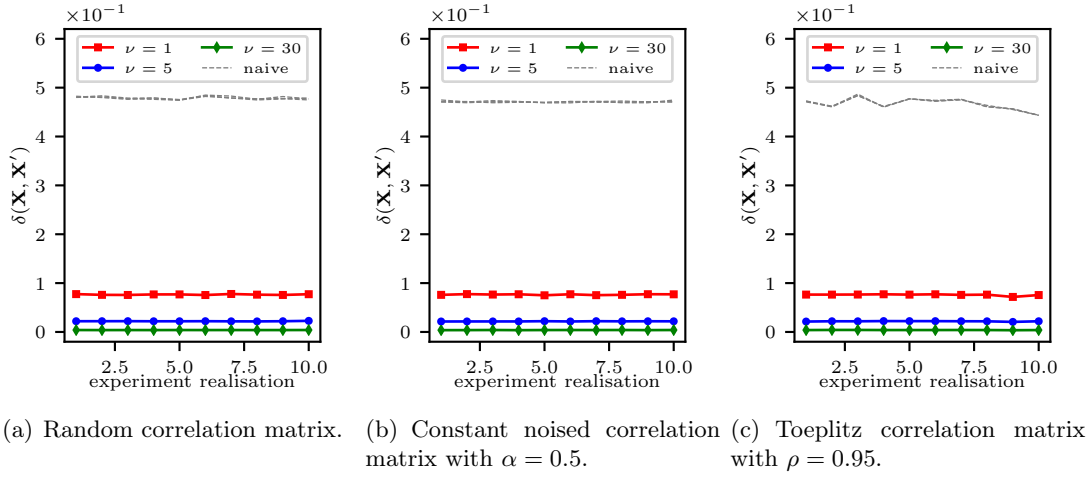
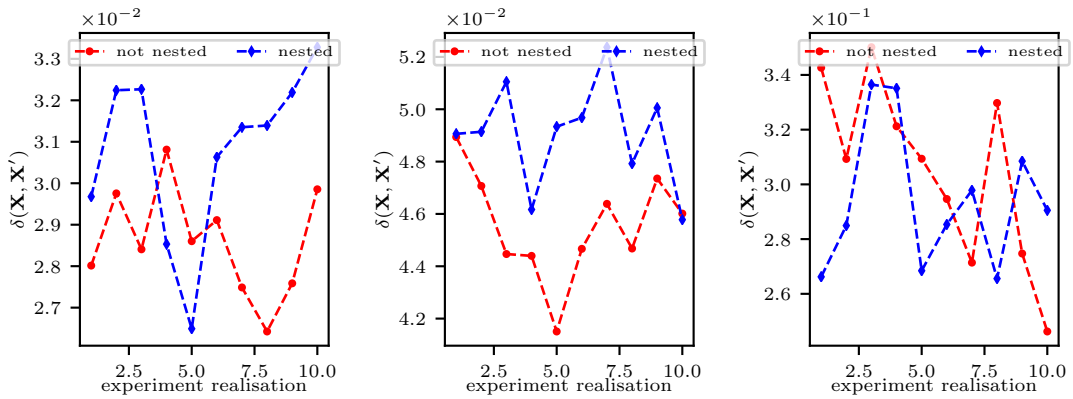
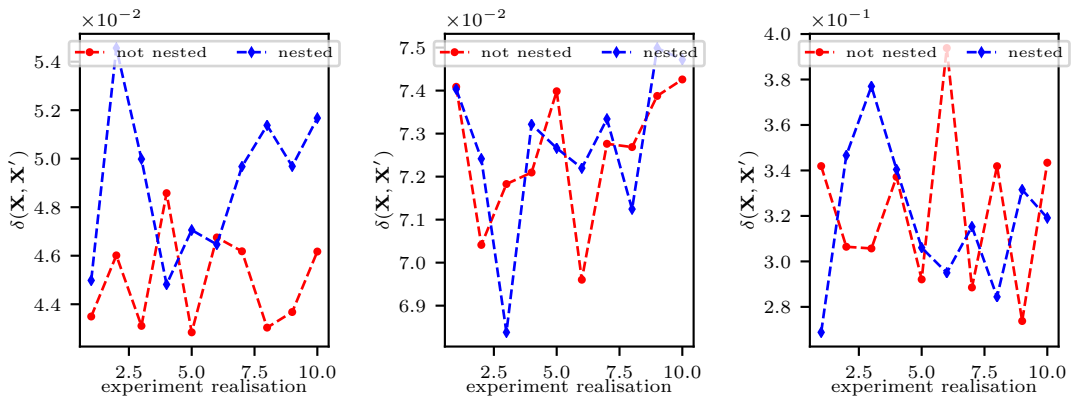


Figure 4.4: The measure of the difference of the correlation matrix due to data transformation with $k = 10$ and $n = 75$ for the t -Student copula (a), (b) and (c), the Fréchet copula (d), (e) and (f), and Archimedean not nested copulas (g), (h) and (i).



(a) Random correlation, Gumbel copula. (b) Constant noised correlation $\alpha = 0.5$, Gumbel copula. (c) Toeplitz correlation $\rho = 0.95$, Gumbel copula.



(d) Random correlation, Frank copula. (e) Constant noised correlation $\alpha = 0.5$, Frank copula. (f) Toeplitz correlation $\rho = 0.95$, Frank copula.

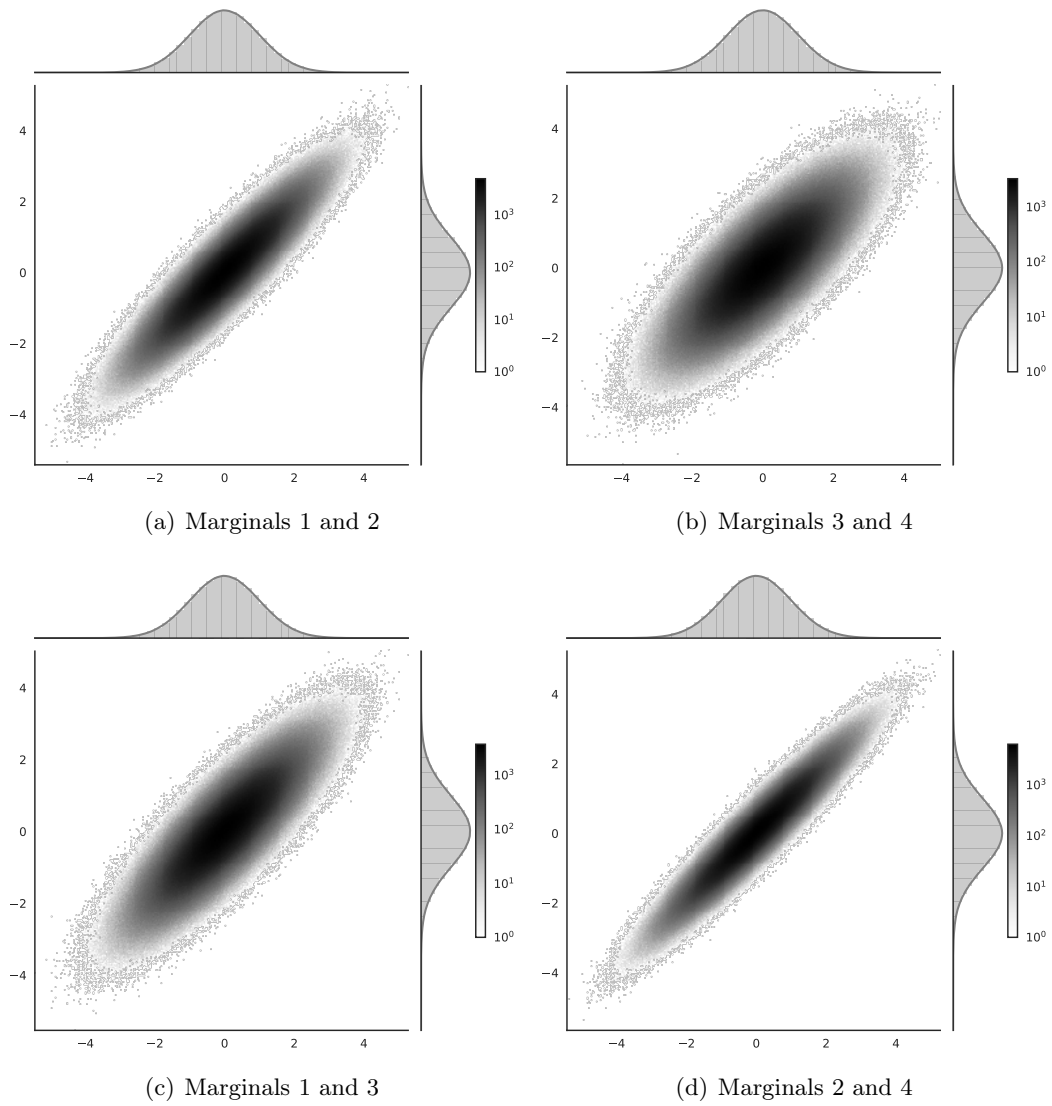
Figure 4.5: The measure of the difference of the correlation matrix due to data transformation. The comparison of nested and not-nested Archimedean copulas, mind different scales on y axis.

lose some information about the cross-correlation between subsets \mathbf{r} and $(1 : n) \setminus \mathbf{r}$. For the Toeplitz matrix, see Figure 4.4(i) we have poor results similar to those of the Fréchet copula. Hence for such correlation matrix the transformation discussed in Algorithm 10 is ineffective while concerning the preservation of the information between the changed and unchanged data subset.

In Figure 4.5 we compare nested and not-nested Archimedean copulas on the example of the Gumbel and the Frank ones. In general, outcomes are similar. This is due to two competing issues. On the one hand, nesting allows for non-uniform correlation matrix inside changed data subset. Such non-uniform correlation is determined by means of Algorithm 11. On the other hand, however, as discussed in Subsection 4.4.3 the transfer of information about the correlation between changed and unchanged subsets of marginals through Algorithm 8 (nested case) may be less efficient than through Algorithm 6 (not nested case). This is due to the fact that Algorithm 6 is simpler than Algorithm 8. Nevertheless, the nested case is more interesting since marginals can be grouped inside a changed subset.

Concluding the t -Student copula's algorithm is effective for all investigated here correlations matrices, especially for large ν . For other copulas we use Algorithm 10 that requires correlation matrices with rather moderate variations in elements values, as in Figure 4.3(a) and Figure 4.3(b) for the information preserving transformation. Given such correlations, Clayton and Gumbel copulas are comparable with the t -Student one and even may outperform the second for some values of its parameter ν . Apart from this, the AMH copula requires additionally low correlations (due to the parameter's limitations), while Frank and Fréchet copulas require rather high correlations. Hence given the random correlation matrix, as in Figure 4.3(a), all copulas apart from the AMH have their optimal results. It is why such a correlation matrix will be used for experiments in Section 6. Finally the performance of nested and not-nested Archimedean copulas are similar, but the first case is more interesting.

Finally for the graphical presentation on results in Figure 4.6 we present univariate and bivariate histograms of $\mathbf{X} \sim \mathcal{N}(0, \mathbf{R})$ with high cross-correlations. In Figures 4.7 we present similarly univariate and bivariate histograms of transformed data \mathbf{X}' in such a way, that marginals number 1 and 2 have been changed employing the Clayton copula, while marginals number 3 and 4 remind unchanged. Observe the intermediate case of marginals 1 versus 3 and 2 versus 4. Given such insight into multivariate non-Gaussian distributions we can move in next chapter to higher order multivariate statistics and higher order multivariate cumulants that can be used to measure higher-order correlations introduced by non-Gaussian distributions as in Figures 4.7(a) 4.7(c) and 4.7(d).

Figure 4.6: Univariate and bivariate histograms of the original data \mathbf{X}

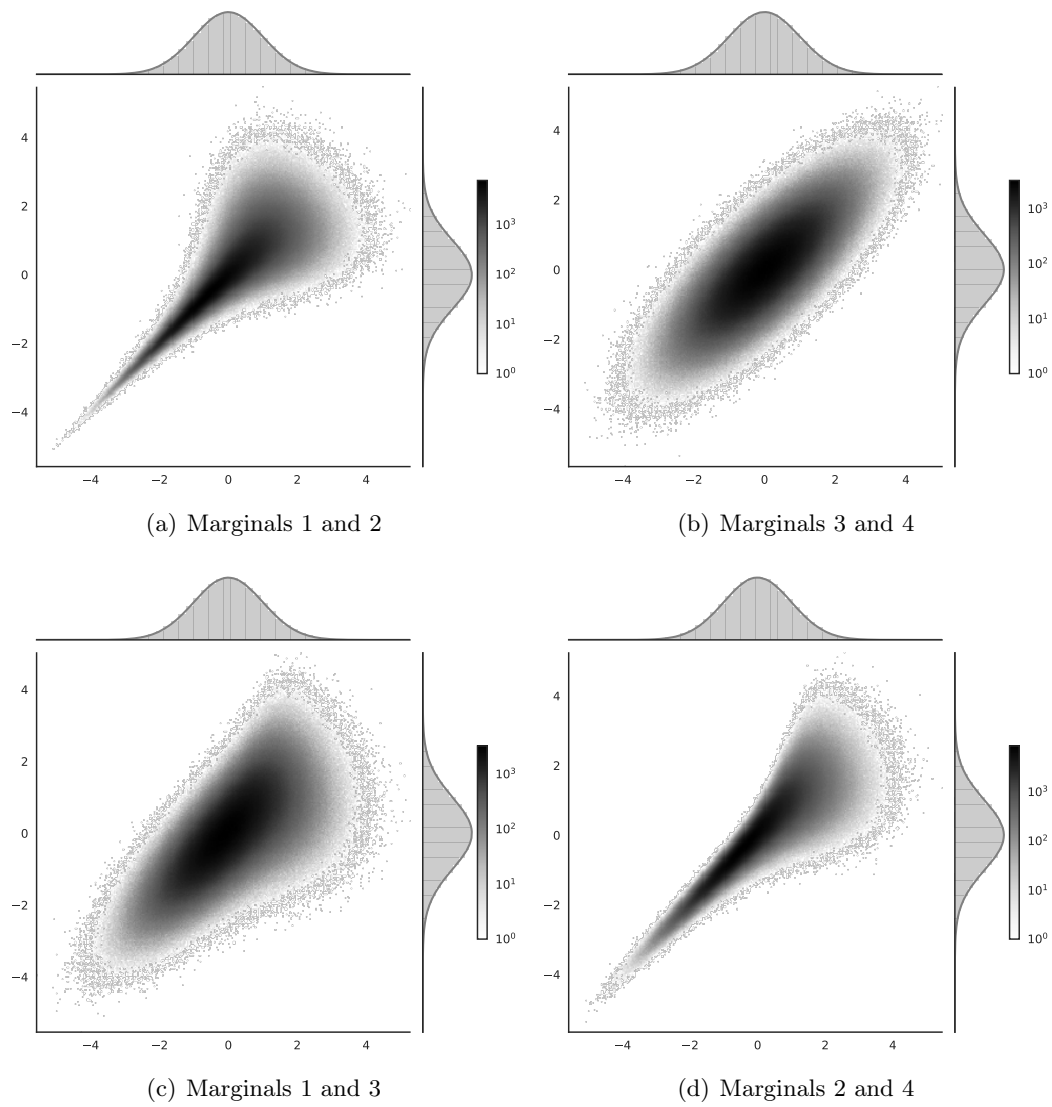


Figure 4.7: Univariate and bivariate histograms of transformed data \mathbf{X}' by means of the Clayton copula.

Chapter 5

Higher order statistics of multivariate data

In this chapter we discuss higher order statistics of multivariate data, *i.e.* statistics of order d , where $d > 2$. Classical example of univariate higher order statistics are asymmetry ($d = 3$) and kurtosis ($d = 4$). These are normalised univariate higher order cumulants. In this chapter, we will concentrate on multivariate higher order cumulants, applicable to analyse non-Gaussian distributed multivariate data. For their practical application in multivariate non-Gaussian data analysis refer to signals analysis, for example in signal filtering [207, 208], finding the direction of received signals [17, 18, 19, 20] and signal auto-correlation analysis [95]. Furthermore, those cumulants are used in hyper-spectral image analysis [47], financial data analysis [209, 210] and neuroimage analysis [211, 212]. Additionally univariate higher order cumulants are used in quantum noise investigation [213], and computer network traffic analysis [48, 49]. We focus on the multivariate data case, which can be easily simplified to the univariate case.

Let us start first with some technical definitions including tensors [75] and their super-symmetry [214], since we use super-symmetric tensors to store higher order cumulants. In our approach, the d -dimensional tensor is simply the d -dimensional array.

Definition 5.0.1. Given the multi-index $\mathbf{i} = (i_1, \dots, i_d)$, where $i_k \in (1 : I_k)$, see Table 1 for notation explanation, and $|\mathbf{i}| = d$, the d mode tensor is the following d -dimensional array of data [75]

$$\mathcal{T} = \{t_{\mathbf{i}}\}_{\mathbf{i}=1}^{I_1, \dots, I_d} \in \mathbb{R}^{I_1 \times \dots \times I_d} \quad (5.1)$$

where the k^{th} element of the multi-index - i_k corresponds to the mode k .

The 3 mode tensor is simply the 3 dimensional data box, see [75] and Figure 1.1 within.

Definition 5.0.2. Let π be a permutation of the multi-index \mathbf{i} , for $d = 3$ one of the permutations is

$$\pi(i_1, i_2, i_3) = (i_2, i_1, i_3). \quad (5.2)$$

Let Π_d be a set of all permutations of the set $(1, 2, \dots, d)$. Tensor $\mathcal{T} \in \mathbb{R}^{\underbrace{n \times \dots \times n}_d}$ is super-symmetric [214] iff

$$\forall \pi \in \Pi_d \quad \forall \mathbf{i} \quad t_{\mathbf{i}} = t_{\pi(\mathbf{i})}. \quad (5.3)$$

To be consistent with [34] we use the following notation for the super-symmetric tensor

$$\mathcal{T} \in \mathbb{R}^{[n, d]}. \quad (5.4)$$

Definition 5.0.3. Following [2, 3], let $\mathbf{f}(\mathbf{v}) : \mathbb{R}^n \rightarrow \mathbb{R}$ be the continuous n -variate Probability Density Function (PDF), its characteristic function is given by

$$\varphi : \mathbb{R}^n \rightarrow \mathbb{C} \quad \varphi(\mathbf{v}) = \int_{\mathbb{R}^n} \exp(\mathbf{i}\mathbf{v}^\top \mathbf{x}) \mathbf{f}(\mathbf{x}) d\mathbf{x}, \quad (5.5)$$

where \mathbf{i} is an imaginary unit. The d^{th} cumulant element of \mathbf{f} , indexed by i_1, \dots, i_d is given by

$$c_{i_1, \dots, i_d} = (-\mathbf{i})^d \frac{\partial^d}{\partial v_{i_1}, \dots, \partial v_{i_d}} \log(\varphi(\mathbf{v})) \Big|_{\mathbf{v}=0}. \quad (5.6)$$

The element c_{i_1, \dots, i_d} may be considered as a part of the d -mode super-symmetric tensor since differentiation in Eq. (5.6) is commutative. Hereafter, for the d^{th} order cumulant's tensor we use the following notation

$$\mathcal{C}_d \in \mathbb{R}^{[n, d]}. \quad (5.7)$$

Remark, that sometimes in literature one uses the cumulant generation function

$$\kappa : \mathbb{R}^n \rightarrow \mathbb{C} \quad \kappa(\mathbf{v}) = \log(\varphi(\mathbf{v})). \quad (5.8)$$

Remark 5.0.1. It is easy to show from Eq. (5.5), that if we use $\mathbf{f}'(\mathbf{x}) = \mathbf{f}(\mathbf{x} - \mathbf{a})$ where $\mathbf{a} \in \mathbb{R}^n$ is a vector of constants, corresponding characteristic function φ' is

$$\varphi'(\mathbf{v}) = \varphi(\mathbf{v}) \exp(-\mathbf{i}\mathbf{v}^\top \mathbf{a}) \quad (5.9)$$

yielding

$$\kappa'(\mathbf{v}) = \kappa(\mathbf{v}) - \mathbf{i}\mathbf{v}^\top \mathbf{a}. \quad (5.10)$$

What is important the term $-\mathbf{i}\mathbf{v}^\top \mathbf{a}$ would vanish after double differentiation over \mathbf{v} in Eq. (5.6). Hence cumulants tensors of order $d \geq 2$ of \mathbf{f} and \mathbf{f}' would be the same. We can note it formally by $c_{\mathbf{i}} = c'_{\mathbf{i}}$ if $|\mathbf{i}| \geq 2$. Hereafter as \mathbf{f}' we will use the zero mean frequency distribution: $\mathbf{f}'(\mathbf{x}) = \mathbf{f}(\mathbf{x} - \mu)$, where $\mu = [\mu_1, \dots, \mu_n]$ is a mean vector of \mathbf{f} . Such approach will make the cumulant computation simpler.

Definition 5.0.4. Analogically to Definition 5.0.3 the d^{th} moment element is

$$m_{i_1, \dots, i_d} = (-\mathbf{i})^d \frac{\partial^d}{\partial v_{i_1}, \dots, \partial v_{i_d}} \varphi(\mathbf{v}) \Big|_{\mathbf{v}=0}, \quad (5.11)$$

for $\varphi(\mathbf{v})$ see Eq. (5.5). As in the cumulant's case, the above is an element of the super-symmetric moment tensor

$$\mathcal{M}_d \in \mathbb{R}^{[n,d]}. \quad (5.12)$$

By performing differentiation of Eq. 5.11 we have

$$m_{i_1, \dots, i_d} = \int_{\mathbb{R}^n} x_{i_1} \cdots x_{i_d} \mathbf{f}(\mathbf{x}) d\mathbf{x}. \quad (5.13)$$

Having introduced cumulant's and moment's tensors from $\mathbf{f}(\mathbf{x})$ that is the PDF function, observe from Eq. (4.5) that $\mathbf{f}(\mathbf{x})$ can be split onto the copula density \mathbf{c} and univariate marginal PDFs f_i . The later correspond with univariate marginal CDFs F_i . From Eq. (5.13) we have

$$m_{i_1, \dots, i_d} = \int_{\mathbb{R}^n} x_{i_1} \cdots x_{i_d} \cdot \mathbf{c}(F_1(x_1), \dots, F_n(x_n)) \prod_{i=1}^n f_i(x_i) dx_i. \quad (5.14)$$

Concluding, we have an impact on the moment's tensors elements both from a copula and from marginal distributions, what is rather complicated and will be discussed further in this book.

Remark 5.0.2. We can shown that the super-diagonal element of \mathcal{M}_d , *i.e.* such indexed by $i_1 = i_2 = \dots = i_d = i$, corresponds to the d^{th} moment of the i^{th} marginal distribution and is copula independent. For the proof, let us start with

$$m_{i, \dots, i} = \int_{\mathbb{R}^n} (x_i)^d \mathbf{c}(F_1(x_1), \dots, F_i(x_i), \dots, F_n(x_n)) \prod_{i'=1}^n f_{i'}(x_{i'}) dx_{i'}. \quad (5.15)$$

Using $u_{i'} = F_{i'}(x_{i'})$ and $du_{i'} = f_{i'}(x_{i'}) dx_{i'}$, where $u_{i'} \in [0, 1]$, we can perform following integrations

$$\begin{aligned} & \int_{[0,1]^{n-1}} \mathbf{c}(u_1, \dots, u_{i-1}, u_i, u_{i+1}, \dots, u_n) du_1 \cdots du_{i-1} du_{i+1} \cdots du_n \\ &= \frac{\partial \mathbf{C}(1, \dots, 1, u_i, 1, \dots, 1)}{\partial u_i} = \frac{\partial u_i}{\partial u_i} = 1. \end{aligned} \quad (5.16)$$

We use here the relation between a copula density and a copula in Eq. (4.3), and the point 2 of Definition 4.0.1. Next, using $x_i = F_i^{-1}(u_i)$ we have

$$m_{i, \dots, i} = \int_0^1 (F_i^{-1}(u_i))^d du_i, \quad (5.17)$$

and converting back to original marginal variable:

$$m_{i, \dots, i} = \int_{\mathbb{R}} (x_i)^d f_i(x_i) dx_i. \quad (5.18)$$

5.1 Cumulants of multivariate Gaussian distribution

In this section we conclude the meaning of higher order cumulants tensors in non-Gaussian data analysis, by showing that they are zero if data are multivariate Gaussian distributed. For this purpose, consider the following quadratic cumulant generation function

$$\kappa(\mathbf{v}) = i\mathbf{v}^\top \boldsymbol{\mu} - \frac{1}{2} \mathbf{v}^\top \boldsymbol{\Sigma} \mathbf{v}. \quad (5.19)$$

where $\boldsymbol{\mu} = [\mu_1, \dots, \mu_n]$. The first cumulant's element would be

$$c_i = -i \frac{\partial}{\partial v_i} \kappa(\mathbf{v}) \Big|_{\mathbf{v}=0} = \mu_i, \quad (5.20)$$

and the second cumulant's element

$$c_{i_1, i_2} = \frac{\partial^2}{\partial v_{i_1} \partial v_{i_2}} \kappa(\mathbf{v}) \Big|_{\mathbf{v}=0} = s_{i_1, i_2}, \quad (5.21)$$

where s_{i_1, i_2} is an element of $\boldsymbol{\Sigma}$. Obviously as κ is quadratic in \mathbf{v} , for $d > 2$ we have

$$\forall_{d>2} c_{i_1, \dots, i_d} = \frac{\partial^d}{\partial v_{i_1} \dots \partial v_{i_d}} \kappa(\mathbf{v}) \Big|_{\mathbf{v}=0} = 0. \quad (5.22)$$

From $\kappa(\mathbf{v})$ given in Eq. (5.19), we can reconstruct the following characteristic function

$$\varphi(\mathbf{v}) = \exp \left(i\mathbf{v}^\top \boldsymbol{\mu} - \frac{1}{2} \mathbf{v}^\top \boldsymbol{\Sigma} \mathbf{v} \right). \quad (5.23)$$

This is a characteristic function of multivariate Gaussian distribution, see Eq. (3.5) and [215].

Oppositely, if the multivariate frequency distribution is non-Gaussian its characteristic function will have different form and higher than quadratic terms may appear yielding non-zero higher order cumulants. It is why the strong suggestion appears, that we can use higher order cumulants to extract information about the frequency distribution that is non-Gaussian. Given these, higher order cumulants have specific meaning as they carries information about the divergence from Gaussian model. And finally, higher order cumulants have an advantage over higher order moments, that are non-necessary non-zero for multivariate Gaussian distributed data.

5.2 Tensors and tensor networks - quantum mechanics inspired tools

In this section we use the tensor and graphical notation to discuss relation between higher order cumulants and higher order moments. As such the approach is inspired on the quantum mechanics.

5.2.1 Moments tensors

Suppose we have the random vector $\mathfrak{X}^{(n)}$, and its t realisations are stored in the matrix form $\mathbf{X} \in \mathbb{R}^{t \times n}$, here the j^{th} realisation is $\mathbf{x}_j = [x_{j,1}, \dots, x_{j,n}]$. Suppose now, each such realisation is equal probable, what is a fair assumption for large t - such that extreme events are sampled properly. Given the probability of each realisation as equal to $\frac{1}{t}$ moment's tensor's elements can be estimated as way

$$m_{\mathbf{i}}(\mathbf{X}) = \mathbb{E}(X_{i_1} \cdot \dots \cdot X_{i_d}) = \frac{1}{t} \sum_{j=1}^t \prod_{k=1}^d x_{j,i_k} \quad (5.24)$$

Here $X_i = [x_{1,i}, \dots, x_{t,i}]^\top$ is a vector of all realisations of the i^{th} marginal and \mathbb{E} is the expectation value operator. We can present Eq. (5.24) using tensor operation and corresponding graphical notation.

Definition 5.2.1. Suppose we have d -mode tensor $\mathcal{T} \in \mathbb{R}^{t \times \dots \times t}$ and matrix $\mathbf{A} \in \mathbb{R}^{n \times t}$. We defined the matrix times tensor multiple in all modes [75],

$$\mathbb{R}^{n \times \dots \times n} \ni \mathcal{T}' = \mathbf{A} \times_{1, \dots, d} \mathcal{T}, \quad (5.25)$$

by the following multiple contraction

$$t'_{i_1, \dots, i_d} = \sum_{j_1, \dots, j_d} a_{i_1, j_1} \cdot \dots \cdot a_{i_d, j_d} \cdot t_{j_1, \dots, j_d}. \quad (5.26)$$

Obviously if \mathcal{T} is super-symmetric, tensor \mathcal{T}' would be super-symmetric as well.

Definition 5.2.2. Let us define the identity tensor $\mathbb{1}_{(d)} \in \mathbb{R}^{[t, d]}$ as the n 'th mode tensor with 1 on the super-diagonal [75] and zeros elsewhere

$$(\mathbb{1}_{(d)})_{\mathbf{i}} = \begin{cases} 1 & \text{if } i_1 = i_2 = \dots = i_d \\ 0 & \text{otherwise} \end{cases}. \quad (5.27)$$

For an exemplary $\mathbb{1}_{(3)}$ see Figure 5.1.

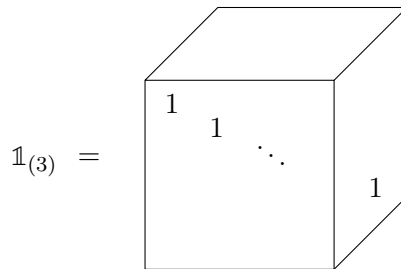
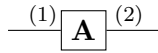


Figure 5.1: The $\mathbb{1}_{(3)}$ example.

Remark 5.2.1. By taking $\mathbb{R}^{n \times t} \ni \mathbf{A} = \mathbf{X}^\top$ and $\mathbb{1}_{(d)} \in \mathbb{R}^{[t,d]}$, Eq. (5.24) can be rewritten into the following form using tensor notation

$$\mathcal{M}_d(\mathbf{X}) = \frac{1}{t} \mathbf{X}^\top \times_{1,\dots,d} \mathbb{1}_{(d)}. \tag{5.28}$$

Definition 5.2.3. The matrix $\mathbf{A} \in \mathbb{R}^{n_a \times t}$ is the 2 mode tensor. As such, it can be presented using the graphic notation



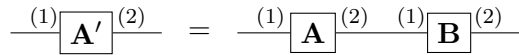
where (1) and (2) enumerates its modes [75]. Furthermore, let $\mathbf{B} \in \mathbb{R}^{t \times n_b}$ be another matrix. Their multiplication

$$\mathbb{R}^{n_a \times n_b} \ni \mathbf{A}' = \mathbf{A}\mathbf{B} \tag{5.29}$$

is the contraction

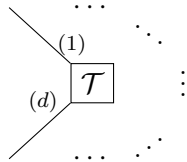
$$a'_{i,j} = \sum_k a_{i,k} b_{k,j} \tag{5.30}$$

that can be represented by means of the graphic notation

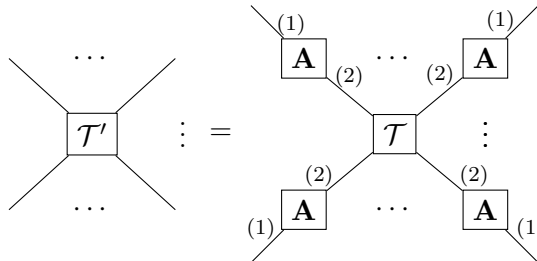


The connection of node (2) in \mathbf{A} with node (1) in \mathbf{B} means the contraction of mode (2) of \mathbf{A} with mode (1) of \mathbf{B} , as in Eq. (5.30).

Definition 5.2.4. The d mode tensor \mathcal{T} can be represented graphically as



In this representation, particular node of the graph corresponds to particular mode of the tensor. If a tensor (or a matrix) is super-symmetric we drop nodes numeration because it does not matter. Suppose we have the super-symmetric tensor $\mathcal{T} \in \mathbb{R}^{[n,d]}$, its multiplication with a matrix in all modes $\mathcal{T}' = \mathcal{T} \times_{1,\dots,d} \mathbf{A}$ can be represented graphically:



Note that only the numeration of modes for the matrix matters.

Having introduced the graphic notation, referring to Eq. (5.28) the d^{th} moment tensor can be represented in the graphical form:

operation $\frac{1}{t} \cdot \mathbb{1}_{(d)}$ is simply a scalar element-wise multiple of $\mathbb{1}_{(d)}$ by $\frac{1}{t}$.

Remark 5.2.2. If we use zero mean frequency distribution *i.e.* such that $\mathbf{f}'(\mathbf{x}) = \mathbf{f}(\mathbf{x} - \mu)$, we can calculate central moments m'_i , see Eq.s (5.5) and (5.11). Obviously, the first central moment would be zero. For large t , we can use following central moments estimators

$$m'_i(\mathbf{X}) = m_i(\tilde{\mathbf{X}}) = \mathbb{E}(\tilde{X}_{i_1} \cdots \tilde{X}_{i_d}) = \frac{1}{t} \sum_{j=1}^t \prod_{k=1}^d (x_{j,i_k} - \mu_{i_k}), \quad (5.31)$$

where \tilde{X}_i is a vector with zero mean, and $\tilde{\mathbf{X}}$ column (marginal) wisely centred data. Elements of $\tilde{\mathbf{X}}$ given original data \mathbf{X} , are:

$$\tilde{x}_{j,i} = x_{j,i} - \mu_i, \quad (5.32)$$

where:

$$\mu_i = m_i(\mathbf{X}) = \mathbb{E}(X_i) = \frac{1}{t} \sum_{j=1}^t x_{j,i}. \quad (5.33)$$

What is important, following [34], we use central moments to compute cumulants since such approach allows to simplify formulas. For graphic representation of central moment we can simply to replace \mathbf{X} by $\tilde{\mathbf{X}}$.

5.2.2 Cumulants tensors

Having discussed higher order moments tensors estimators we can move to cumulant's calculation formulas that uses corresponding moments. Formulas for calculation cumulants of order 1 – 3 are relatively simple, hence to give some examples we can derive them step by step from Definition 5.0.3, see also Appendix B in [34].

Example 5.2.1. To compute 1^{st} cumulant let us single differentiate Eq. (5.6)

$$c_i = -i \frac{\partial}{\partial v_i} \log(\varphi(\mathbf{v})) \Big|_{\mathbf{v}=0} = -i \frac{\frac{\partial}{\partial v_i} \varphi(\mathbf{v})}{\varphi(\mathbf{v})} \Big|_{\mathbf{v}=0} = -i \frac{\partial}{\partial v_i} \varphi(\mathbf{v}) \Big|_{\mathbf{v}=0} = m_i, \quad (5.34)$$

we used Definition 5.0.4 and the fact that according to Eq. (5.5) we have

$$\varphi(\mathbf{v} = 0) = \int_{\mathbb{R}^n} \exp(0) \mathbf{f}(\mathbf{x}) d\mathbf{x} = \int_{\mathbb{R}^n} \mathbf{f}(\mathbf{x}) d\mathbf{x} = 1, \quad (5.35)$$

due to the normalisation of the PDF function.

Example 5.2.2. The second cumulant is

$$\begin{aligned} c_{i_1, i_2} &= - \frac{\partial^2}{\partial v_{i_1} \partial v_{i_2}} \log(\varphi(\mathbf{v})) \Big|_{\mathbf{v}=0} = - \left(\frac{\varphi(\mathbf{v}) \frac{\partial^2}{\partial v_{i_1} \partial v_{i_2}} \varphi(\mathbf{v}) - \left(\frac{\partial}{\partial v_{i_1}} \varphi(\mathbf{v}) \right) \left(\frac{\partial}{\partial v_{i_2}} \varphi(\mathbf{v}) \right)}{(\varphi(\mathbf{v}))^2} \right) \Big|_{\mathbf{v}=0} \\ &= - \frac{\frac{\partial^2}{\partial v_{i_1} \partial v_{i_2}} \varphi(\mathbf{v})}{\varphi(\mathbf{v})} \Big|_{\mathbf{v}=0} + \frac{\left(\frac{\partial}{\partial v_{i_1}} \varphi(\mathbf{v}) \right) \left(\frac{\partial}{\partial v_{i_2}} \varphi(\mathbf{v}) \right)}{(\varphi(\mathbf{v}))^2} \Big|_{\mathbf{v}=0} = m_{i_1, i_2} - m_{i_1} m_{i_2}. \end{aligned} \quad (5.36)$$

Example 5.2.3. The third cumulant requires another differentiation of Eq. (5.36). Hereafter, for clarity we use φ for $\varphi(\mathbf{v})$ and $\frac{\partial \varphi}{\partial v_i}$ for $\left(\frac{\partial}{\partial v_i} \varphi(\mathbf{v}) \right)$ etc. We have

$$\begin{aligned} c_{i_1, i_2, i_3} &= i \frac{\partial^3}{\partial v_{i_1} \partial v_{i_2} \partial v_{i_3}} \log(\varphi) \Big|_{\mathbf{v}=0} \\ &= i \left(\frac{\varphi \frac{\partial^3 \varphi}{\partial v_{i_1} \partial v_{i_2} \partial v_{i_3}} - \frac{\partial^2 \varphi}{\partial v_{i_1} \partial v_{i_2}} \frac{\partial \varphi}{\partial v_{i_3}}}{\varphi^2} \right. \\ &\quad \left. - \frac{\varphi^2 \left(\frac{\partial^2 \varphi}{\partial v_{i_1} \partial v_{i_3}} \frac{\partial \varphi}{\partial v_{i_2}} + \frac{\partial \varphi}{\partial v_{i_1}} \frac{\partial^2 \varphi}{\partial v_{i_2} \partial v_{i_3}} \right) - 2 \varphi \frac{\partial \varphi}{\partial v_{i_1}} \frac{\partial \varphi}{\partial v_{i_2}} \frac{\partial \varphi}{\partial v_{i_3}}}{\varphi^4} \right) \Big|_{\mathbf{v}=0} \\ &= i \frac{\frac{\partial^3 \varphi}{\partial v_{i_1} \partial v_{i_2} \partial v_{i_3}}}{\varphi} \Big|_{\mathbf{v}=0} - i \frac{\frac{\partial^2 \varphi}{\partial v_{i_1} \partial v_{i_2}} \frac{\partial \varphi}{\partial v_{i_3}} + \frac{\partial^2 \varphi}{\partial v_{i_1} \partial v_{i_3}} \frac{\partial \varphi}{\partial v_{i_2}} + \frac{\partial \varphi}{\partial v_{i_1}} \frac{\partial^2 \varphi}{\partial v_{i_2} \partial v_{i_3}}}{\varphi^2} \Big|_{\mathbf{v}=0} \\ &\quad + 2i \frac{\varphi \frac{\partial \varphi}{\partial v_{i_1}} \frac{\partial \varphi}{\partial v_{i_2}} \frac{\partial \varphi}{\partial v_{i_3}}}{\varphi^4} \Big|_{\mathbf{v}=0} \end{aligned} \quad (5.37)$$

what leads to

$$c_{i_1, i_2, i_3} = m_{i_1, i_2, i_3} - m_{i_1, i_2} m_{i_3} - m_{i_1, i_3} m_{i_2} - m_{i_2, i_3} m_{i_1} + 2m_{i_1} m_{i_2} m_{i_3}. \quad (5.38)$$

Referring to Eqs. (5.34) and (5.36) we can simplify this as

$$m_{i_1, i_2, i_3} = c_{i_1, i_2, i_3} + c_{i_1, i_2} c_{i_3} + c_{i_1, i_3} c_{i_2} + c_{i_2, i_3} c_{i_1} + c_{i_1} c_{i_2} c_{i_3}. \quad (5.39)$$

To simplify this relation further let us introduce c'_i , the element of the cumulant's tensor of the zero mean frequency distribution $\mathbf{f}'(\mathbf{x}) = \mathbf{f}(\mathbf{x} - \mu)$. By Remark 5.0.1 we have

$$c'_i = \begin{cases} 0 & \text{if } |\mathbf{i}| = 1 \\ c_i & \text{if } |\mathbf{i}| \geq 2 \end{cases}. \quad (5.40)$$

Following [34] such approach simplifies cumulant's calculation formulas.

Remark 5.2.3. In the case of the 2nd cumulant, we can simplify Eq. (5.36)

$$c_{i_1, i_2} = c'_{i_1, i_2} = m'_{i_1, i_2} - m'_{i_1} m'_{i_2} = m'_{i_1, i_2} \quad (5.41)$$

in a graphic tensor notation, using Definition 5.2.3 we have

$$\text{---} \boxed{C_2} \text{---} = \text{---} \begin{matrix} (2) \\ \boxed{\tilde{\mathbf{X}}} \\ (1) \end{matrix} \text{---} \boxed{\frac{1}{t} \cdot \mathbb{1}} \text{---} \begin{matrix} (1) \\ \boxed{\tilde{\mathbf{X}}} \\ (2) \end{matrix} \text{---} = \frac{1}{t} \cdot \begin{matrix} (2) \\ \boxed{\tilde{\mathbf{X}}} \\ (1) \end{matrix} \text{---} \begin{matrix} (1) \\ \boxed{\tilde{\mathbf{X}}} \\ (2) \end{matrix} \text{---}$$

Where $\mathbb{1}$ is simply the identity matrix. In the matrix notation we have

$$C_2(\mathbf{X}) = \frac{1}{t} \tilde{\mathbf{X}}^\top \tilde{\mathbf{X}} \quad (5.42)$$

Remark 5.2.4. In the case of the 3rd cumulant, we can simplify Eq. (5.39)

$$c_{i_1, i_2, i_3} = c'_{i_1, i_2, i_3} = m'_{i_1, i_2, i_3} - c'_{i_1, i_2} c'_{i_3} - c'_{i_1, i_3} c'_{i_2} - c'_{i_2, i_3} c'_{i_1} - c'_{i_1} c'_{i_2} c'_{i_3} = m'_{i_1, i_2, i_3}, \quad (5.43)$$

in a graphic notation, see Definition 5.2.4, we have:

For the the 4th cumulant its relation with central moments becomes more complex. To understand this observe that if we differentiate Eq. (5.37) again besides $\frac{1}{\varphi} \frac{\partial^4 \varphi}{\partial v_{i_1} \partial v_{i_2} \partial v_{i_3} \partial v_{i_4}} \Big|_{\mathbf{v}=0}$ corresponding to 4th moment, we have

$$-\frac{1}{\varphi^2} \left(\frac{\partial^2 \varphi}{\partial v_{i_1} v_{i_2}} \frac{\partial^2 \varphi}{\partial v_{i_3} v_{i_4}} + \frac{\partial^2 \varphi}{\partial v_{i_1} v_{i_3}} \frac{\partial^2 \varphi}{\partial v_{i_2} v_{i_4}} + \frac{\partial^2 \varphi}{\partial v_{i_1} v_{i_4}} \frac{\partial^2 \varphi}{\partial v_{i_2} v_{i_3}} \right) \Big|_{\mathbf{v}=0}, \quad (5.44)$$

corresponding to the combinatorics symmetrizing sum of the product of second moments, which do not vanish while using central cumulants and moments. Now, one can show that 4th cumulant elements are [34]

$$c_{i_1, i_2, i_3, i_4} = c'_{i_1, i_2, i_3, i_4} = m'_{i_1, i_2, i_3, i_4} - m'_{i_1, i_2} m'_{i_3, i_4} - m'_{i_1, i_3} m'_{i_2, i_4} - m'_{i_1, i_4} m'_{i_2, i_3}, \quad (5.45)$$

or in the equivalently

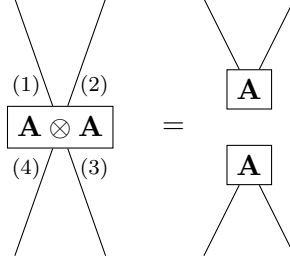
$$c_{i_1, i_2, i_3, i_4} = m'_{i_1, i_2, i_3, i_4} - c_{i_1, i_2} c_{i_3, i_4} - c_{i_1, i_3} c_{i_2, i_4} - c_{i_1, i_4} c_{i_2, i_3}. \quad (5.46)$$

For the graphic notation, we need a few additional definitions.

Definition 5.2.5. The outer product of symmetric matrix $\mathbf{A} \in \mathbb{R}^{[n,2]}$ by itself in the 4-mode tensor representation is $\mathbb{R}^{n \times n \times n \times n} \ni \mathcal{T} = \mathbf{A} \otimes \mathbf{A}$, with elements

$$t_{i_1, i_2, i_3, i_4} = a_{i_1, i_2} a_{i_3, i_4}. \quad (5.47)$$

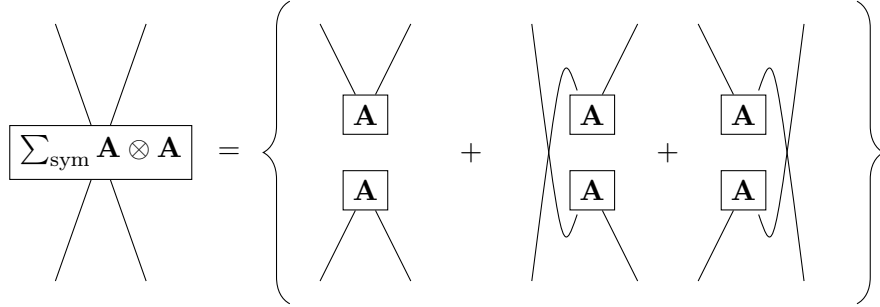
In a graphic notation we have



However, such tensor is not super-symmetric. To overcome this problem refer to [46], where the idea of symmetries of tensor products of symmetrical matrices is discussed. To get the super-symmetric tensor we need the symmetrising sum of such outer products $\mathcal{T}_{\text{sym}} = \sum_{\text{sym}} \mathbf{A} \otimes \mathbf{A}$, which is defined element wisely:

$$(t_{\text{sym}})_{i_1, i_2, i_3, i_4} = a_{i_1, i_2} a_{i_3, i_4} + a_{i_1, i_3} a_{i_2, i_4} + a_{i_1, i_4} a_{i_2, i_3}. \quad (5.48)$$

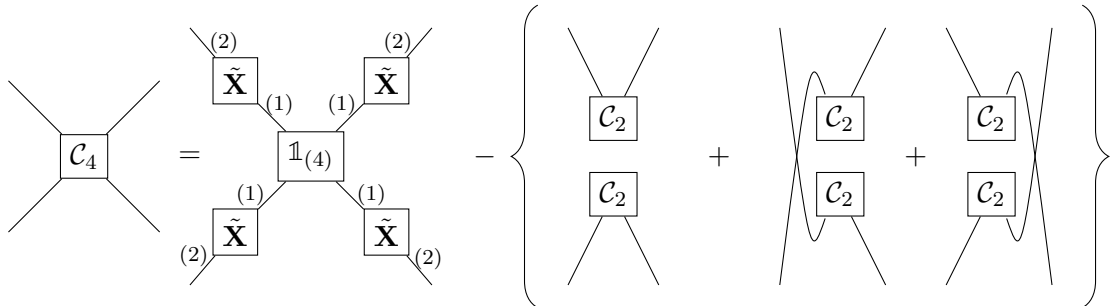
In a graphic notation we have



Remark 5.2.5. Referring to Eq. (5.46), the 4th cumulant in a tensor notation would be:

$$\mathcal{C}_4(\mathbf{X}) = \mathcal{M}_4(\tilde{\mathbf{X}}) - \sum_{\text{sym}} \mathcal{C}_2 \otimes \mathcal{C}_2. \quad (5.49)$$

In a graphic notation we have

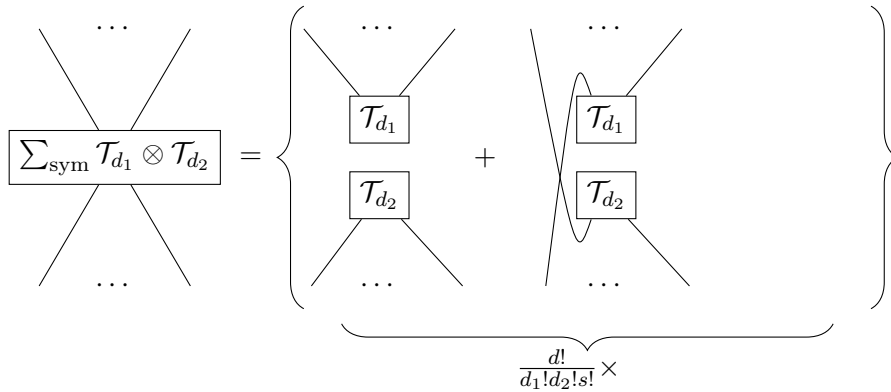


In the case of the 5th cumulant double differentiation of Eq. (5.37) produces a term $\frac{1}{\varphi} \frac{\partial^5 \varphi}{\partial v_{i_1} \partial v_{i_2} \partial v_{i_3} \partial v_{i_4} \partial v_{i_5}} \Big|_{\mathbf{v}=0}$ and additional 10 terms $-\frac{1}{\varphi^2} \left(\frac{\partial^2 \varphi}{\partial v_{i_1} \partial v_{i_2}} \frac{\partial^3 \varphi}{\partial v_{i_3} \partial v_{i_4} \partial v_{i_5}} \right) \Big|_{\mathbf{v}=0}$, $-\frac{1}{\varphi^2} \left(\frac{\partial^2 \varphi}{\partial v_{i_1} \partial v_{i_5}} \frac{\partial^3 \varphi}{\partial v_{i_2} \partial v_{i_3} \partial v_{i_4}} \right) \Big|_{\mathbf{v}=0}, \dots$ that do not vanish. Remaining terms will have a single derivative of φ leading to first moments that vanishes due to the centring. Given these, and the fact, that cumulants of order 2 and 3 equals to corresponding central moments, the 5th cumulant element is given by

$$c_{i_1, \dots, i_5} = m'_{i_1, \dots, i_5} - \underbrace{c_{i_1, i_2} c_{i_3, i_4, i_5} - c_{i_1, i_3} c_{i_2, i_4, i_5} - c_{i_1, i_4} c_{i_2, i_3, i_5} - \dots}_{\times 10} \quad (5.50)$$

Here again we have a symmetrising sum of outer products of second cumulant's matrix and third cumulant's tensor, that have 10 terms.

Definition 5.2.6. The symmetrising sum of tensors' outer products. Suppose we have d_1 and d_2 modes super-symmetric tensors \mathcal{T}_{d_1} and \mathcal{T}_{d_2} , the symmetrised sum of outer products of these tensors in a graphic notation is given by

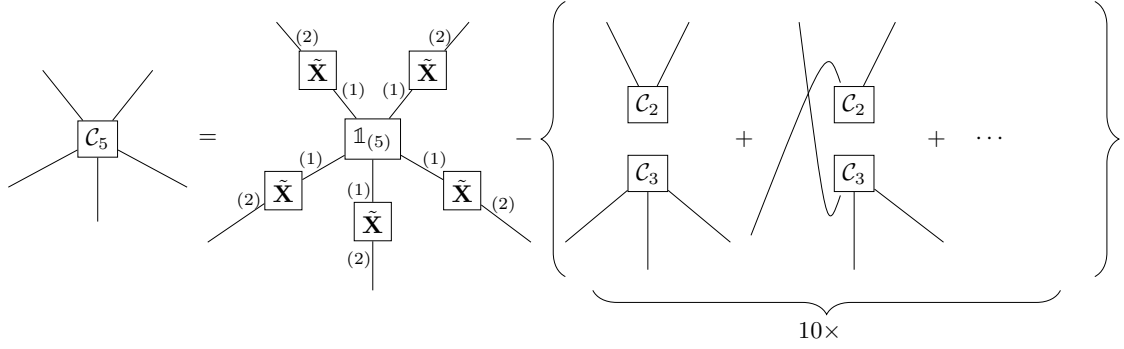


If $d_1 = d_2$ we have the outer product of the \mathcal{T}_{d_1} by itself and set $s = 2$, otherwise we set $s = 1$.

Remark 5.2.6. Referring to Eq. (5.50), in the tensor notation the 5th cumulant is given by

$$\mathcal{C}_5(\mathbf{X}) = \mathcal{M}_5(\tilde{\mathbf{X}}) - \sum_{\text{sym}} \mathcal{C}_2(\mathbf{X}) \otimes \mathcal{C}_3(\mathbf{X}), \quad (5.51)$$

and in a graphic notation by



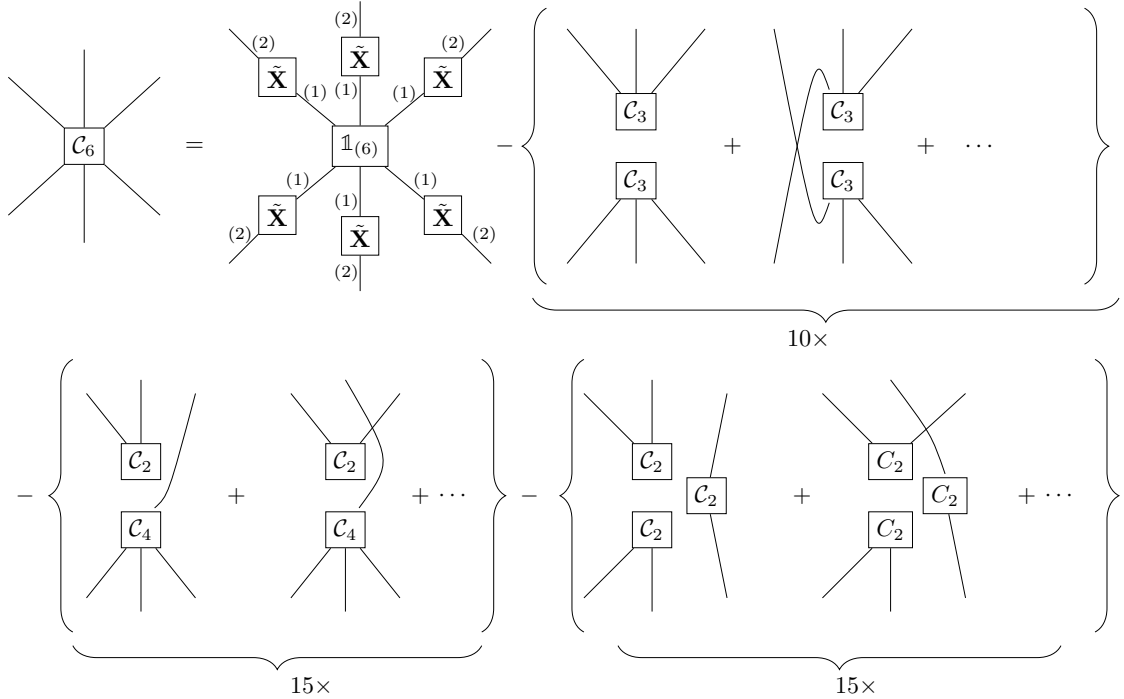
Remark 5.2.7. The 6th cumulant's tensor formula is much more complicated. For the general formula in the tensor notation we can refer to [34], yielding:

$$\mathcal{C}_6(\mathbf{X}) = \mathcal{M}_6(\tilde{\mathbf{X}}) - \sum_{\text{sym}} \mathcal{C}_4(\mathbf{X}) \otimes \mathcal{C}_2(\mathbf{X}) - \sum_{\text{sym}} \mathcal{C}_3(\mathbf{X}) \otimes \mathcal{C}_3(\mathbf{X}) - \sum_{\text{sym}} \mathcal{C}_2(\mathbf{X}) \otimes \mathcal{C}_2(\mathbf{X}) \otimes \mathcal{C}_2(\mathbf{X}) \quad (5.52)$$

The last term is the symmetrising sum of the outer produce of 3 symmetric matrices. $\mathbb{R}^{[n,6]} \in \mathcal{T}_{\text{sym}} = \sum_{\text{sym}} \mathbf{A} \otimes \mathbf{A} \otimes \mathbf{A}$ where $\mathbf{A} \in \mathbb{R}^{[n,2]}$ what can be represented by the following element wise notation:

$$(t_{\text{sym}})_{i_1, \dots, i_6} = \underbrace{a_{i_1, i_2} a_{i_3, i_4} a_{i_5, i_6} + a_{i_1, i_3} a_{i_2, i_4} a_{i_5, i_6} + a_{i_1, i_4} a_{i_2, i_3} a_{i_5, i_6} + \dots}_{\times 15} \quad (5.53)$$

Finally in a graphic notation we have



5.2.3 Calculation and programming implementation

As discussed in Section 5.2.1 and Section 5.2.2 both moments tensors and cumulants tensors are super-symmetric. Hence it is sufficient to store and calculate only one hyper-pyramid part of such tensor. Such storage scheme was discussed in [34]. Let us mention here only a symmetric matrix example that can be stored in blocks in the following form

$$\mathbb{R}^{[n,2]} \ni \mathbf{A} = \begin{bmatrix} (\mathbf{A})_{11} & (\mathbf{A})_{12} & \cdots & (\mathbf{A})_{1\bar{n}} \\ \text{Void} & (\mathbf{A})_{22} & \cdots & (\mathbf{A})_{2\bar{n}} \\ \vdots & \vdots & \ddots & \vdots \\ \text{Void} & \text{Void} & \cdots & (\mathbf{A})_{\bar{n}\bar{n}} \end{bmatrix}. \quad (5.54)$$

The use of blocks makes a computation implementation simpler and more efficient, see also [214]. As discussed in [34], given a block size parameter b and $\bar{n} = \frac{n}{b}$ and assuming that $b|n$, the super-symmetric tensor have $\binom{\bar{n}+d-1}{\bar{n}}$ blocks, hence we store $b^d \binom{\bar{n}+d-1}{\bar{n}}$ elements out of n^d in an naive approach. For $n \gg b$ we save up to the $\frac{1}{d!}$ computer memory and computational power. Those block storage scheme was implemented in the Julia programming language in the `SymmetricTensors.jl` module, see [216] GitHub repository. Algorithms for the calculation of moment's and cumulant's were implemented as well in `Cumulants.jl` module, see [35] GitHub repository.

5.3 Cumulants of copulas

Having introduced higher order cumulants we can discuss their significance in the copula determination of multivariate data. Given data probabilistic model including marginals and the copula, multivariate moments tensors can be computed by Eq. (5.14). These moments tensors are the base to compute multivariate cumulants tensors. We are interested in this section rather on the impact of copulas on multivariate cumulants, since non-Gaussian univariate marginal distributions are easy to detect and analyse by means of univariate statistics. Following [203] and inspired by the fact, that univariate Gaussian distribution results in zero higher order univariate cumulants, we present in this section examples of cumulants of many non-Gaussian copulas with univariate standard Gaussian marginals hoping to reveal in cumulants characteristics of copulas. For each experiment we use the sample of size $t = 5 \times 10^6$ to ensure accurate approximation of cumulants.

Further in this section we have measured the simultaneous interdependence of 3 or 4 marginals by means of cumulants. What is important, we have shown by experiments, that these interdependences are meaningful. Alternative approach to the use of univariate Gaussian marginals is to use uniform marginals on $[0, 1]$. However such marginals have its own impact on even order higher order cumulants, due to highly negative kurtosis of the uniform distribution. Examples, where uniform marginals have a dominant impact on elements of the 4th cumulant's tensor are presented at the end of this section.

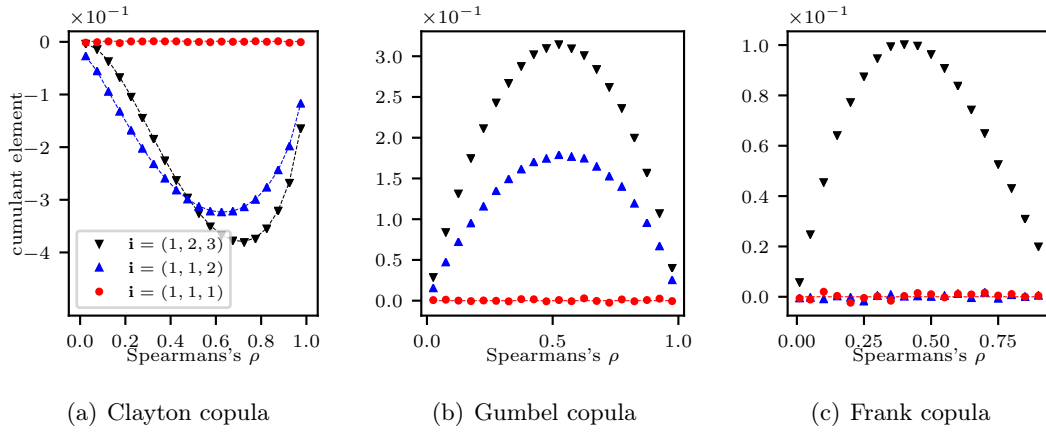


Figure 5.2: 3th cumulant's elements of Archimedean copulas, and standard Gaussian marginals. Solid lines represent theoretical outcomes, while points represent outcomes form generated data.

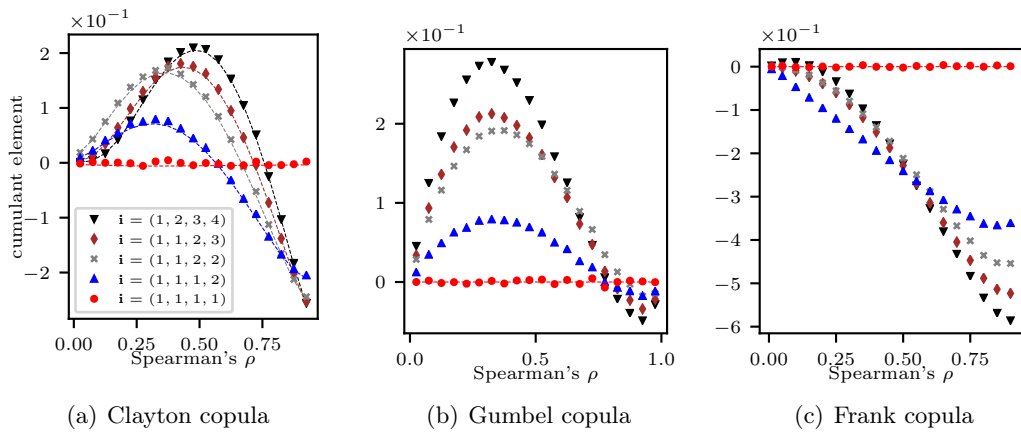


Figure 5.3: 4th cumulant's elements of Archimedean copulas, and standard Gaussian marginals. Solid lines represent theoretical outcomes, while points represent outcomes form generated data.

5.3.1 Archimedean copulas

We start with the (non nested) Archimedean copula, as introduced in Definition 4.3.3. It is easy to show that such copula is unchanged under any permutation of marginals,

$$\forall_{i,j \in (1:n)} \mathbf{C}_{\psi_\theta}(u_1, \dots, u_i, \dots, u_j, \dots, u_n) = \mathbf{C}_{\psi_\theta}(u_1, \dots, u_j, \dots, u_i, \dots, u_n), \quad (5.55)$$

and we call such feature the symmetry of the Archimedean copula.

The simplest approach to investigate distinct elements of 3rd cumulant tensor of the Archimedean copula with standard Gaussian marginals will be to take the tri-variate Archimedean copula. The probabilistic model is given by:

$$\mathbf{C}_{\psi_\theta}(u_1, u_2, u_3) \text{ and } x_i = F_{\mathcal{N}(0,1)}^{-1}(u_i). \quad (5.56)$$

Following [203], we have here 3 distinct 3rd cumulant's elements:

- $c_{1,1,1} = c_{2,2,2} = c_{3,3,3} = 0$ – diagonal elements, zero due to Gaussian marginal distributions;
- $c_{1,1,2} = c_{1,2,2} = c_{1,3,3} = c_{3,3,1} \dots$ – partially diagonal elements, equal due to copula symmetry, identical marginal distributions, and cumulants super-symmetry;
- $c_{1,2,3} = c_{2,1,3} = c_{3,1,2} = \dots$ - off-diagonal elements, equal due to cumulants super-symmetry.

In Figure 5.2 we present elements of the 3rd cumulant calculated for data sampled from Gumbel, Clayton or Frank Archimedean copulas, for a further discussion see [203]. In the case of the Clayton copula 5.2(a) we present in addition theoretical values obtained by integrating numerically Eq. (5.14). For all Archimedean copulas, we determine the copula parameter θ from the Spearman's ρ correlation coefficient, using Eq. (4.8).

Analogically we have 5 distinct elements of the 4th cumulant's tensor given 4-variate Archimedean copula (with standard Gaussian marginals in our case). Values of these elements computed from data sampled from these copula are presented in Figure 5.3.

From Figures 5.2 and 5.3 one can conclude that higher order cumulants of different Archimedean copulas with Gaussian marginals have different patterns, hence such cumulants can be used to distinguish between copulas. Moreover, from Figure 5.2(c), one can conclude that given the Frank copula, the 3rd cumulant has only non-zero off-diagonal elements. These elements are calculated from three distinct marginals. This is a meaningful example of the tri-variate 3rd order cross-correlation measure that is non-zero given zero bivariate 3rd order cross-correlation measures, such as $c_{1,1,2}$. For the practical discussion of cumulants based d -variate interdependence measures (where $d > 2$) in data analysis see [217]. There cumulants are used to analyse information from the hyper-spectral data.

5.3.2 Fréchet copula

In this subsection, we discuss cumulants of the n -variate 1-parameter Fréchet copula with standard Gaussian marginals, see Definition 4.2.3. It is easy to show that this

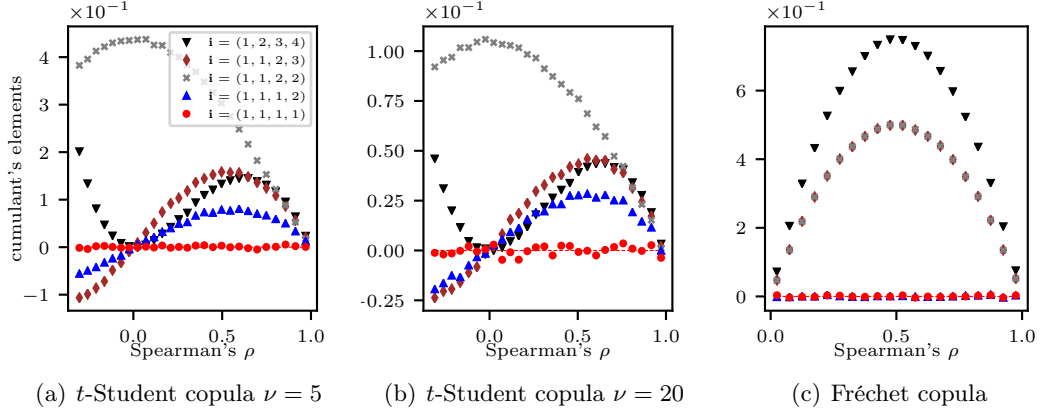


Figure 5.4: 4th cumulant's elements of t -Student and Fréchet copula, and standard Gaussian marginals.

copula has the same symmetry as an Archimedean one, see Eq. (5.55). Further it can be demonstrated, at least numerically, that higher order odd cumulants of such copula with symmetric marginals (such as Gaussian marginals) should be zero, see Figure 6.2 for justification.

For experiments results, in Figure 5.4(c) we present distinguishable 4th cumulant's elements of discussed here Fréchet copula. One can observe that the pattern of the 4th cumulant differs from patterns of Archimedean copulas, presented in Figure 5.3. Importantly for each Spearman's ρ value, off-diagonal cumulant's tensor's elements of the Fréchet copula, are distinguishable (due to their higher values) in comparison with partially diagonal ones. These off-diagonal elements (such as $c_{1,2,3,4}$) correspond to the 4th order 4-variate cross-correlation measure between marginals.

5.3.3 t -Student copula

Next, we analyse the t -Student copula with standard Gaussian marginals parametrised by an integer parameter ν and the matrix \mathbf{R} with constant off-diagonal elements $r_{1,2} = r_{1,3} = \dots = r$ - see the constant correlation matrix in [203]. Given such parametrisation, similar marginals exchange symmetry appears to Archimedean and Fréchet copulas cases, hence similar presentation of results is possible. For experiments we use the 4-variate t -Student copula parametrised by r and ν and standard Gaussian marginals. We use the following limitation for the r parameter $-\frac{1}{3} < r < 1$ to ensure the matrix $\mathbf{R} \in \mathbb{R}^{[4,2]}$ to be positive definite given 1 on its diagonal. In Figures 5.4(a) 5.4(b) we present results of our experiments concerning the 4th cumulant's tensors. For further analysis of cumulants of t -Student copula see [204]. The pattern of the t -Student copula differs from patterns of other copulas (Archimedean and Fréchet), what gives an advantage for 4th order cumulant in copula detection. For the t -Student copula, we discuss 4th cumulant, since in the case of the t -Student copula with symmetric marginals higher order odd cumulants

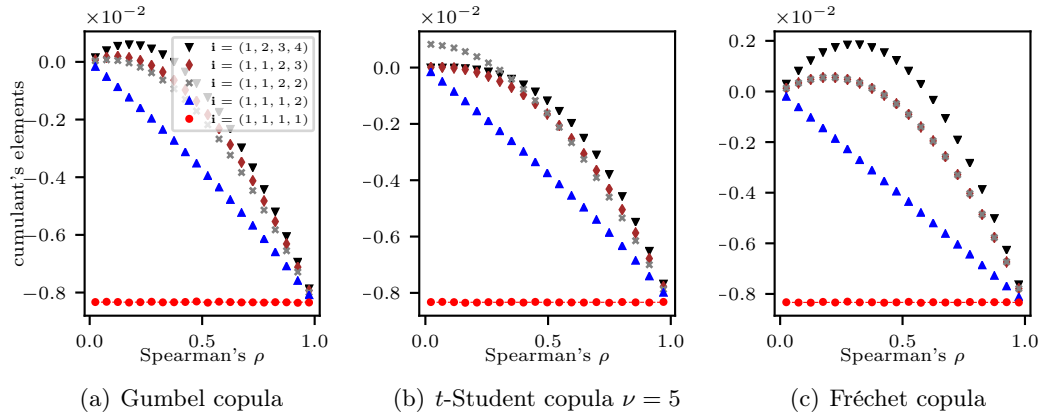


Figure 5.5: 4th cumulant's elements given uniform marginals on $[0, 1]$.

are supposed to be zero as it is in a case of t -Student multivariate distribution [176]. See also a discussion on elliptical copulas (including t -Student one) in [183].

To demonstrate the significance of univariate Gaussian marginals to reveal in cumulants features of copulas, refer to Figure 5.5, where we present values of elements of the 4th cumulants tensors of various cumulants with uniform marginals on $[0, 1]$. Here patterns are similar, for different copulas, and the proper copula's determination on the base of these cumulants is difficult. This is due a high negative kurtosis of the uniform distribution and its impact on multivariate cumulant of order 4.

5.4 Auto-correlation function and cumulants

Having discussed the use of cumulants to analyse interdependency between marginals of multivariate data we can mention their potential use to analyse auto-correlation of univariate data. What is interesting, the combination of both approaches is possible as well.

Suppose we have a random process represented by a series of univariate random variables $\mathfrak{Z}_1, \dots, \mathfrak{Z}_i, \dots, \mathfrak{Z}_j, \dots, \mathfrak{Z}_k$ and want to analyse the auto-correlation inside such series. The simplest approach would be to use the Pearson's correlation based auto-correlation coefficient [78]:

$$\text{acc}_{i,j} = \frac{\text{acf}_{i,j}}{\sigma_i \sigma_j} = \frac{\mathbb{E}((\mathfrak{Z}_i - \mu_i)(\mathfrak{Z}_j - \mu_j))}{\sigma_i \sigma_j} \tag{5.57}$$

here μ_i and σ_i are the mean and the standard deviation of \mathfrak{Z}_i , and \mathbb{E} is expecting value operator. It is easy to show, that the auto-correlation function is simply an element of the 2nd cumulant of k - variate random vector $\mathfrak{Z}^{(k)}$ with marginals $\mathfrak{Z}_1, \dots, \mathfrak{Z}_k$. If $\mathfrak{Z}^{(k)} \sim \mathcal{N}(\mu, \Sigma)$ the covariance matrix carries all information about the auto-correlation, and $\text{acf}_{i,j} = s_{i,j}$. Given some assumptions about statistics of these variables, further simplification of the auto-correlation function is possible.

Remark 5.4.1. If all random variables \mathfrak{Z}_i are from the same distribution we have: $\sigma_i = \sigma_j = \sigma$ and $\mu_i = \mu_j = \mu$. Further if the auto-correlation function $\text{acf}_{i,j}$ is only the function of $\tau = |i - j|$ we have a stationary process and we can parametrize the auto-correlation function or coefficient by one lag parameter τ . Suppose we have $\tilde{Z} \in \mathbb{R}^t$ being a vector of t realisations of zero mean univariate random variable. Given stationary of \tilde{Z} the auto-correlation function can be estimated by [78]

$$\text{acf}_\tau(Z) = \frac{1}{t - \tau} \sum_{i=1}^{t-\tau} \tilde{z}_i \tilde{z}_{i+\tau} \quad (5.58)$$

If our series is represented by $\mathfrak{Z}^{(k)}$ that is not distributed according to multivariate Gaussian, we may want to consider higher order cumulants approach in place of standard auto-correlation function, see [40, 95].

Example 5.4.1. *Let us present some examples of cumulants based auto-correlation functions, namely*

1. 3rd order in analogy to 3rd cumulant

$$\text{acf}_{\tau_1, \tau_2}(Z) = \frac{1}{t - \max(\tau_1, \tau_2)} \sum_{i=1}^{t - \max(\tau_1, \tau_2)} \tilde{z}_i \tilde{z}_{i+\tau_1} \tilde{z}_{i+\tau_2} \quad (5.59)$$

2. 4th order in analogy to 4th cumulant

$$\begin{aligned} \text{acf}_{\tau_1, \tau_2, \tau_3}(Z) &= \frac{1}{t - \tau} \sum_{i=1}^{t-\tau} \tilde{z}_i \tilde{z}_{i+\tau_1} \tilde{z}_{i+\tau_2} \tilde{z}_{i+\tau_3} - \left(\frac{1}{t - \tau} \right)^2 \\ &\left(\sum_{i=1}^{t-\tau} \tilde{z}_i \tilde{z}_{i+\tau_1} \sum_{i=1}^{t-\tau} \tilde{z}_{i+\tau_2} \tilde{z}_{i+\tau_3} + \sum_{i=1}^{t-\tau} \tilde{z}_i \tilde{z}_{i+\tau_2} \sum_{i=1}^{t-\tau} \tilde{z}_{i+\tau_1} \tilde{z}_{i+\tau_3} + \sum_{i=1}^{t-\tau} \tilde{z}_i \tilde{z}_{i+\tau_3} \sum_{i=1}^{t-\tau} \tilde{z}_{i+\tau_1} \tilde{z}_{i+\tau_2} \right) \\ &= \frac{1}{t - \tau} \sum_{i=1}^{t-\tau} \tilde{z}_i \tilde{z}_{i+\tau_1} \tilde{z}_{i+\tau_2} \tilde{z}_{i+\tau_3} - \text{acf}_{\tau_1} \text{acf}_{|\tau_3 - \tau_2|} - \text{acf}_{\tau_2} \text{acf}_{|\tau_3 - \tau_1|} - \text{acf}_{\tau_3} \text{acf}_{|\tau_2 - \tau_1|}, \end{aligned} \quad (5.60)$$

where $\tau = \max(\tau_1, \tau_2, \tau_3)$. Here products of one parameter auto-correlation functions ensures that $\text{acf}_{\tau_1, \tau_2, \tau_3}(Z)$ carries additional information included in those one parameter auto-correlation functions.

To show a significance of higher order cumulants in auto-correlation analysis in the computer science refer to [95], where the parallel computer architecture for the calculation of 4th order cumulant that measures auto-correlation is discussed. Further in [218] the novel algorithm for the FPGA (Field Programmable Gate Array) based architecture was used to calculate the third order auto-correlation cumulant. Let us present further potential applications of cumulant based auto-correlations in real life biomedical data analysis.

Example 5.4.2. *While analysing biomedical signals one is often interested in a correlation of two signals in a frequency domain. For justification of such approach consider [219] where the spectral distance analysis of the neurological EEG signals was introduced. To determine the correlation of two signals as a function of frequency the coherence function [220] is used. Such coherence is the normalised Fourier transform of auto-correlation function between two signals. In details, suppose we have two zero mean signals $\tilde{Z} \in \mathbb{R}^t$ and $\tilde{W} \in \mathbb{R}^t$. First we compute their auto-correlation function:*

$$acc_\tau(Z, W) = \frac{1}{\sigma(Z)\sigma(W)(t - \tau)} \sum_{i=1}^{t-\tau} \tilde{z}_i \tilde{w}_{i+\tau}, \quad (5.61)$$

where $\sigma(Z)\sigma(W)$ are corresponding standard deviations of signals. Next we perform the Fourier transform of the result over τ , moving to frequency domain since τ for biomedical data indicates often a time lag. Finally the coherence $-1 \leq \kappa_{Z,W}^2(f) \leq 1$ is normalised Fourier transform of the auto-correlation function as in Eq. (5.61).

For application of the coherence function in biomedical data analysis see [221, 222, 223]. However consider for example [224] where 3 biomedical signals are analysed and the pairwise coherence was computed for those signals. Such approach can be generalised using the 3rd cumulants i.e. computing following auto-correlation

$$acc_\tau(Z, W, V) = \frac{1}{\sigma(Z)\sigma(W)\sigma(V)(t - \tau)} \sum_{i=1}^{t-\tau} \tilde{z}_i \tilde{w}_{i+\tau_1} \tilde{v}_{i+\tau_2}, \quad (5.62)$$

where $\tau = \max(\tau_1, \tau_2)$. Next by the double Fourier transform and corresponding normalisation we can have the double frequencies coherence that can be compared with pairwise results.

Chapter 6

Cumulants in machine learning

In this chapter, we consider multivariate data where marginal variables are features. Next, we discuss algorithms applying cumulants that can be used for feature selection or feature extraction when new features are linear combinations of original ones. We focus on examples, where interesting information is associated with the joint non-Gaussian distribution of a subset of features. In general, such an approach is applicable when searching for outliers that represent extreme events often resulting from non-usual dynamics of the complex (physical) system producing data, e.g. [23, 63]. Such dynamics may result in non-Gaussian distribution. In other words, outliers lie in the tail of the multivariate distribution of data. Hence outliers may be modelled by non-Gaussian models. Apart from this, the majority of algorithms presented in this chapter can be modified in such a way, that they can be used to search for/find subsets of Gaussian-distributed features. These can then be used in machine learning algorithms that rely on assumption that data are normally distributed.

For the practical example, consider financial data analysis in the safe investment portfolio determination. We are searching for such a portfolio (the linear combination of assets being features) where potential extreme events, being high drops in the portfolio's value are unlikely. The standard approach that uses Gaussian multivariate distribution [64], although simple applicable, fails to anticipate extreme events. To overcome this problem, one can use higher order cumulants tensors, that reflect higher order cross-correlations between marginals and hence can be used to anticipate simultaneous extreme events occurring for many marginals [225]. The practical use of higher order cumulants tensors in the safe investment portfolios determination, during the crisis on the Warsaw Stock Exchange, is discussed in [39].

As another example, let us consider non-Gaussian distributed data collected utilising the hyper-spectral imaging (HSI). Analysis of such images is complicated due to their high dimensionality, lack of training examples for classification and the presence of feature redundancy phenomena [69].

Example 6.0.1. *In this example we discuss data collected by means of the hyper-spectral camera. Such camera outputs for each pixel (a position on 2D plane) a vector of n features being intensities of light (reflectance) recorded for n different wavelengths: $\lambda_1, \dots, \lambda_n$.*

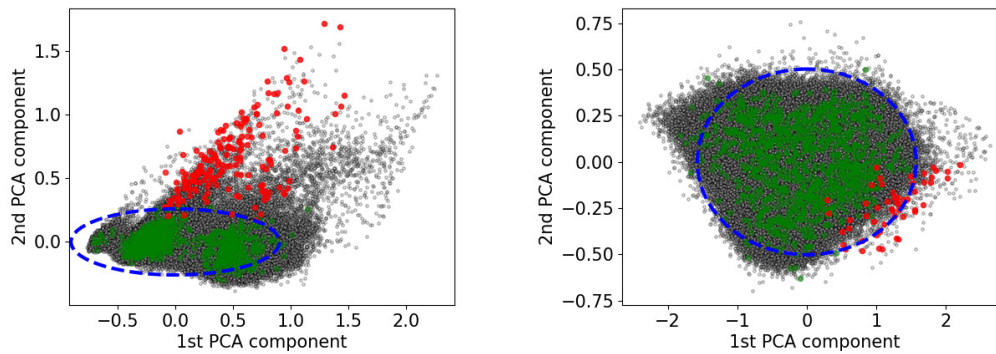
Hyper-spectral images are represented by a 3 mode tensor $\mathcal{X} \in \mathbb{R}^{x \times y \times n}$. One can analyse hyper-spectral data in the spectral approach or the spatial approach [68]. In the spectral approach, each feature is a reflectance vector tied to the given wavelength. Here pixels index realisations. Hence, we can represent data in the form of matrix $\mathbf{X} \in \mathbb{R}^{t \times n}$. Such representation gives naturally n features and $t = xy$ realisations. The disadvantage of such representation is the loose of the spatial information, what is the cost of the use of the spectral approach. Alternatively, in the spatial approach, we examine n different monochrome images of data that correspond to n different wavelengths.

In [226] authors discussed the detection of the gunshot residue (GSR) on various fabrics types utilizing a hyper-spectral imaging. For this purpose, the authors used advanced machine learning algorithms. Such an approach is potentially applicable to support the forensic analyst in the objective evidence collection and follows the active research in forensic science of the GSR identification and analysis [227]. In more details, in [226], authors used spectral approach together with unsupervised and supervised machine learning algorithms, the first being the (RX) Reed-Xiaoli Detector [228], and the second the (SVM) Support Vector Machine classifier [229]. Authors focused on the anomaly detection scenario, where the GSR pattern occupies a small portion of pixels. For the purpose of experiments, authors have created the dataset by annotating, by hand, some of the pixels reflecting the fabric itself (background) and GSR (outliers). Even though GSR patterns have a distinct spatial characteristics: spherical or elliptical, the spectral approach applied here gives a straightforward application of probabilistic models in detection.

The detection performance in both unsupervised RX detector and supervised SVM classification varied between materials. In majority cases most of the annotated outliers have been detected. However there was a notable number of false positives. To demonstrate unsupervised detection, the visualisation of both background and GSR data is presented in Figure 6.1. Here the PCA projection of features on two most significant components is presented. Further, some realisations are annotated as background data or outliers. The ellipse represents the approximate threshold of the multivariate Gaussian model at 95% confidence. Hence, if data were multivariate Gaussian distributed (with the same covariance matrix for data and outliers), the ellipse should refer to the detection threshold. Given those, most of the outliers are supposed to lay outside the ellipse. Analogically most (95%) of background data are supposed to lay inside the ellipse. In Figure 6.1(a) we demonstrate the result, where most of the outliers are detected.

Nevertheless, we have a significant number of false detections due to the non-Gaussian structure of the background. In Figure 6.1(b), although outliers are on the side of the background data, the vast number of them lie within the background model. One can see here the non-Gaussian structure of data as well, however different than in Figure 6.1(a) case. Given those, in [226] authors have concluded, that data pattern suggests the non-Gaussian distribution of outliers, as well as of background data given some (mainly not uniform) materials.

For the supervised approach the detection rate is consistent or slightly better than in the unsupervised case and the number of false positives is lower. What is important from the application point of view, authors have shown that the hyper-spectral imaging



(a) A mixture of cotton and polyester (a military uniform).

(b) White cotton (a shirt).

Figure 6.1: Each figure presents a PCA projection on two most significant components. Dark grey dots mark projections of not annotated hyper-spectral vectors, light grey dots mark projections of vectors annotated as background, while black dots mark projections of vectors annotated as GSR.

in general outperforms the RGB (red green blue) imaging in term of the GSR detection accuracy.

Promising directions of further research include the development of background model, possibly using copulas, to build background's non-Gaussian probabilistic model. Further one can evolve features selection algorithm to find such features that have highly non-Gaussian joint distribution and carry meaningful information about outliers. Alternatively, one can find such linear combination of features that carries most information about non-Gaussian joint distribution of features in the features extraction procedure. Both of above can be performed by means of higher order cumulants tensors.

From such examples, one can conclude that it would be beneficial to have the measure determining how far the multivariate distribution of data or its subset (a background data, outliers, etc...) is from the multivariate Gaussian one. Such measure may be introduced, by means of higher order cumulants tensors that are zero for multivariate Gaussian distributed data, see Section 5.1. As discussed in [230] the simple approach, to construct such measure, would be to compute the Frobenius norm of higher order cumulants tensors. For an arbitrary tensor $\mathcal{T} \in \mathbb{R}^{d_1 \times \dots \times d_n}$ the Frobenius norm is given by

$$\|\mathcal{T}\| = \sqrt{\sum_{i_1, \dots, i_d} (t_{i_1, \dots, i_d})^2}. \quad (6.1)$$

The norm in Eq. (6.1) is easily implementable for the super-symmetric tensor (such as cumulant's tensor), that uses blocks to store only its meaningful part, see Section 5.2.3. For the algorithmic implementation see [230] and Algorithm 5 within, while for implementation in Julia programming language see [231] and `norm()` function within. Following

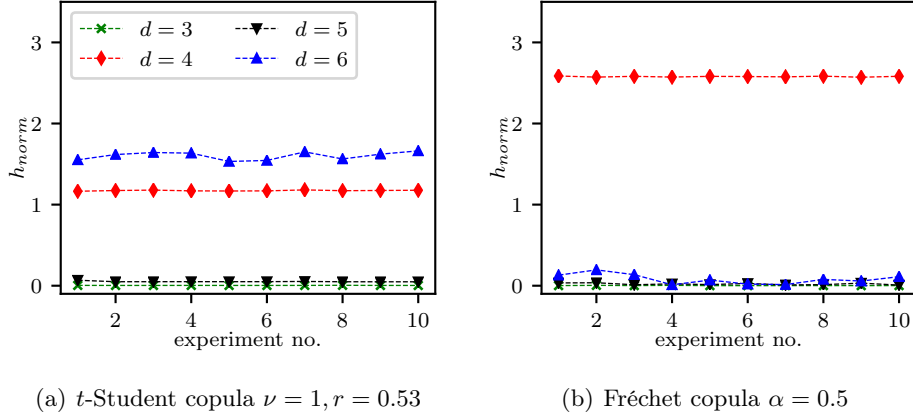


Figure 6.2: $h_{\text{norm},d}$ of higher order cumulants for t -Student and 1-parameter Fréchet copulas with standard Gaussian marginals and $n = 30$ features. Given such parametrisation both copulas have similar cross-correlation between marginals. For t -Student and Fréchet copulas with standard Gaussian marginals we have a strong suggestion of zero odd order cumulants. Observe the characteristic case of the 1-parameter Fréchet copula, where only the 4th cumulant’s tensor is non-zero, while other cumulants (of order 3, 5, 6) appear to be zero.

discussion in [230] we use the normalised norm

$$h_{\text{norm},d}(\mathcal{C}_2, \mathcal{C}_d) = \frac{\|\mathcal{C}_d\|}{\|\mathcal{C}_2\|^{d/2}} \text{ for } d \geq 3, \quad (6.2)$$

to measure how much the probabilistic model of data diverges from the multivariate Gaussian distribution. The motivation for such normalisation in denominator comes from the fact that in an univariate case, *i.e.* $n = 1$ we reproduce the module of the asymmetry for $d = 3$ and the module of the kurtosis for $d = 4$.

In Figure 6.2 we present $h_{\text{norm},d}$ for artificial data modelled by the t -Student copula (Figure 6.2(a)) and the Fréchet copula (Figure 6.2(b)). The t -Student copula is parametrised by the scalar parameter $\nu = 1$ and the matrix parameter \mathbf{R} with constant off-diagonal elements equal to $r = 0.53$ and ones on the diagonal. This reflect constant cross-correlation between marginals. The Fréchet copula is parametrised by $\alpha = 0.5$. The cross-correlation between marginals in the t -Student copula case is similar to the cross-correlation in the Fréchet copula case. Further, in both cases we use standard Gaussian marginals (with zero kurtosis), to reveal only copulas properties, see Section 5.3 to justify such approach. We performed all computations for $t = 5 \times 10^6$ realisations of $n = 30$ features.

Analysing Figure 6.2, we can conclude that for both copulas, there is a strong suggestion that odd order higher order cumulants are zero. In the case of the t -Student copula it results from the specific symmetry of the t -Student multivariate distribution [176] that

is the base of the t -Student copula. In the case of the 1-parameter Fréchet copula there is a strong suggestion that cumulant of order 6 is zero as well, while cumulant of order 4 is not zero. Interestingly the 6th cumulant is not zero for bivariate 2-parameters Fréchet copula introduced by Definition 4.2.2, however such copula is not applicable for $n > 2$.

Concluding, the $h_{\text{norm},d}$ can be used in features selection given various copulas models. Given Gaussian univariate marginals we have

1. $h_{\text{norm},4} = h_{\text{norm},6} = 0$ for Gaussian copula,
2. $h_{\text{norm},4} \neq 0$ and $h_{\text{norm},6} \approx 0$ for Fréchet copula,
3. $h_{\text{norm},4} \neq 0$ and $h_{\text{norm},6} \neq 0$ for t -Student copula.

While using other copulas families (such as Archimedean) the $h_{\text{norm},d}$ for odd d would be non-zero as well, see Subsection 5.3.1. Hence more selection scenarios are possible. Apart from this, norms of higher order cumulants can be used to analyse real-life data, as in following example.

Example 6.0.2. *Consider the analysis of real-life biomedical data analysis [232] where electromyographic (EMG) [233] signals recorded on the porcine uterine walls, during the pre-fertilisation and early pregnancy periods. The motivation for such research comes from the fact, that pigs uterine activity has been used to model those of humans due to their close similarities [234]. Refer to researches on the role of the uterine activity in promotion of the fertilization [235]. In [232] the novelty of the study comes from the fact that the analytic tools there are higher order cumulants tensors.*

In practice, the EMG signal organises in the form of bursts reflecting the electrical activity in the uterus. In [232], these bursts are investigated employing commonly used features in the EMG signal analysis. Features in the time domain [236, 237] are Duration of the burst, Pause – length of the pause between bursts, Amplitude of the burst, and RMS – root mean square of the burst. Features in the frequency domain [238] are MaxP – maximum power of the burst, MinP – minimum power of the burst, and DF – dominant frequency of the burst. The motivation for the second approach comes from the fact, that frequency domain features were suggested to be more effective than the conventional time-dependent features while analysing the uterine dynamics [239]. Given those, quantitative multivariate data in [232] were discussed here features of the EMG signal recorded in different part of the porcine uterus and different days of the pre-fertilisation and early pregnancy periods. These locations are: the tip of the right uterine horn (channel 1), the middle of the right uterine horn (channel 2), and the corpus uteri (channel 3), see Figure 6.3. Data were collected from 8 Polish Landrace sows and aggregated together for a given location and a given day of the experimental period.

Due to complex biochemical process associated with the uterine behaviour [240], authors expect non-Gaussian joint distribution of the features. For each day of the pre-fertilisation and early pregnancy periods and each channel, features are represented in the form of matrix $\mathbf{X} \in \mathbb{R}^{t \times n}$. Each time we have $t = 400$ realisations and $n = 7$ features (Duration; Pause; Amplitude; RMS; MaxP; MinP; DF). Since values of different features

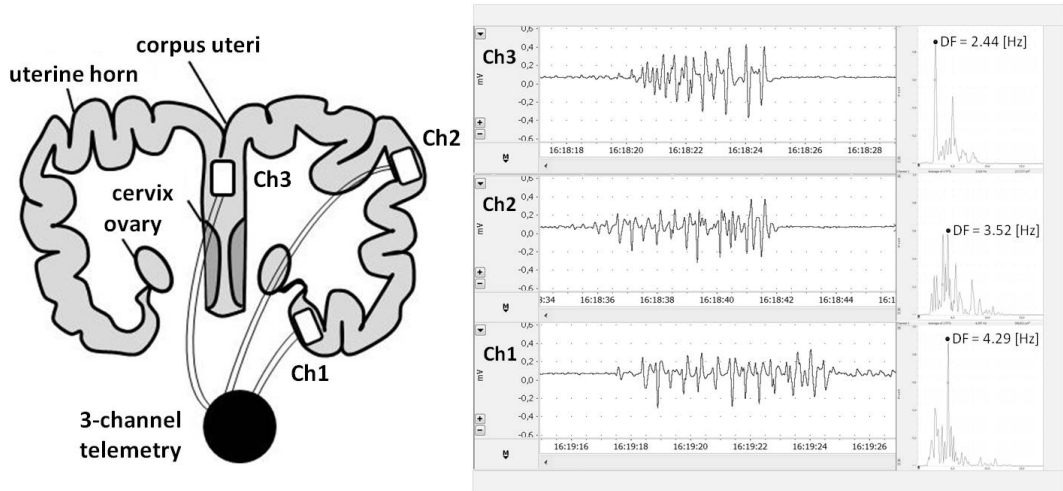


Figure 6.3: The experimental setting used for data acquisition in [232]. Here channels correspond to various locations of probes on the uterus on the left panel. Example of rough EMG data recorded are presented on the right panel.

(marginals) differs by many orders of magnitude, authors normalise each column vector of \mathbf{X} by its standard deviation. Normalised data are represented in the form of matrix $\hat{\mathbf{X}} \in \mathbb{R}^{t \times n}$, see Eq. (4) in [232]. Such normalisation facilitates the analysis of the joint distribution and higher order cross-correlations between features.

The goal of [232] was to apply higher order cumulants tensors to analyse probabilistic models of data for distinct days of the pre-fertilization period and the early pregnancy. To measure how much the probabilistic model of features diverged from the Gaussian model, one uses the Frobenius norm of the cumulants tensors of order 3 and 4, see Eq. (6.1). Results of such analysis are presented in Figure 6.4. A straight forward conclusion is that analysed features do not have multivariate Gaussian distribution, what should be taken into account in their analysis. Further multivariate higher order cumulants indicates that probabilistic models of these features changes expressly on the daily basis. As discussed in [232], these changes appears in concordance with crucial periods of the development and maintenance of pregnancy.

1. Authors suggest the first pick of $\|\mathcal{C}_d\|$ that begins in the corpus uteri in day -4 , see Figures 6.4(a) 6.4(d) is the signal of the estrus cycle synchronization. Next it spreads along the uterine horn (days -3 to 0 in Figures 6.4(b) 6.4(e)) into the tip of the uterine horn (day -3 in Figures 6.4(c) 6.4(f)).
2. The second pick of $\|\mathcal{C}_d\|$ occurs shortly after the Artificial Insemination (AI) in the corpus uteri (day 1, Figures 6.4(a) 6.4(d)), next it moves to the middle of the utters horn (day 2, Figures 6.4(b) 6.4(e)) and finally to the tip of the uterine horn (day 3,4, Figures 6.4(c) 6.4(f)). Authors suggest that such behaviour is related to the sperm cells transport.

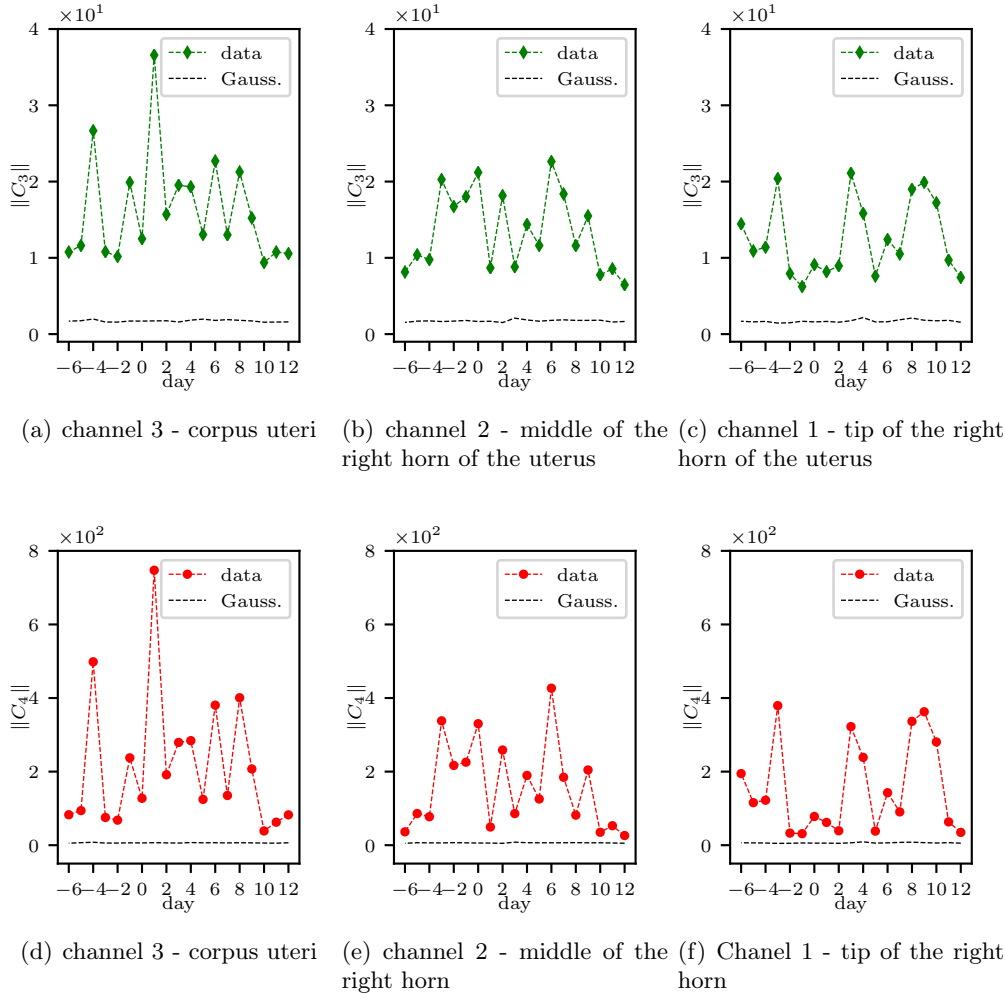


Figure 6.4: Frobenius norms of higher order cumulant tensors calculated for $\hat{\mathbf{X}}$ - features of EMG signals, collected on pigs uterus. Channels indicates position on the uterus where data are collected. On the horizontal scale we have days of the per-fertilisation and early pregnancy cycle. Dashed black line indicates 0.975 percentile of $\|\mathcal{C}_d\|$ given hypothetical Gaussian model. Day 0 corresponds to the Artificial Insemination (AI), see [232].

3. The third pick occurs only at the middle in the uterine horn (days 6 to 8, Figures 6.4(b) 6.4(e)) and in the tip (days 8 to 10, Figures 6.4(c) 6.4(f)). It is probably caused by the he descent of embryos into the uterine lumen.

To summarize, in [232] cumulant tensors of order 3 and 4 were used to anticipate information about the probabilistic model of data. It is why authors used the 3rd cumulant tensor based features selection procedure to achieve a rank of features importance. For this purpose authors applied the features selection procedure introduced in [47] for hyper-

spectral data analysis. This procedure is called the JSBS (Joint Skewness Band Selection) and is discussed in this book in Section 6.1.2. Results of the ranking of the importance of features for all days and channels are presented in Table 1 of [232]. Based on these authors speculate for investigated animals, features: MinP, MaxP and Pause are crucial elements of the middle of the uterine horn activity. This is an important result in evolving models of the uterine activity, that partially approves the outcome of [239], hence we have two features in a frequency domain.

Concluding, modelling based on higher order cumulants tensors offers a unique opportunity to understand the mechanisms underlying uterine contractility and development of early pregnancy in animals. Further such novel approaches may point the direction of research aimed to develop uterine models, hence improve management of the early pregnancy both in animals and in human, due to close similarities [234] of models in both cases. The 3rd cumulant's tensor bases JSBS features selection used in [232] is a member of the wider family of features selection methods that are introduced and discussed in next section of this book.

Using the analogical approach in [241] authors have applied higher order cumulants tensors to analyse features of the EMG signal of the estrus cycle in pigs. Here, in contrary to the classical statistical approach, the higher order cumulants tensors model shows evidences of large EMG activity during induced estrus. This is in contrary to the spontaneous estrus. Authors of [241] concludes, that higher order cumulants tensors are indicator revealing a probabilistic model of dynamic changes in the myometrial electrical activity as a result of positive and negative feedback of the reproductive hormones.

Referring to the last two paragraphs of Example 6.0.2, and the application of the cumulants tensors in the features selection for hyper-spectral data [47] we can move to the discussion of cumulant's based features selection algorithms in next section.

6.1 Features selection

In this section we discuss algorithms aimed to select a subset of marginals $\mathbf{r} \in (1 : n)$ of multivariate data that carries a meaningful information tied to the non-Gaussian joint distribution of such subset. Suppose we have n -variate random vector $\mathfrak{X}^{(n)}$ with marginals $\mathfrak{X}_1, \dots, \mathfrak{X}_n$ and data are given in a form of matrix $\mathbf{X} \in \mathbb{R}^{t \times n}$, where columns correspond to marginals. Following [47, 204, 217] we can introduce a family of features selection algorithms that uses higher order cumulants tensors to select a subset of marginals with non-Gaussian joint distribution.

Definition 6.1.1. Let $\mathcal{T} \in \mathbb{R}^{[n,d]}$ be the super-symmetric tensor. Following [47, 217], we define its r^{th} fibres cut, as the following tensor $\mathcal{T}_{(-r)} = \mathcal{T}' \in \mathbb{R}^{[(n-1),d]}$, where

$$t'_{i'_1, \dots, i'_d} = t_{i_1, \dots, i_d} : i'_k = \begin{cases} i_k & \text{if } i_k < r \\ i_{k-1} & \text{if } r \leq i_k < n, \end{cases} \quad (6.3)$$

and $i'_k \in (1 : n - 1)$. Referring to [75] we simply remove all r^{th} fibres from \mathcal{T} , obviously such transformation preserves super-symmetry.

Algorithm 12 Cumulants based features selection, see also [217].

```

1: Input:  $\mathcal{C}_{d_1} \in \mathbb{R}^{[n, d_1]}, \mathcal{C}_{d_2} \in \mathbb{R}^{[n, d_2]}, \dots$  - cumulant's tensors,  $h$  - target function,  $s < n$ 
   - Int, a stop condition.
2: Output: a subset of marginals that carries important information.
3: function FEATURES SELECT( $\mathcal{C}_{d_1}, \mathcal{C}_{d_2}, \dots, h, s$ )
4:   for  $n'$  in  $n, n-1, \dots, s$  do
5:     for  $i \leftarrow 1$  to  $n'$  do
6:        $m_i = h(\mathcal{C}_{d_1(-i)}, \mathcal{C}_{d_2(-i)}, \dots)$ 
7:     end for
8:     set  $r$  such that  $m_r = \max(\{m_1, \dots, m_{n'}\})$ 
9:      $\mathcal{C}_{d_1}, \mathcal{C}_{d_2}, \dots = \mathcal{C}_{d_1(-r)}, \mathcal{C}_{d_2(-r)}, \dots$ 
10:  end for
11:  return reminding  $s$  marginals.
12: end function

```

It is easy to show referring to Definition 5.0.3, that given $\mathfrak{X}^{(n)}$ and its cumulant's tensor \mathcal{C}_d if we change $\mathfrak{X}^{(n)}$ to $\mathfrak{X}^{(n-1)}$ by removing r^{th} marginal, the new cumulant's tensor would be $\mathcal{C}'_d = \mathcal{C}_{d(-r)}$. Hence following [47, 204, 217] we can use the following target function

$$h(\mathcal{C}_{d_1}, \mathcal{C}_{d_2}, \dots) \quad (6.4)$$

and maximise it at each iterative step, while removing a feature that carries little information tied to non-Gaussian joint distribution of features. Such procedure, see Algorithm 12, is discussed in [204], and [217] where it was applied to analyse hyper-spectral data in the small target detection problem. For the implementation in the Julia programming language see [242]. In following subsections we discuss various target functions.

6.1.1 Classical method MEV

Before moving to higher order cumulants, for the sake of comparison, consider the MEV (Maximum Ellipsoid Volume) [70] that uses information stored in the covariance matrix - hence the MEV is appropriate for multivariate Gaussian distributed data. Following [70] the MEV measures information stored in the covariance matrix by means of the volume of the hyper-ellipsoid spanned on its eigenvectors. It follows from fact that the covariance matrix Σ , being real valued, symmetric, and positively semi definite, can be decomposed according to Eq. (3.9):

$$\Sigma = \mathbf{A} \Sigma_{(d)} \mathbf{A}^\top, \quad (6.5)$$

where $\Sigma_{(d)}$ is a diagonal matrix with elements $\lambda_1, \dots, \lambda_n$ on its diagonal. Here each $\lambda_i \geq 0$ is a non-negative eigenvector of Σ . Columns of \mathbf{A} , *i.e.* A_1, \dots, A_n are normalised eigenvectors of Σ . Since \mathbf{A} is an unitary matrix, the determinant of the covariance matrix can be written as:

$$\det(\Sigma) = \det(\Sigma_{(d)}) = \prod_{i=1}^n \lambda_i. \quad (6.6)$$

This determinant is proportional to the hyper-ellipsoid volume span by vectors $\lambda_1 A_1, \dots, \lambda_n A_n$. Thus, as discussed in [70], we can use such decomposition in data processing, if we have multivariate Gaussian distributed data and the meaningful information is tied to the variance of features (we are not interested in the mean vector). In such approach, the higher the absolute value of the cross-correlation between two features (marginals) the more information carried by the first one is carried by the second one as well. Having a pair of highly (positively or negatively) cross-correlated marginals, two columns of the correlation matrix Σ would be similar (or approximately proportional) and one eigenvalue in Eq. (6.6) would be small (near zero) affecting strongly the determinant. Suppose now, that we remove one marginal, in such a way, that the determinant of reminding data is maximised. Here we would remove one of two highly cross-correlated marginals, but we would preserve most information. Based on these, we can have the iterative dimensionality reduction procedure. At each step we remove one marginal in such a way, that we maximise the determinant of the correlation matrix of reminding data. Performing iterations, we would obtain a subset of marginals that carry significant part of information. Nevertheless the discussion on the lose of information, and acceptable information error is necessary to determine the stop condition of iterations. For further discussion on the MEV see [70]. Importantly, if the multivariate distribution of data is non-Gaussian, not all information would be tie to the covariance matrix and the MEV procedure may not be optimal. Such scenarios will be discussed in the reminding part of this section.

At the end let us refer to the simple example. Suppose we have two repeating marginals. The covariance matrix would have two the same columns, one of its eigenvalue would be zero, and the determinant in Eq. (6.6) would be zero. By removing one of the two marginals (assuming all other marginals differs from each other) we have a non-zero determinant of reminding data set, but the information carried by data is not reduced.

6.1.2 Cumulant based features selection

Following [204, 217] we propose to modify the MEV algorithm to handle non-Gaussian distributed data. Suppose, we have data for with information is tied to non-Gaussian joint distribution of features. To analyse such data, we apply method based on the High Order Singular Value Decomposition (HOSVD), see [243, 244, 210] of the higher order cumulant's tensor.

Definition 6.1.2. Let $\mathcal{C} \in \mathbb{R}^{[n,d]}$ be the super-symmetric tensor. The relation

$$\mathcal{C} = \mathbf{1} \times_{1,\dots,d} \mathcal{C} = \mathbf{A}\mathbf{A}^\top \times_{1,\dots,d} \mathcal{C} = \mathbf{A} \times_{1,\dots,d} \mathcal{C}', \quad (6.7)$$

is called its HOSVD decomposition, for used there notation see Definition 5.2.1. Here $\mathbf{A} \in \mathbb{R}^{n \times n}$ is an unitary factor matrix and $\mathbf{A}\mathbf{A}^\top = \mathbf{1}$. Tensor

$$\mathbb{R}^{[n,d]} \ni \mathcal{C}' = \mathbf{A}^\top \times_{1,\dots,d} \mathcal{C} \quad (6.8)$$

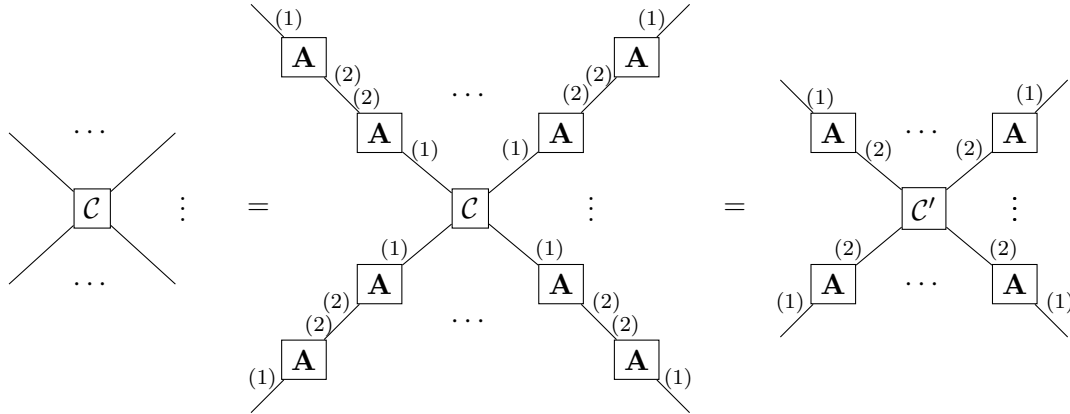
is called the core-tensor. Eq. (6.8) can be shown using element wise notation, where

$$t'_{j_1, \dots, j_n} = \sum_{i_1, \dots, i_n} a_{i_1, j_1} \dots a_{i_n, j_n} t_{i_1, \dots, i_n}. \quad (6.9)$$

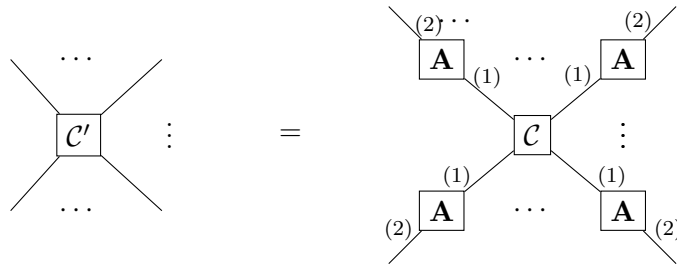
To introduce a graphic notation observe that by Definition 5.2.3 for an unitary matrix the $\mathbf{A}\mathbf{A}^\top = \mathbb{1}$ can be represented graphically by

$$\text{---} \boxed{\mathbb{1}} \text{---} = \text{---} \boxed{\mathbf{A}}^{(1)} \boxed{\mathbf{A}}^{(2)} \text{---} \boxed{\mathbf{A}}^{(2)} \boxed{\mathbf{A}}^{(1)} \text{---}$$

Hence, Eq. (6.7) can be represented in a graphic notation (see Definition 5.2.4), from which clearly comes Eq. (6.8)



The Eq. (6.8) can be represented in the graphical notation as



Observe, that definition 6.1.2 concerns only the HOSVD of the super-symmetric tensor being of our interest since cumulants tensors are super-symmetric. In the general tensor case [244], the HOSVD is more complex, yielding d distinct factor matrices.

Let us now discuss the standard method of finding the factor matrix [244] of the HOSVD of the super-symmetric tensor case.

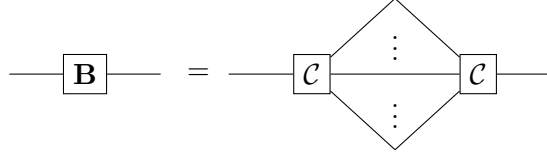
Definition 6.1.3. Let $\mathcal{C} \in \mathbb{R}^{[n,d]}$ be a super-symmetric tensor, its contraction with itself in $d - 1$ modes (all modes but first) produces the following symmetric matrix

$$\mathbb{R}^{[n,2]} \ni \mathbf{B} = \sum_{\mathbf{i} \setminus (i_1)} \mathcal{C}\mathcal{C}, \tag{6.10}$$

with elements

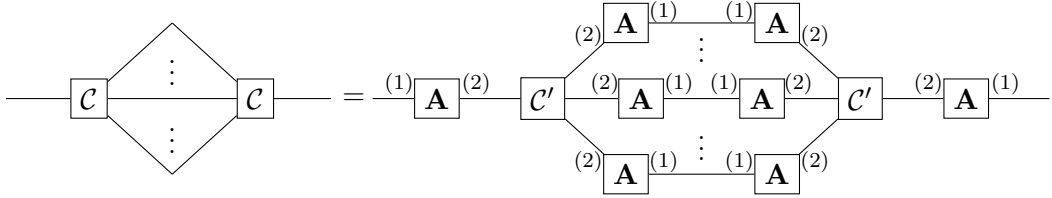
$$b_{j_1, j_2} = \sum_{i_2, \dots, i_n} c_{j_1, i_2, \dots, i_n} c_{j_2, i_2, \dots, i_n}. \tag{6.11}$$

The matrix \mathbf{B} is symmetric, since indices j_1 and j_2 are exchangeable in Eq. (6.11). Further due to the super-symmetry of \mathcal{C} it does not matter in which $d - 1$ modes we contract \mathcal{C} by itself. We can introduce a graphic notation analogical to Definition 5.2.3 and Definition 5.2.4. On the graphic notation, each connection between tensors accounts for the contraction in one mode. In Eq. (6.11) we have contractions over $n - 1$ indices (corresponding to $n - 1$ modes). These correspond to the following graphical notation (with $n - 1$ connections between \mathcal{C} and \mathcal{C}),

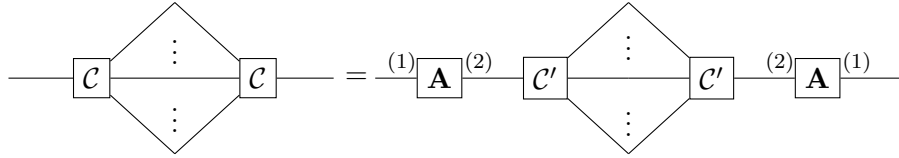


We do not number edges due to symmetry / super-symmetry of all objects involved.

Replacing \mathcal{C} by its HOSVD, we have



Using $\mathbf{A}^\top \mathbf{A} = \mathbb{1}$ we have



Analogically, using tensor notation

$$\sum_{\mathbf{i} \setminus i_1} \mathcal{C} \mathcal{C} = \mathbf{A} \left(\sum_{\mathbf{i} \setminus i_1} \mathcal{C}' \mathcal{C}' \right) \mathbf{A}^\top. \quad (6.12)$$

Recall now that Eq. (6.12) is similar to Eq. (6.5) in such a way in which the HOSVD is similar to the Eigenvalue Decomposition. Our strategy is to perform the Singular Value Decomposition of the $\sum_{\mathbf{i} \setminus i_1} \mathcal{C} \mathcal{C}$ matrix, yielding $\sum_{\mathbf{i} \setminus i_1} \mathcal{C}' \mathcal{C}'$ that is a diagonal matrix of eigenvalues of $\sum_{\mathbf{i} \setminus i_1} \mathcal{C} \mathcal{C}$. Importantly, in Eq. (6.10) we can rearrange summation over i_2, \dots, i_d to the summation over one index

$$j = 1 + \sum_{k=2}^d (i_k - 1) d^{k-2}. \quad (6.13)$$

Hence j is uniquely determined by i_2, \dots, i_d . Now Eq. (6.10) is equivalent to

$$\mathbf{B} = \mathbf{V}^T \mathbf{V} = \sum_{\mathbf{i} \setminus i_1} \mathcal{C} \mathcal{C}, \quad (6.14)$$

where $\mathbf{V} \in \mathbb{R}^{n^{d-1} \times n}$ is a matrix being a transposition of the unfold in first mode of the tensor \mathcal{C} according to definition [75]. Elements of \mathbf{V} are

$$v_{j, i_1} = c_{i_1, i_2, \dots, i_d}, \quad (6.15)$$

where index j is given by Eq. (6.13). Due to Eq. (6.14) we expect \mathbf{B} to be positive definite. To enlighten the meaning of the \mathbf{V} in higher order cross-correlation analysis let us refer to the following remark and example.

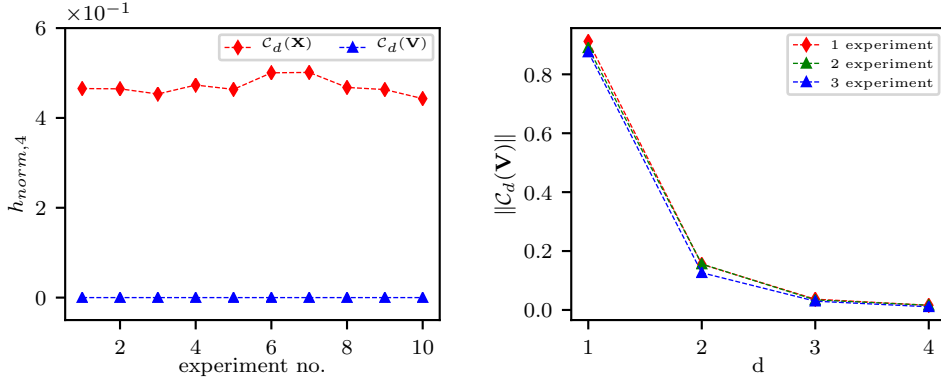
Remark 6.1.1. Suppose, \mathbf{V} is an unfold of the d^{th} order cumulant of original data \mathbf{X} , see Eq. (6.15). We, can treat \mathbf{V} as a data vector of n marginals and n^{d-1} realisations. Its i^{th} column (V_i) contains all possible d^{th} order cross-correlation between the i^{th} marginal of original data \mathbf{X} and all other marginals. See also [204] for further discussion on the 4th cumulant's case. Hence \mathbf{V} carries information about higher order cross-correlation between margins of original data. Each column of V_i contains a lot of combinations of d^{th} order correlations with all other marginals, hence there is a hope for some sort of the Central Limit Theorem, yielding that \mathbf{V} would be Gaussian or almost Gaussian distributed. Furthermore there is a suggestion, based on experiments, that $\mathbf{V} \in \mathbb{R}^{n^{d-1} \times n}$ is much nearer to the multivariate Gaussian distribution than the original data \mathbf{X} , see Example 6.1.1.

Example 6.1.1. *Let us take the artificial data $\mathbf{X} \in \mathbb{R}^{t \times n}$ sampled for the t -Student copula parametrised by the Topelitz \mathbf{R} matrix with $\rho = 0.95$, see Figure 4.3(c), and $\nu = 5$. As priorly we assume standard normal marginals. Next we compute $\mathcal{C}_4(\mathbf{X})$ and its unfold $\mathbf{V} \in \mathbb{R}^{n^3 \times n}$ as in Eq. (6.15). We use $n = 50$ and $t = 50^3$ to compare data of the same size. In Figure 6.5 we present measures based on the Frobenius norms of cumulants of \mathbf{V} and \mathbf{X} . It results, that \mathbf{V} is much nearer to the Gaussian distribution than \mathbf{X} , see $h_{\text{norm},4}$ in Figure 6.5(a). Further most of information of \mathbf{V} is stored in the mean vector, see Figure 6.5(b), hence we can not use zero mean \mathbf{V} for analysis.*

Based on the discussion above we use \mathbf{B} , as in Eq. (6.14) to measure higher order cross-correlation in \mathbf{X} . In fact \mathbf{B} is a sum of the covariance matrix of \mathbf{V} and an outer produce of the mean vector and mean vector transposition of \mathbf{V} . Further \mathbf{V} is assumed to be Gaussian or almost Gaussian assumed. Henceforth the transformation $\mathcal{C} \rightarrow \mathcal{C}'$, see Eq. (6.12) is consistent with the transformation of the \mathbf{B} matrix. Although, since \mathbf{A} is unitary we have the following equality in the sense of the Frobenius norm

$$\|\mathbf{B}\| = \|\mathbf{V}^T \mathbf{V}\| = \left\| \sum_{\mathbf{i} \setminus i_1} \mathcal{C} \mathcal{C} \right\| = \left\| \sum_{\mathbf{i} \setminus i_1} \mathcal{C}' \mathcal{C}' \right\| \text{ and } \|\mathcal{C}\| = \|\mathcal{C}'\| \quad (6.16)$$

As \mathbf{V} is expected to be Gaussian distributed or at least near the Gaussian distribution, we can measure the information while using the Frobenius norm. This will be further



(a) Comparison of $h_{\text{norm},4}(\mathbf{X})$ and $h_{\text{norm},4}(\mathbf{V})$ and (b) Norms $\|C_d(\mathbf{V})\|$ for experiments from 6.5(a)

Figure 6.5: Cumulants based measures the distance form the multivariate Gaussian distribution for \mathbf{X} and \mathbf{V} . Original data \mathbf{X} are generated by means of the t -Student copula parametrised by the Topelitz matrix \mathbf{R} and the scalar parameter $\nu = 5$, with standard Gaussian marginals. The \mathbf{V} is an unfold of the $C_4(\mathbf{X})$. Using the $h_{\text{norm},4}$ measure, one can conclude that \mathbf{V} is nearer to the multivariate Gaussian distribution than \mathbf{X} .

related to the mean squared approximation of Gaussian distributed data. We can assume that by the transformation $\mathcal{C} \rightarrow \mathcal{C}'$ we do not lose significantly information [244] stored in \mathcal{C} .

Referring to Eq. (6.16), in general $\|\mathcal{C}\| \neq \|\sum_{\mathbf{i} \setminus i_1} \mathcal{C}\mathcal{C}'\|$. Nevertheless we expect some monotone relation between $\|\mathcal{C}\|$ and $\|\sum_{\mathbf{i} \setminus i_1} \mathcal{C}\mathcal{C}'\|$, to tie information carried by \mathcal{C} with information carried by $\sum_{\mathbf{i} \setminus i_1} \mathcal{C}'\mathcal{C}'$. See [244] and discussion in Remark 6.1.1. Further, since \mathbf{A} is unitary we have:

$$\det \left(\sum_{\mathbf{i} \setminus i_1} \mathcal{C}\mathcal{C}' \right) = \det \left(\sum_{\mathbf{i} \setminus i_1} \mathcal{C}'\mathcal{C}' \right) = \prod \left(\text{diag} \left(\sum_{\mathbf{i} \setminus i_1} \mathcal{C}'\mathcal{C}' \right) \right). \quad (6.17)$$

The last term is the product of diagonal elements of $\sum_{\mathbf{i} \setminus i_1} \mathcal{C}'\mathcal{C}'$, that is a diagonal matrix.

Based on proposed relation between \mathcal{C} and the product of diagonal elements of $\sum_{\mathbf{i} \setminus i_1} \mathcal{C}'\mathcal{C}'$, in the informative sense, we will use $\det \left(\sum_{\mathbf{i} \setminus i_1} \mathcal{C}_d \mathcal{C}_d \right)$ to measure information tied to d^{th} order cross-correlations between marginals of data for which \mathcal{C}_d is computed. Hence we introduce following general target function for non-Gaussian features selection.

$$h_{\det,d}(\mathcal{C}_2, \mathcal{C}_d) = \frac{\det \left(\sum_{\mathbf{i} \setminus i_1} \mathcal{C}_d \mathcal{C}_d \right)}{\det(\mathcal{C}_2)^d} \quad (6.18)$$

The normalisation (denominator) assures that in univariate case we reproduce the module of asymmetry if $d = 3$ and the module of kurtosis if $d = 4$. See [217] for further discussion

on the normalisation and the application of Eq. (6.18) to analyse real life hyper-spectral data.

Following the argumentation from subsection 6.1.1 the determinant in the numerator would be near zero in two cases. The first case concerns two similar columns of the matrix $\mathbf{B} = \mathbf{V}^T \mathbf{V} = \det \left(\sum_{i \setminus i_1} \mathcal{C}_d \mathcal{C}_d \right)$. This would correspond to two features with similar d^{th} order cross-correlations with all other features. Hence, from the informative point of view, one of these features would be redundant. The second case concerns zero all d^{th} order cross-correlations of the i^{th} feature. Such feature may be suspected to be Gaussian distributed. Hence, we expect to remove such Gaussian features by Algorithm 12.

Experiments concerning features selection based on $h_{\text{det},d}$ are widely discussed in [203, 204]. For some experiments on artificial data, see also next subsection.

6.1.3 Experiments

In this subsection we test algorithms introduced in this chapter on artificial data generated, see Section 4.4. For each experiment's realisation we start with data $\mathbf{X} \in \mathbb{R}^{t \times n}$ randomly sampled from multivariate Gaussian distribution $\mathcal{N}(0, \mathbf{R})$. The \mathbf{R} is the positive definite symmetric correlation matrix with ones on a diagonal, generated at random for each experiment, see random method in Subsection 4.5.2 and Figure 4.3(a). Next we change chosen at random subset of marginals $|\mathbf{r}| = k$ by means of t -Student, Fréchet or Archimedean nested copulas. The transformation is performed in such a way that the correlation matrix of changed data is similar to the covariance matrix of an original data. Next, we perform the features selection procedure. We remove iterative low-informative features using one of following target functions: $h_{\text{det},d}$, $h_{\text{norm},d}$ or the MEV. See also [217] for the application of the $h_{\text{det},d}$ on real life hyper-spectral data and the iteration algorithm. We perform the iterative elimination of features as long as there remains k features left, that are most informative according to the target function. Next we check how many of these k features are correctly selected as features from the non-Gaussian copula subset. We denote number of correctly selected features by $|\mathbf{r}_{\text{detected}}|$, obviously in our setting the perfect outcome would give $|\mathbf{r}_{\text{detected}}| = k$. In Figure 6.6 we present the empirical probability of the number of detections, given different target functions in Figure 6.6(a) or different non-Gaussian copulas of changed subset of features in Figure 6.6(b). For further experiments see [204] in the case of the t -Student copula and [203] in the case of Archimedean Copulas.

Referring to Figure 6.6(a) we have a poor performance of the MEV similar to the random guess. This is due to the fact that the transformation of marginal's subset does not affect significantly the covariance matrix, that is used by the MEV method to extract information, see Subsection 4.5.2. On the other hand, we have a good performance of the 3rd cumulant based method, as absolute values of 3rd cumulant's tensor's elements for the Clayton copula (with Gaussian marginals) are relatively large, see Figure 5.2(a) and compare it with Figure 5.3(a) for 4th cumulant's elements for this copula. In these experiments we use cross-correlation between marginals, as in Figure 4.3(a), due the random \mathbf{R} matrix generation algorithm. For the 4th cumulant case the $h_{\text{det},4}$ function is

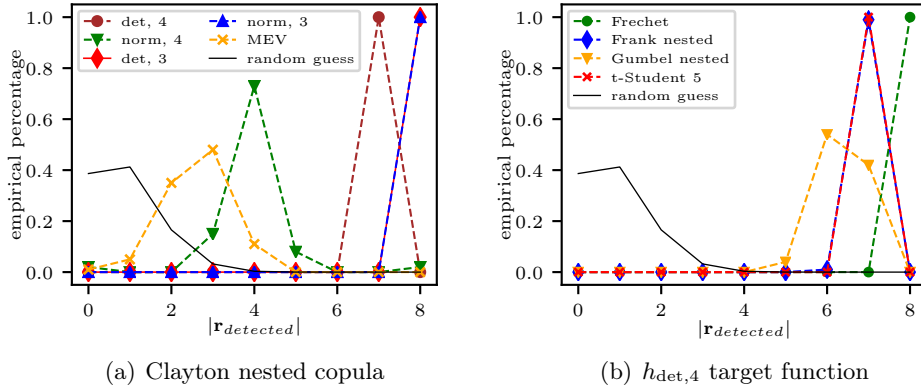


Figure 6.6: Features selection experiments $t = 10^5$, $n = 75$, $k = 8$, and 100 experiments realisations. Cumulant’s based methods are compared with the MEV and the random guess. On the horizontal axis there are numbers of correctly detected features, the more to the right the better the results. Results of the MEV are poor as it was expected. Results of the $h_{\text{det},4}$ for Fréchet, t -Student and Frank copula are good. For Clayton copula methods using the 3rd cumulant seems to work better than these using the 4th cumulant.

much better than $h_{\text{norm},4}$ and almost as good as the 3rd cumulant’s based methods. Hence sophisticated HOSVD based method discussed in Subsection 6.1.2 have an advantage over the simple norm of the cumulant’s tensor.

Nevertheless the 4th cumulant’s based methods are more general, since there are copulas (such as a t -Student one, widely used in the financial data analysis) for which elements of the 3rd cumulant’s tensor are zero, given symmetric marginal distributions. Hence, we will use the target function $h_{\text{det},4}$ to analyse more general case for various copulas. Referring to Figure 6.6(b) we have good detection for all copulas, far from the random guess case. Best results gives the Fréchet copula, next we have t -Student and Frank copulas. We observe, the worse detectability of features modelled by the Gumbel copula if using the 4th cumulant’s based method. This comes from the fact that for the Gumbel copula with high cross-correlations, 4th cumulant’s elements are small, see Figure 5.3(b). For the corss-correlation level between marginals during experiments see Figure 4.3(a).

6.2 Features extraction

Having discussed the cumulant’s based features selection, we can move to another dimensionality reduction scenario, the features extraction. Let us start as in the previous section with n -variate random vector $\mathfrak{X}^{(n)}$. Its t realisations are given in a form of a matrix $\mathbf{X} \in \mathbb{R}^{t \times n}$, where n marginals are features. Features extraction is the projec-

tion of features onto directions that carry most meaningful information [65]. In other words we want to find such linear combinations of marginals that carry most meaningful information. Suppose we have the following factor matrix $\mathbf{A}' \in \mathbb{R}^{n \times n'}$, where $n' < n$. In our case we would use the orthonormal columns corresponding to n' 'independent' features, hence $(\mathbf{A}')^\top \mathbf{A}' = \mathbf{1}$, but $\mathbf{A}'(\mathbf{A}')^\top \neq \mathbf{1}$. We can reduce dimensionality of data by performing the transformation

$$\mathbb{R}^{t \times n'} \ni \mathbf{Y}' = \mathbf{X}\mathbf{A}' \quad (6.19)$$

Columns of \mathbf{Y}' represent linear combinations of original features. If matrix \mathbf{A} is properly determined most of information from \mathbf{X} will remain in \mathbf{Y}' .

Suppose that n is large, it would be computationally complex to use whole $\mathbf{X} \in \mathbb{R}^{t \times n}$ in some sophisticated machine learning algorithm e.g. classifying realisations $\mathbf{x}_j \in \mathbb{R}^n$ to given classes, detecting outlier realisations or fitting some model to data. Further it may require large computer memory to store or process a whole \mathbf{X} especially if t is large. But, if we chose such \mathbf{A}' that most of meaningful information from \mathbf{X} is still present in $\mathbf{Y}' \in \mathbb{R}^{t \times n'}$ and $n' \ll n$, we would have a significant gain on computational complexity or computational memory, see [65].

Example 6.2.1. *In the case of financial data analysis, consider investment portfolio management, where we are basically interested in finding such portfolios of assets that are characterised by low risk. It can be done, in a statistical approach, by the analysis of statistics of historical assets values. Obviously, we assume that the probabilistic model of future data will be similar to the probabilistic model of past data. Suppose $\mathbf{X} \in \mathbb{R}^{t \times n}$ represents data of t past records of n assets returns. To minimise risk, we need to find such linear combination of assets that has low variability, what is an opposite approach to the information maximisation. We have*

$$\mathbb{R}^{t \times n''} \ni \mathbf{Y}'' = \mathbf{X}\mathbf{A}'', \quad (6.20)$$

suppose another factor matrix \mathbf{A}'' is determined in such a way, that it projects data on directions caring most information about the variability of data. Hence we can search for directions, orthogonal to those in \mathbf{A}' projecting data onto directions with low variability. Assuming such directions are orthonormal to each other, they can be stored in the orthonormal factor matrix \mathbf{A}'' . One of the methods of obtaining \mathbf{A}'' will be searching for columns orthogonal to columns from \mathbf{A}' .

The most popular method of determining the factor matrix \mathbf{A}' (and \mathbf{A}'') is the Singular Value Decompositions (SVD) of a covariance matrix. Let us concentrate on \mathbf{A}' , following Eq. (6.5) we have

$$\mathcal{C}_2 = \mathbf{A}\boldsymbol{\Sigma}_{(d)}\mathbf{A}^\top. \quad (6.21)$$

If we shuffle columns of \mathbf{A} in such a way that eigenvalues are in decreasing order (these eigenvalues are real and non-negative) first columns of matrix \mathbf{A} would correspond to largest information or highest variability of linear combination of features in reference to the covariance matrix. Here by taking first n' columns of \mathbf{A} we can determine the

factor matrix that preserves most of information, see [245]. The covariance matrix $\Sigma'_{(d)} = \mathbf{A}'^T \mathcal{C}_2 \mathbf{A}'$ of new data $\mathbf{Y} = \mathbf{X} \mathbf{A}'$ would be a diagonal one composed of highest n' eigenvectors of \mathcal{C}_2 .

For a graphic representation clarity, we assume centred $\tilde{\mathbf{X}}$, such that $\mathcal{C}_1(\tilde{\mathbf{X}}) = 0$, hence $\mathcal{C}_1(\tilde{\mathbf{Y}}) = 0$. We can discuss $\tilde{\mathbf{Y}}$ using a graphic notation. Starting with:

$$\text{---} \boxed{\tilde{\mathbf{Y}}} \text{---}^{(1)} \text{---}^{(2)} = \text{---} \boxed{\tilde{\mathbf{X}}} \text{---}^{(1)} \text{---}^{(2)} \text{---} \boxed{\mathbf{A}'} \text{---}^{(2)}$$

the covariance matrix of $\tilde{\mathbf{Y}}$ is

$$\text{---} \boxed{\mathcal{C}'_2} \text{---} = \text{---} \boxed{\tilde{\mathbf{Y}}} \text{---}^{(2)} \text{---} \boxed{\tilde{\mathbf{Y}}} \text{---}^{(1)} \text{---} \boxed{\tilde{\mathbf{Y}}} \text{---}^{(2)} \text{---} = \text{---} \boxed{\mathbf{A}'} \text{---}^{(2)} \text{---} \boxed{\tilde{\mathbf{X}}} \text{---}^{(1)} \text{---} \boxed{\tilde{\mathbf{X}}} \text{---}^{(1)} \text{---} \boxed{\tilde{\mathbf{X}}} \text{---}^{(2)} \text{---} \boxed{\mathbf{A}'} \text{---}^{(2)}$$

but

$$\text{---} \boxed{\mathcal{C}_2} \text{---} = \text{---} \boxed{\tilde{\mathbf{X}}} \text{---}^{(2)} \text{---} \boxed{\tilde{\mathbf{X}}} \text{---}^{(1)}$$

The covariance matrix of $\tilde{\mathbf{Y}}$ will be:

$$\text{---} \boxed{\mathcal{C}'_2} \text{---} = \text{---} \boxed{\mathbf{A}'} \text{---}^{(2)} \text{---} \boxed{\mathcal{C}_2} \text{---} \boxed{\mathbf{A}'} \text{---}^{(1)}$$

In the case of non-centred data \mathbf{X} we need to observe that if $\mathbf{Y}' = \mathbf{X} \mathbf{A}'$ than $\tilde{\mathbf{Y}}' = \tilde{\mathbf{X}} \mathbf{A}'$ and use $\mathcal{C}_2(\tilde{\mathbf{Y}}) = \mathcal{C}_2(\mathbf{Y})$.

If we use $\mathbf{A}' \in \mathbb{R}^{n \times n'}$ where $n > n'$ and $\mathbf{A}'^T \mathbf{A}' = \mathbf{1}$, the transformation $\mathbf{Y}' = \mathbf{X} \mathbf{A}'$ will loose some information in the sense of the Frobenius norm

$$\|\mathcal{C}_2\| < \|\mathcal{C}'_2\| \text{ or } \|\mathbf{Y}'\| < \|\mathbf{X}\|. \quad (6.22)$$

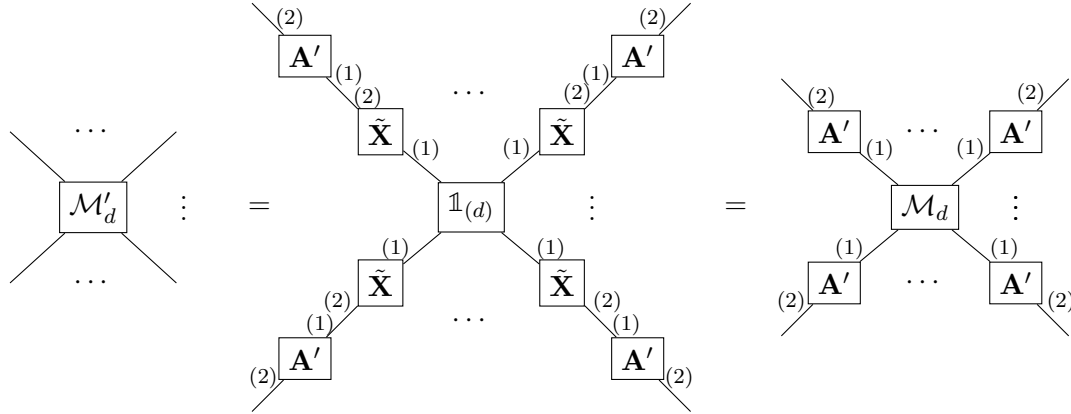
hence we have to chose a proper value of n' to make an information lose acceptable. In these approximation the lose of information is minimised by the minimisation of the mean square error measured by the Frobenius norm. Such approach is optimal for Gaussian distributed multivariate data. Unfortunately most of real life data, such as financial one are usually non-Gaussian distributed. Hence, these simple approach is not optimal. Higher order statistics may play a vital role in more adequate approach for these data.

6.2.1 High Order Singular Value Decomposition

Suppose now we have a following linear data transformation $\mathbf{Y}' = \mathbf{X} \mathbf{A}'$. We can take zero mean example $\tilde{\mathbf{Y}}' = \tilde{\mathbf{X}} \mathbf{A}'$ for simplicity. One can show, that the d^{th} order cumulant for $d \geq 2$ (for $d = 1$ we do not have equity between the cumulant of centred and non-centred data) of \mathbf{Y} or $\tilde{\mathbf{Y}}$ would be

$$\mathbb{R}^{[n',d]} \ni \mathcal{C}'_d = (\mathbf{A}')^T \times_{1,\dots,d} \mathcal{C}_d, \quad (6.23)$$

where $\mathcal{C}_d \in \mathbb{R}^{[n,d]}$ is the d^{th} order cumulant of \mathbf{X} or $\tilde{\mathbf{X}}$, and $\mathbf{A} \in \mathbb{R}^{n \times n'}$ is a factor matrix. Let us refer to a notation for the d^{th} order central moment, see Definition 5.2.4, of $\tilde{\mathbf{Y}}' = \tilde{\mathbf{X}} \mathbf{A}'$. For the proof of Eq. (6.23) refer to graphical notation



shows the relation between central moments of \mathbf{Y}' and \mathbf{X} , namely

$$\mathbb{R}^{[n',d]} \ni \mathcal{M}'_d = (\mathbf{A}')^\top \times_{1,\dots,d} \mathcal{M}_d. \quad (6.24)$$

Hence, Eq. (6.23) holds for cumulant of order $d = 2$ and $d = 3$ as these are central moments. For $d > 3$, one need to refer to the graphic representation of corresponding cumulant, see Remarks 5.2.5 5.2.6 5.2.7, use Eq. (6.24) and the fact that Eq. (6.23) holds for $2, \dots, d - 2$.

Now our task is to find such factor matrix that gives highly informative features with respect to the d^{th} order cumulant. This can be performed by means of the HOSVD procedure of the corresponding cumulant's tensor. Suppose $\mathbf{A} \in \mathbb{R}^{n \times n}$ is an unitary column matrix of eigenvectors of $\sum_{\mathbf{i} \setminus i_1} \mathcal{C}_d \mathcal{C}_d$, see Eq. (6.12). The core-tensor fulfils $\mathcal{C}'_d = (\mathbf{A})^\top \times_{1,\dots,d} \mathcal{C}_d$, and referring to Eq. (6.12) we get

$$\sum_{\mathbf{i} \setminus i_1} \mathcal{C}_d \mathcal{C}_d = \mathbf{A} \left(\sum_{\mathbf{i} \setminus i_1} \mathcal{C}'_d \mathcal{C}'_d \right) \mathbf{A}^\top. \quad (6.25)$$

where $\sum_{\mathbf{i} \setminus i_1} \mathcal{C}'_d \mathcal{C}'_d$ is diagonal eigenvalue matrix. Hence, if we shuffle columns of \mathbf{A} is such a way that its eigenvalues are sorted in decreasing order (given they are real and non-negative) first columns of \mathbf{A} should give a linear combination of data with high information measured by the d^{th} cumulant. To discuss this in more details consider $\mathbf{V}_y \in \mathbb{R}^{n^{d-1} \times n}$, that is the matrix representation of \mathcal{C}' with elements given by Eq. (6.15). We have

$$(\mathbf{V}_y)^\top \mathbf{V}_y = \sum_{\mathbf{i} \setminus i_1} \mathcal{C}'_d \mathcal{C}'_d. \quad (6.26)$$

Following Remark 6.1.1 the i^{th} column of \mathbf{V}_y contains d^{th} order cross-correlations of the i^{th} marginal of $\mathbf{Y} = \mathbf{X}\mathbf{A}$ with all other marginals of \mathbf{Y} . Further as discussed in Remark 6.1.1 data in \mathbf{V}_y should be n -variate Gaussian distributed or have a probabilistic model near to the Gaussian one. Due to the Singular Value Decomposition matrix $(\mathbf{V}_y)^\top \mathbf{V}_y$ is diagonal. Concluding, columns of \mathbf{V}_y can be ordered with respect to the information they carry about the d^{th} order cross-correlation of data. Assuming the

Gaussian model of \mathbf{V}_y we can use the mean square error approximation in the analysis of the decomposition.

Analogically to the Singular Value Decomposition of the covariance matrix case, if we use unitary $\mathbf{A} \in \mathbb{R}^{n \times n}$ we have the following information conservation in the sense of the Frobenius norm,

$$\|(\mathbf{A})^\top \times_{1,\dots,d} \mathcal{C}_d\| = \|\mathcal{C}_d\| \text{ and } \|\mathbf{X}\mathbf{A}\| = \|\mathbf{X}\|. \quad (6.27)$$

Given the eigenvalues ordering, one can conclude, that elements of the following core tensor $\mathcal{C}'_d = (\mathbf{A})^\top \times_{1,\dots,d} \mathcal{C}_d$ indexed by low multi-index (left right corner in the $d = 3$ case), should have relatively large impact to the Frobenius norm of this core tensor $\|\mathcal{C}'_d\|$ [244]. Such ordering leads to $\mathbf{A}' \in \mathbb{R}^{n \times n'}$ composed of first n' columns of \mathbf{A} . Such \mathbf{A}' can be used to achieve a linear combination of data carrying most of information with respect to d^{th} order cumulant. We have here

$$\|(\mathbf{A}')^\top \times_{1,\dots,d} \mathcal{C}_d\| < \|\mathcal{C}_d\|. \quad (6.28)$$

Hence, we have to chose such n' to make an information lose acceptable. In the next subsection we will discuss a real life data application of the procedure.

6.2.2 Multi-cumulant higher order singular value decomposition

In this subsection, following [39], we discuss the procedure of the real life financial data analysis where we want to find such factor matrix that gives low risk investment portfolios. Investment portfolio is composed of many assets, negative quantity of assets is possible and correspond to the ‘short sale’. The value of the portfolio is the linear combination of values of these assets (often being shares prices). To determine the low risk portfolio we want to reduce its variability measured by cumulants of order $2, 3, \dots, d$. In [39] the author has shown, that such approach, given $d = 6$, gives relatively save portfolios of shares traded on the Warsaw Stock Exchange, during the crisis of year 2015. On average, the losses on such portfolios were smaller than the loss of the benchmark being the stock exchange index (WIG20).

To determine safe portfolios we use the Alternating Least Squares (ALS) algorithm, which is some composition of the HOSVD of cumulants tensors and the Singular Value Decomposition of the covariance matrix [225, 246, 247]. The ALS searches for the local maximum of the function

$$\xi_d(\mathbf{A}') = \frac{1}{2!} \|\mathbf{A}'^\top \mathcal{C}_2 \mathbf{A}'\| + \sum_{k=3}^d \frac{1}{k!} \|(\mathbf{A}')^\top \times_{1,\dots,k} \mathcal{C}_k\|, \quad (6.29)$$

given $\mathbf{A}'^\top \mathbf{A}' = \mathbb{1}$ where $\mathbf{A}' \in \mathbb{R}^{n \times n'}$ and $n' < n$, where n' is a parameter. Following [39], we discuss here the following iterative approach.

1. In the first step we construct the matrix

$$\mathbb{R}^{[n,2]} \ni \mathbf{T}_\xi = \frac{1}{2!} \mathcal{C}_2 \mathcal{C}_2 + \sum_{k=3}^d \frac{1}{k!} \sum_{\mathbf{i} \setminus (i_1)} \mathcal{C}_k \mathcal{C}_k. \quad (6.30)$$

2. We perform the eigenvalue decomposition of \mathbf{T}_ξ ,

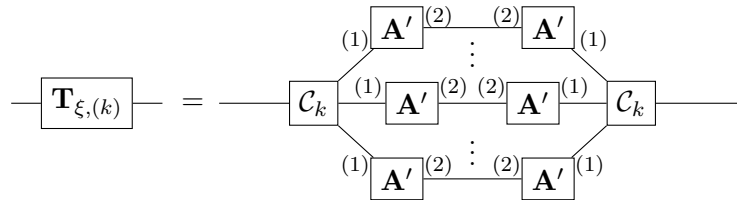
$$\mathbf{T}_\xi = \mathbf{A}\mathbf{T}_{(d)}\mathbf{A}^\top \tag{6.31}$$

where \mathbf{A} is unitary matrix which columns are eigenvectors of \mathbf{T}_ξ and $\mathbf{T}_{(d)}$ is diagonal matrix of real non-negative eigenvalues sorted in decreasing order. Here $\mathbf{A}' \in \mathbb{R}^{n \times n'}$ is supposed to carry meaningful information. Such information would be tied both to its standard measure being a covariance of features and not-standard measures being higher order cross-correlations of order $(3, 4, \dots, d)$.

3. In the p^{th} step we take a factor matrix from the $(p - 1)^{\text{th}}$ step, compute

$$\mathbf{T}_{\xi,(k)} = \sum_{\mathbf{i} \setminus (i_1)} \mathcal{T}_k \mathcal{T}_k \text{ where } \mathcal{T}_k = \mathbf{A}'_{(p-1)}^\top \times_{2,\dots,k} \mathcal{C}_k, \tag{6.32}$$

what can be represented graphically as



compute

$$\mathbf{T}_\xi = \sum_{k=2}^d \frac{1}{k!} \mathbf{T}_{\xi,(k)}, \tag{6.33}$$

and repeat point 2.

4. The procedure is repeated to satisfy the stop condition.

Recall that if we take $n = n'$ the Eq. (6.32) would give the Eq. (6.29), see graphic notation for justification and the fact that for $n = n'$ we have $\mathbf{A}\mathbf{A}^\top = \mathbf{1}$. Nevertheless since the factor matrix is not uniquely determined by Eq. (6.32), some iterations may be still useful, e.g. requiring $\det(\mathbf{A}) = +1$ in a stop condition to make an outcome deterministic, see [39]. If taking $n = n'$, last columns of \mathbf{A} will give a linear combination of features with low variability. The variability measures both by the variance and higher order cumulants $3, \dots, d$ as well. These linear combination of features with low variability, correspond to safe portfolios especially for a crisis. During the crisis we have simultaneous high drops of values of many assets, what is modelled by higher order correlations [60, 225].

Alternatively, to take a full advantage of the iterative procedure, we may use $\mathbf{A}' \in \mathbb{R}^{n \times n'}$, where $n' < n$. The output would be a factor matrix giving portfolios with high variability. Next, one has to search for the factor matrix \mathbf{A}'' with columns orthonormal to the output matrix. Such \mathbf{A}'' is supposed to give a factor matrix reflecting linear combinations with variability - safe portfolios.

6.2.3 Experiments

To show that last columns of the factor matrix of the HOSVD of the d^{th} cumulant's tensors gives mainly a linear combination of such marginals that have little d order cross-correlation, we propose a following experiment. In the experimental set we use $t = 10^5$ and $n = 5$, and for each experimental realisation we generate randomly positive definite symmetric correlation matrix \mathbf{R} with ones on the diagonal, using random method discussed in Section 4.5, see Figure 4.3(a) there. Next, we sample \mathbf{X} from $\mathcal{N}(0, \mathbf{R})$, and change first two marginals of \mathbf{X} by means of a non-Gaussian copula. Next we perform the HOSVD of the \mathcal{C}_d computed for changed data, see Eq. (6.25), to get a factor matrix $\mathbf{A} \in \mathbb{R}^{n \times n}$. Such factor matrix, is a matrix of columns that are eigenvectors of $\sum_{i \setminus i_1} \mathcal{C}_d \mathcal{C}_d$. In our procedure, these eigenvectors are ordered by the information significance, which is measured by the d^{th} order cumulant of the corresponding linear combination of features. Hence if we take the last column of the factor matrix - $A_5 \in \mathbb{R}^n$, it corresponds to the lowest eigenvalue of $\sum_{i \setminus i_1} \mathcal{C}_d \mathcal{C}_d$. Such column should generally correspond to the linear combination of marginals that have small d^{th} order cross-correlation. This linear combination should have small d^{th} order cumulant, see [225]. Given the last column A_5 and its first two elements $a_{1,5}$ and $a_{2,5}$ that correspond to the impact of non-Gaussian features, we use the norm

$$w = \frac{\sqrt{a_{1,5}^2 + a_{2,5}^2}}{\|A_5\|}, \quad (6.34)$$

which should be low if there is a little impact of the non-Gaussian distributed subset in the linear combination of features given by A_5 .

Results are presented in Figure 6.7, ideally we expect $w = 0$. We have $w \approx 0$ for many realisations of the experiment given the HOSVD of \mathcal{C}_3 for data changed by the Gumbel copula and of the HOSVD of \mathcal{C}_4 for data changed by the t -Student copula. In the Gumbel copula case, observe that absolute values of elements 3rd cumulant's tensor's are basically larger than those corresponding to the 4th cumulant's tensor's, compare Figures 5.2(b) and 5.3(b). Nevertheless the performance of the HOSVD of \mathcal{C}_4 is almost as good as those of the HOSVD of \mathcal{C}_3 , especially in comparison with the performance of the SVD of the covariance matrix.

In the t -Student copula case, see Figure 6.7(b), we did not present outcomes of the HOSVD of odd cumulants, hence these cumulants are zero and the HOSVD of these cumulants would produce random results. Importantly in the t -Student copula case, the HOSVD of \mathcal{C}_4 produces good results, better than the HOSVD of \mathcal{C}_6 . This is probably due to higher estimation error of \mathcal{C}_6 in comparison with \mathcal{C}_4 , see Appendix A in [34]. Nevertheless, the HOSVD of \mathcal{C}_6 is still better than the SVD of \mathcal{C}_2 .

As a conclusion one can observe, that last columns of the factor matrix of the HOSVD of higher order cumulants tensors are good candidates for such linear combination of features in which non-Gaussian features have a little representation. Nevertheless the order of the cumulant for which the HOSVD is performed has to be determined on the base of the probabilistic mode of data.

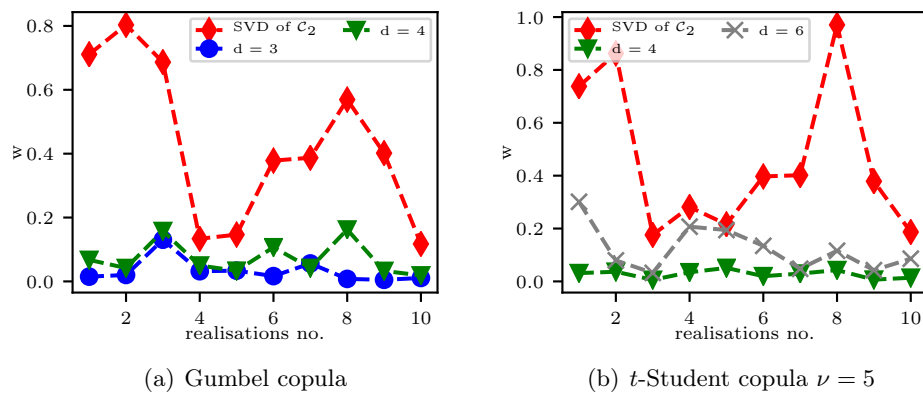


Figure 6.7: An impact of non-Gaussian features on linear combination that is supposed to have small d^{th} cumulant. Here, following Eq. (6.34), w is the measure of the participation of non-Gaussian features in the linear combination of features, given by the last column of the factor matrix. The lower w the lower participation of non-Gaussian features. For Gumbel copula best results gives the HOSVD of 3rd cumulant, while for t -Student copula the HOSVD of the 4th cumulant.

Chapter 7

Discussion

In this book, we discuss stochastic models of real-life data that break the Central Limit Theorem assumptions both in a univariate and a multivariate case. Such models give motivation for the developments of algorithms applicable to the analysis of non-Gaussian distributed data. To discuss and develop some of such algorithms we analyse probabilistic models of data, including copulas and univariate marginal distributions. Further, to analyse these probabilistic models, we use higher order multivariate statistics and, notably, higher order multivariate cumulants. This leads to particular algorithms presented in Chapter 6 of the book.

In Chapter 6 we discuss different methods of dimensionality reduction applicable for non-Gaussian distributed data. These methods provide the core of various features selection or feature extraction schemes, all based on higher order cumulants tensors. One should keep in mind that dimensionality reduction is vital in many machine learning scenarios where we either want to reduce the dimensionality of data to such that carries only interesting us information or to filter out data that are not informative or carry a noise. There we can either improve a score of further analysis or reduce the size of the data set to be further processed.

Discussed dimensionality reduction methods were tested successfully on specifically prepared artificial data with higher order dependencies within a subset of marginals. Marginals from this subset were modelled by some non-Gaussian copula, while reminding were modelled by the Gaussian copula. The discussion on the optimal dimensionality reduction schemes given various probabilistic models is provided as well in Chapter 6. For example, if we have higher order dependencies modelled by the t -Student copula, we need even higher order cumulants to analyse it, since odd ones are supposed to be zero. The wide discussion on copulas and copula-based algorithms for data preparation is presented in Chapter 4, while a wide discussion on cumulants is presented in Chapter 5.

Apart from this, we present some applications of cumulants based dimensionality reduction algorithms in real-life data analysis. In particular we concentrate on financial data analysis, hyper-spectral imaging data analysis, or biomedical data analysis. We hope for the further applications on real data, given the fact cumulants based dimensionality reduction algorithms are tested both on artificial and real-life data. Finally, these

algorithms are implemented in a modern and efficient Julia programming language and available in the `GitHub` repository.

Potential applications involve the further analysis of various non-Gaussian distributed data, both from sources mentioned in preceding paragraph, and from other sources not mentioned there. The vast source of non-Gaussian data provided from the hyper-spectral imaging. Here we can refer to various hyper-spectral analysis scenarios. One of these is the search for features (or features combinations) that carry meaningful information about small targets in detection scenarios. Another is the introduction of non-Gaussian models of hyper-spectra data.

Large sources of non-Gaussian data are financial systems as well. Referring to financial data one can use stochastic models as discussed in Chapter 2 to predict crises or other periods of high and unusual variability of financial data. In such periods extreme changes in financial data values, simultaneous on many marginals, are possible. Such dynamics can be analysed by higher order cumulants. In practice, different algebraic multi-linear methods may be applied to find such linear combinations of assets—the portfolio—that have small variability and are relatively safe. For example, one can improve the ALS approach discuss in Chapter 6, to be applicable to the practical problem of finding portfolios with low variability and positive portions of all assets, and to exclude the problematic short sale (negative portions) case. Such algorithm can be tested on a vast amount of financial data from around the world.

Analogically one can investigate non-Gaussian distributions of various multi-features biomedical data—such as multi-sources EMG or EEG data—employing higher order cumulants tensors. The proposed approach of cumulant-based multilag autocorrelation analysis of such signals is presented at the end of Chapter 5. By using advanced statistical models to analyse existing biomedical data, new knowledge can be retained without further data acquisition involving experiments on animals or human based research.

There are much more non-Gaussian real-life data that can be analysed by higher order cumulants, such as traffic data. Analysis of these data can be beneficial in computer network modelling or road, rail or air traffic modelling. Here non-Gaussian patterns can be analysed by copulas or higher order cumulants, while data dynamics by various stochastic models. There is also a potential for quantum computing in handling traffic data. Observe finally, that non-Gaussian are also weather data and solar activity data. These can be analysed in the climate and weather research, especially as extreme events are now more probable due to the climate changes. Such analysis can be beneficial both in analysing a human impact on the climate and in civil engineering.

We believe that this book will significantly contribute to the development of algorithms applicable for the non-Gaussian data analysis. As mentioned before, such analysis is crucial for various scientific disciplines and humanity development.

Bibliography

- [1] R. B. Nelsen, *An introduction to copulas*. Springer, 2007.
- [2] M. G. Kendall *et al.*, “The advanced theory of statistics,” *The advanced theory of statistics.*, no. 2nd Ed, 1946.
- [3] E. Lukacs, “Characteristics functions,” *Griffin, London*, 1970.
- [4] J. Bezanson, S. Karpinski, V. B. Shah, and A. Edelman, “Julia: A fast dynamic language for technical computing,” *arXiv:1209.5145*, 2012.
- [5] J. Bezanson, A. Edelman, S. Karpinski, and V. B. Shah, “Julia: A fresh approach to numerical computing,” *SIAM review*, vol. 59, no. 1, pp. 65–98, 2017.
- [6] U. Cherubini, E. Luciano, and W. Vecchiato, *Copula methods in finance*. John Wiley & Sons, 2004.
- [7] G. L. Vasconcelos, “A guided walk down Wall Street: an introduction to econophysics,” *Brazilian Journal of Physics*, vol. 34, no. 3B, pp. 1039–1065, 2004.
- [8] J. Domańska, *Markowskie modele nateżenia przesyłków internetowych*. IITiS PAN, 2014.
- [9] I. Norros, “On the use of fractional brownian motion in the theory of connectionless networks,” *IEEE Journal on selected areas in communications*, vol. 13, no. 6, pp. 953–962, 1995.
- [10] M. Li and S. Chen, “Fractional Gaussian noise and network traffic modeling,” in *Proceedings of the 8th WSEAS International Conference on Applied Computer and Applied Computational Science*, 2009.
- [11] B. Chandrasekaran, “Survey of network traffic models,” 2009. Washington University in St. Louis.
- [12] G. Terdik and T. Gyires, “Lévy flights and fractal modeling of internet traffic,” *IEEE/ACM Transactions on Networking*, vol. 17, no. 1, pp. 120–129, 2009.
- [13] F. Dong, K. Wu, and V. Srinivasan, “Copula analysis for statistical network calculus,” in *IEEE Conference on Computer Communications (INFOCOM)*, pp. 1535–1543, 2015.

-
- [14] F. Dong, *Copula theory and its applications in computer networks*. PhD thesis, University of Victoria, 2017.
- [15] P. Kidmose, "Alpha-stable distributions in signal processing of audio signals," in *41st Conference on Simulation and Modelling*, pp. 87–94, 2000.
- [16] A. Swami, G. B. Giannakis, and G. Zhou, "Bibliography on higher-order statistics," *Signal Processing*, vol. 60, no. 1, pp. 65–126, 1997.
- [17] B. Porat and B. Friedlander, "Direction finding algorithms based on high-order statistics," *IEEE Transactions on Signal Processing*, vol. 39, no. 9, pp. 2016–2024, 1991.
- [18] E. Moulines and J.-F. Cardoso, "Second-order versus fourth-order music algorithms: an asymptotical statistical analysis," in *Proc. IEEE Signal Processing Workshop on Higher-Order Statistics, Chamrousse, France, June, 1991*.
- [19] J.-F. Cardoso and E. Moulines, "Asymptotic performance analysis of direction-finding algorithms based on fourth-order cumulants," *IEEE Transactions on Signal Processing*, vol. 43, no. 1, pp. 214–224, 1995.
- [20] J. Liang, "Joint azimuth and elevation direction finding using cumulant," *IEEE Sensors Journal*, vol. 9, no. 4, pp. 390–398, 2009.
- [21] S. G. Iyengar, "Decision-making with heterogeneous sensors—a copula based approach," Master's thesis, Syracuse University, 2011.
- [22] R.-G. Cong and M. Brady, "The interdependence between rainfall and temperature: copula analyses," *The Scientific World Journal*, vol. 2012, p. 405675, 2012.
- [23] K. Domino, T. Błachowicz, and M. Ciupak, "The use of copula functions for predictive analysis of correlations between extreme storm tides," *Physica A: Statistical Mechanics and its Applications*, vol. 413, p. 489–497, 2014.
- [24] B. Ozga-Zielinski, M. Ciupak, J. Adamowski, B. Khalil, and J. Malard, "Snow-melt flood frequency analysis by means of copula based 2D probability distributions for the Narew River in Poland," *Journal of Hydrology: Regional Studies*, vol. 6, pp. 26–51, 2016.
- [25] D.-B. Pougaza, A. Mohammad-Djafari, and J.-F. Bercher, "Using the notion of copula in tomography," *arXiv:0812.1316*, 2008.
- [26] S. G. Iyengar, J. Dauwels, P. K. Varshney, and A. Cichocki, "Quantifying EEG synchrony using copulas," in *International Conference on Acoustics Speech and Signal Processing (ICASSP)*, pp. 505–508, 2010.
- [27] R. J. Scherrer, A. A. Berlind, Q. Mao, and C. K. McBride, "From finance to cosmology: The copula of large-scale structure," *The Astrophysical Journal Letters*, vol. 708, no. 1, p. L9, 2009.

-
- [28] E. Eban, G. Rothschild, A. Mizrahi, I. Nelken, and G. Elidan, "Dynamic copula networks for modeling real-valued time series," in *Artificial Intelligence and Statistics*, pp. 247–255, 2013.
- [29] K. Domino and A. Glos, "DatagenCopulaBased.jl: Data generator based on copulas," 2018. <https://github.com/ZKSI/DatagenCopulaBased.jl>.
- [30] A. Sundaresan, P. K. Varshney, and N. S. Rao, "Copula-based fusion of correlated decisions," *IEEE Transactions on Aerospace and Electronic Systems*, vol. 47, no. 1, pp. 454–471, 2011.
- [31] G. Mercier, G. Moser, and S. B. Serpico, "Conditional copulas for change detection in heterogeneous remote sensing images," *IEEE Transactions on Geoscience and Remote Sensing*, vol. 46, no. 5, pp. 1428–1441, 2008.
- [32] A. Voisin, V. A. Krylov, G. Moser, S. B. Serpico, and J. Zerubia, "Supervised classification of multisensor and multiresolution remote sensing images with a hierarchical copula-based approach," *IEEE Transactions on Geoscience and remote sensing*, vol. 52, no. 6, pp. 3346–3358, 2014.
- [33] J. De Leeuw, "Multivariate cumulants in R," 2012.
- [34] K. Domino, P. Gawron, and Ł. Pawela, "Efficient Computation of Higher-Order Cumulant Tensors," *SIAM Journal on Scientific Computing*, vol. 40, no. 3, pp. A1590–A1610, 2018.
- [35] K. Domino, Ł. Pawela, T. Kelman, and P. Gawron, "Cummulants.jl: Multivariate cumulants of any order," 2018. <https://github.com/ZKSI/Cumulants.jl>.
- [36] R. C. Mittelhammer, *Mathematical statistics for economics and business*. Springer, 1996.
- [37] D. Sornette, J. Andersen, and P. Simonetti, "'nonlinear' covariance matrix and portfolio theory for non-Gaussian multivariate distributions," *Physics Report*, vol. 335, pp. 19–92, 2000.
- [38] J.-F. Muzy, D. Sornette, J. Delour, and A. Arneodo, "Multifractal returns and hierarchical portfolio theory," *Quantitative Finance*, vol. 1, no. 1, pp. 131–148, 2001.
- [39] K. Domino, "The use of the multi-cumulant tensor analysis for the algorithmic optimisation of investment portfolios," *Physica A: Statistical Mechanics and its Applications*, vol. 467, pp. 267–276, 2017.
- [40] C. L. Nikias and J. M. Mendel, "Signal processing with higher-order spectra," *IEEE Signal Processing Magazine*, vol. 10, no. 3, pp. 10–37, 1993.

-
- [41] J. M. Mendel, "Tutorial on higher-order statistics (spectra) in signal processing and system theory: theoretical results and some applications," *Proceedings of the IEEE*, vol. 79, no. 3, pp. 278–305, 1991.
- [42] C. L. Nikias and A. P. Petropulu, *Higher Order Spectra Analysis: A Non-Linear Signal Processing Framework*. Prentice Hall, 1993.
- [43] J. K. Tugnait, "Identification of linear stochastic systems via second-and fourth-order cumulant matching," *IEEE Transactions on Information Theory*, vol. 33, no. 3, pp. 393–407, 1987.
- [44] S.-W. Nam and E. J. Powers, "Application of higher order spectral analysis to cubically nonlinear system identification," *IEEE Transactions on Signal Processing*, vol. 42, no. 7, pp. 1746–1765, 1994.
- [45] J.-F. Cardoso, "Super-symmetric decomposition of the fourth-order cumulant tensor. Blind identification of more sources than sensors," in *Acoustics, Speech, and Signal Processing, 1991. ICASSP-91., 1991 International Conference on*, pp. 3109–3112, 1991.
- [46] J.-F. Cardoso, "Eigen-structure of the fourth-order cumulant tensor with application to the blind source separation problem," in *Acoustics, Speech, and Signal Processing, 1990. ICASSP-90., 1990 International Conference on*, pp. 2655–2658, 1990.
- [47] X. Geng, K. Sun, L. Ji, H. Tang, and Y. Zhao, "Joint skewness and its application in unsupervised band selection for small target detection," *Scientific Reports*, vol. 5, 2015.
- [48] L. Bai, W. Guan, C. Chen, J. He, and R. Wang, "Modeling High-Speed Network Traffic with Truncated α -Stable Processes," in *Future Communication, Computing, Control and Management*, pp. 599–603, Springer, 2012.
- [49] M. Salagean and I. Firoiu, "Anomaly detection of network traffic based on analytical discrete wavelet transform," in *8th International Conference on Communications (COMM)*, pp. 49–52, 2010.
- [50] W. H. Lam, S. Wong, and H. K. Lo, eds., *Transportation and Traffic Theory 2009: Golden Jubilee*. Springer, 2009.
- [51] A. Gibberd, J. Noble, and E. Cohen, "Characterising dependency in computer networks using spectral coherence," *arXiv:1711.09609*, 2017.
- [52] M. F. Osborne, *Stock market and finance from a physicist's viewpoint*. Crossgar Pr, 1977.
- [53] N. Vandewalle and M. Ausloos, "Coherent and random sequences in financial fluctuations," *Physica A: Statistical Mechanics and its Applications*, vol. 246, no. 3-4, pp. 454–459, 1997.

-
- [54] B. B. Mandelbrot and J. W. Van Ness, “Fractional Brownian motions, fractional noises and applications,” *SIAM Review*, vol. 10, no. 4, pp. 422–437, 1968.
- [55] S. Wim, *Lévy Processes in Finance Pricing Financial Derivatives*. John Wiley & Sons Ltd, 2003.
- [56] R. F. Engle, “Autoregressive conditional heteroscedasticity with estimates of the variance of United Kingdom inflation,” *Econometrica: Journal of the Econometric Society*, pp. 987–1007, 1982.
- [57] R. Engle, “GARCH 101: The use of ARCH/GARCH models in applied econometrics,” *Journal of Economic Perspectives*, vol. 15, no. 4, pp. 157–168, 2001.
- [58] R. Engle, “New frontiers for arch models,” *Journal of Applied Econometrics*, vol. 17, no. 5, pp. 425–446, 2002.
- [59] P. Bak, M. Paczuski, and M. Shubik, “Price variations in a stock market with many agents,” *Physica A: Statistical Mechanics and its Applications*, vol. 246, no. 3-4, pp. 430–453, 1997.
- [60] D. Sornette, *Why stock markets crash: critical events in complex financial systems*. Princeton University Press, 2009.
- [61] D. Sornette and A. Johansen, “A hierarchical model of financial crashes,” *Physica A: Statistical Mechanics and its Applications*, vol. 261, no. 3-4, pp. 581–598, 1998.
- [62] R. Altschaffel, J. Dittmann, C. Kratzer, and S. Kiltz, “A hierarchical model for the description of internet-based communication,” in *Eighth International Conference on IT Security Incident Management & IT Forensics (IMF)*, pp. 85–94, 2014.
- [63] M. Gligor and M. Ignat, “Econophysics: a new field for statistical physics?,” *Interdisciplinary Science Reviews*, vol. 26, no. 3, pp. 183–190, 2001.
- [64] P. Best, *Implementing value at risk*. John Wiley & Sons, 2000.
- [65] R. O. Duda, P. E. Hart, and D. G. Stork, *Pattern classification*. John Wiley & Sons, 2012.
- [66] K. Pearson, “LIII. On lines and planes of closest fit to systems of points in space,” *The London, Edinburgh, and Dublin Philosophical Magazine and Journal of Science*, vol. 2, no. 11, pp. 559–572, 1901.
- [67] I. Jolliffe, *Principal component analysis*. Springer Series in Statistics, Springer, 2002.
- [68] J. A. Benediktsson and P. Ghamisi, *Spectral-spatial classification of hyperspectral remote sensing images*. Artech House, 2015.

-
- [69] P. Ghamisi, N. Yokoya, J. Li, W. Liao, S. Liu, J. Plaza, B. Rasti, and A. Plaza, "Advances in hyperspectral image and signal processing: A comprehensive overview of the state of the art," *IEEE Geoscience and Remote Sensing Magazine*, vol. 5, no. 4, pp. 37–78, 2017.
- [70] C. Sheffield, "Selecting band combinations from multispectral data," *Photogrammetric Engineering and Remote Sensing*, vol. 51, pp. 681–687, 1985.
- [71] S. Jia, G. Tang, J. Zhu, and Q. Li, "A novel ranking-based clustering approach for hyperspectral band selection," *IEEE Transactions on Geoscience and Remote Sensing*, vol. 54, no. 1, pp. 88–102, 2016.
- [72] J. V. Stone, *Independent component analysis: a tutorial introduction*. MIT press, 2004.
- [73] A. Hyvärinen, J. Karhunen, and E. Oja, *Independent Component Analysis. Series on Adaptive and Learning Systems for Signal Processing, Communications, and Control*. Wiley, 2001.
- [74] H. Du, H. Qi, X. Wang, R. Ramanath, and W. E. Snyder, "Band selection using independent component analysis for hyperspectral image processing," in *Applied Imagery Pattern Recognition Workshop, 2003. Proceedings. 32nd*, pp. 93–98, 2003.
- [75] T. G. Kolda and B. W. Bader, "Tensor decompositions and applications," *SIAM Review*, vol. 51, no. 3, pp. 455–500, 2009.
- [76] S. Havlin and D. Ben-Avraham, "Diffusion in disordered media," *Advances in Physics*, vol. 51, no. 1, pp. 187–292, 2002.
- [77] P. Billingsley, *Probability and measure*. Wiley Series in Probability and Mathematical Statistics, Wiley New York, 1995.
- [78] P. F. Dunn and M. P. Davis, *Measurement and data analysis for engineering and science*. CRC press, 2017.
- [79] V. Akgiray, "Conditional heteroscedasticity in time series of stock returns: Evidence and forecasts," *Journal of Business*, pp. 55–80, 1989.
- [80] T. Bollerslev, "A conditionally heteroskedastic time series model for speculative prices and rates of return," *The Review of Economics and Statistics*, pp. 542–547, 1987.
- [81] T. Bollerslev, "Generalized autoregressive conditional heteroskedasticity," *Journal of Econometrics*, vol. 31, no. 3, pp. 307–327, 1986.
- [82] B. Tim, "Glossary to ARCH (GARCH), Volatility and Time Series Econometrics: Essays in Honor of Robert F. Engle, Chapter 8," 2010.

- [83] B. Zhou, D. He, Z. Sun, and W. H. Ng, "Network traffic modeling and prediction with ARIMA/GARCH," in *Proc. of HET-NETs Conference*, pp. 1–10, 2005.
- [84] B. Zhou, D. He, and Z. Sun, "Traffic modeling and prediction using ARIMA/GARCH model," in *Modeling and Simulation Tools for Emerging Telecommunication Networks*, pp. 101–121, Springer, 2006.
- [85] J. W. Taylor and R. Buizza, "A comparison of temperature density forecasts from GARCH and atmospheric models," *Journal of Forecasting*, vol. 23, no. 5, pp. 337–355, 2004.
- [86] S. Mihandoost and M. C. Amirani, "EEG signal analysis using spectral correlation function & garch model," *Signal, Image and Video Processing*, vol. 9, no. 6, pp. 1461–1472, 2015.
- [87] R. Riccelli, L. Passamonti, A. Duggento, M. Guerrisi, I. Indovina, A. Terracciano, and N. Toschi, "Dynamical brain connectivity estimation using GARCH models: An application to personality neuroscience," in *39th Annual International Conference of the IEEE Engineering in Medicine and Biology Society (EMBC)*, pp. 3305–3308, 2017.
- [88] M. Amirmazlaghani and H. Amindavar, "EMG signal denoising via Bayesian wavelet shrinkage based on GARCH modeling," in *Proceedings of the 2009 IEEE International Conference on Acoustics, Speech and Signal Processing*, pp. 469–472, 2009.
- [89] I. Cohen, "Modeling speech signals in the time–frequency domain using GARCH," *Signal Processing*, vol. 84, no. 12, pp. 2453–2459, 2004.
- [90] S. Mousazadeh and I. Cohen, "Anomaly detection in sonar images based on wavelet domain noncausal AR-ARCH random field modeling," in *IEEE 26th Convention of Electrical and Electronics Engineers in Israel (IEEEI)*, pp. 000306–000309, 2010.
- [91] A. Feldmann, A. C. Gilbert, and W. Willinger, "Data networks as cascades: Investigating the multifractal nature of internet wan traffic," in *ACM SIGCOMM Computer Communication Review*, vol. 28, pp. 42–55, 1998.
- [92] A. Nogueira, P. Salvador, R. Valadas, and A. Pacheco, "Modeling network traffic with multifractal behavior," *Telecommunication Systems*, vol. 24, no. 2-4, pp. 339–362, 2003.
- [93] T. Blachowicz, A. Ehrmann, and K. Domino, "Statistical analysis of digital images of periodic fibrous structures using generalized Hurst exponent distributions," *Physica A: Statistical Mechanics and its Applications*, vol. 452, pp. 167–177, 2016.
- [94] K. Marri and R. Swaminathan, "Multifractal analysis of sEMG signals for fatigue assessment in dynamic contractions using Hurst exponents," in *41st Annual North-east Biomedical Engineering Conference (NEBEC)*, pp. 1–2, 2015.

-
- [95] E. S. Manolakos and H. M. Stellakis, "Systematic synthesis of parallel architectures for the computation of higher order cumulants," *Parallel Computing*, vol. 26, no. 5, pp. 655–676, 2000.
- [96] C.-K. Peng, S. V. Buldyrev, S. Havlin, M. Simons, H. E. Stanley, and A. L. Goldberger, "Mosaic organization of DNA nucleotides," *Physical Review E*, vol. 49, no. 2, p. 1685, 1994.
- [97] C.-K. Peng, S. Havlin, H. E. Stanley, and A. L. Goldberger, "Quantification of scaling exponents and crossover phenomena in nonstationary heartbeat time series," *Chaos: An Interdisciplinary Journal of Nonlinear Science*, vol. 5, no. 1, pp. 82–87, 1995.
- [98] J. W. Kantelhardt, S. A. Zschiegner, E. Koscielny-Bunde, S. Havlin, A. Bunde, and H. E. Stanley, "Multifractal detrended fluctuation analysis of nonstationary time series," *Physica A: Statistical Mechanics and its Applications*, vol. 316, no. 1-4, pp. 87–114, 2002.
- [99] H. E. Hurst, *The Nile: a general account of the river and the utilization of its waters*. Constable, 1952.
- [100] C. L. Jones, G. T. Lonergan, and D. Mainwaring, "Wavelet packet computation of the Hurst exponent," *Journal of Physics A: Mathematical and general*, vol. 29, no. 10, p. 2509, 1996.
- [101] I. Simonsen, A. Hansen, and O. M. Nes, "Determination of the hurst exponent by use of wavelet transforms," *Physical Review E*, vol. 58, no. 3, p. 2779, 1998.
- [102] U. R. Acharya, S. V. Sree, P. C. A. Ang, R. Yanti, and J. S. Suri, "Application of non-linear and wavelet based features for the automated identification of epileptic eeg signals," *International Journal of Neural Systems*, vol. 22, no. 02, p. 1250002, 2012.
- [103] R. H. Riedi, M. S. Crouse, V. J. Ribeiro, and R. G. Baraniuk, "A multifractal wavelet model with application to network traffic," *IEEE Transactions on Information Theory*, vol. 45, no. 3, pp. 992–1018, 1999.
- [104] J.-F. Muzy, E. Bacry, and A. Arneodo, "Wavelets and multifractal formalism for singular signals: Application to turbulence data," *Physical Review Letters*, vol. 67, no. 25, p. 3515, 1991.
- [105] B. Podobnik and H. E. Stanley, "Detrended cross-correlation analysis: a new method for analyzing two nonstationary time series," *Physical Review Letters*, vol. 100, no. 8, p. 084102, 2008.
- [106] D. Grech and G. Pamuła, "The local Hurst exponent of the financial time series in the vicinity of crashes on the Polish stock exchange market," *Physica A: Statistical Mechanics and its Applications*, vol. 387, no. 16, pp. 4299–4308, 2008.

- [107] Ł. Czarnecki, D. Grech, and G. Pamuła, “Comparison study of global and local approaches describing critical phenomena on the Polish stock exchange market,” *Physica A: Statistical Mechanics and its Applications*, vol. 387, no. 27, pp. 6801–6811, 2008.
- [108] K. Domino, “The use of the Hurst exponent to investigate the global maximum of the Warsaw Stock Exchange WIG20 index,” *Physica A: Statistical Mechanics and its Applications*, vol. 391, no. 1, pp. 156–169, 2012.
- [109] K. Domino, “The use of the Hurst exponent to predict changes in trends on the Warsaw Stock Exchange,” *Physica A: Statistical Mechanics and its Applications*, vol. 390, no. 1, pp. 98–109, 2011.
- [110] W. L. Maner, L. B. MacKay, G. R. Saade, and R. E. Garfield, “Characterization of abdominally acquired uterine electrical signals in humans, using a non-linear analytic method,” *Medical and Biological Engineering and Computing*, vol. 44, no. 1-2, pp. 117–123, 2006.
- [111] T. Karagiannis, M. Molle, and M. Faloutsos, “Long-range dependence ten years of internet traffic modeling,” *IEEE Internet Computing*, vol. 8, no. 5, pp. 57–64, 2004.
- [112] D. Chakraborty, A. Ashir, T. Suganuma, G. Mansfield Keeni, T. K. Roy, and N. Shiratori, “Self-similar and fractal nature of Internet traffic,” *International Journal of Network Management*, vol. 14, no. 2, pp. 119–129, 2004.
- [113] R. Bove, V. Pelino, and L. De Leonibus, “Complexity in rainfall phenomena,” *Communications in Nonlinear Science and Numerical Simulation*, vol. 11, no. 6, pp. 678–684, 2006.
- [114] P. Lévy, “Calcul des probabilités,” *Paris: Gautier-Villars*, 1925.
- [115] B. Mandelbrot, “The Pareto-Lévy law and the distribution of income,” *International Economic Review*, vol. 1, no. 2, pp. 79–106, 1960.
- [116] M. Abramowitz and I. A. Stegun, *Handbook of Mathematical Functions with Formulas, Graphs, and Mathematical Tables*. United States Department of Commerce, National Bureau of Standards, 10th ed., 1972.
- [117] J. Voit, “Random walks in finance and physics,” in *The Statistical Mechanics of Financial Markets*, pp. 25–48, Springer, 2003.
- [118] J. Voit, *The statistical mechanics of financial markets*. Springer, 2013.
- [119] J. Nolan, *Stable distributions: models for heavy-tailed data*. Birkhauser, 2003.
- [120] L. C. Miranda and R. Riera, “Truncated Lévy walks and an emerging market economic index,” *Physica A: Statistical Mechanics and its Applications*, vol. 297, no. 3-4, pp. 509–520, 2001.

-
- [121] G. M. Viswanathan, V. Afanasyev, S. Buldyrev, E. Murphy, P. Prince, and H. E. Stanley, "Lévy flight search patterns of wandering albatrosses," *Nature*, vol. 381, no. 6581, p. 413, 1996.
- [122] G. M. Viswanathan, "Ecology: Fish in Lévy-flight foraging," *Nature*, vol. 465, no. 7301, p. 1018, 2010.
- [123] P. Barthelemy, J. Bertolotti, and D. S. Wiersma, "A Lévy flight for light," *Nature*, vol. 453, no. 7194, p. 495, 2008.
- [124] X.-S. Yang, "Firefly algorithm, Lévy flights and global optimization," in *Research and development in intelligent systems XXVI*, pp. 209–218, Springer, 2010.
- [125] X.-S. Yang and S. Deb, "Engineering optimisation by cuckoo search," *International Journal of Mathematical Modelling and Numerical Optimisation*, vol. 1, no. 4, pp. 330–343, 2010.
- [126] C. Tsallis, "Nonadditive entropy and nonextensive statistical mechanics-an overview after 20 years," *Brazilian Journal of Physics*, vol. 39, no. 2A, pp. 337–356, 2009.
- [127] M. Gell-Mann and C. Tsallis, *Nonextensive entropy: interdisciplinary applications*. Oxford University Press, 2004.
- [128] W. J. Thistleton, J. A. Marsh, K. Nelson, and C. Tsallis, "Generalized Box Muller Method for Generating q-Gaussian Random Deviates," *IEEE Transactions on Information Theory*, vol. 53, pp. 4805–4810, Dec 2007.
- [129] L. D. Landau and E. M. Lifshitz, *Course of theoretical physics*. Elsevier, 2013.
- [130] S. Kirkpatrick, C. D. Gelatt, and M. P. Vecchi, "Optimization by simulated annealing," *Science*, vol. 220, no. 4598, pp. 671–680, 1983.
- [131] C. Tsallis and D. A. Stariolo, "Generalized simulated annealing," *Physica A: Statistical Mechanics and its Applications*, vol. 233, no. 1-2, pp. 395–406, 1996.
- [132] S. Umarov, C. Tsallis, and S. Steinberg, "On a q-central limit theorem consistent with nonextensive statistical mechanics," *Milan Journal of Mathematics*, vol. 76, no. 1, pp. 307–328, 2008.
- [133] S. Devi, "Financial market dynamics: superdiffusive or not?," *Journal of Statistical Mechanics: Theory and Experiment*, vol. 2017, no. 8, p. 083207, 2017.
- [134] L. Borland, "Option pricing formulas based on a non-Gaussian stock price model," *Physical Review Letters*, vol. 89, no. 9, p. 098701, 2002.
- [135] F. Michael and M. Johnson, "Financial market dynamics," *Physica A: Statistical Mechanics and its Applications*, vol. 320, pp. 525–534, 2003.
- [136] A. d'Onofrio, *Bounded noises in physics, biology, and engineering*. Springer, 2013.

- [137] A. M. C. de Souza and C. Tsallis, “Student’s t-and r-distributions: Unified derivation from an entropic variational principle,” *Physica A: Statistical Mechanics and its Applications*, vol. 236, no. 1-2, pp. 52–57, 1997.
- [138] C. Anteneodo, “Non-extensive random walks,” *Physica A: Statistical Mechanics and its Applications*, vol. 358, no. 2-4, pp. 289–298, 2005.
- [139] W. S. de Lima and E. L. Helena, “qGaussian: Tools to explore applications of Tsallis statistics,” *arXiv:1703.06172*, 2017.
- [140] I. Florescu, M. C. Mariani, H. E. Stanley, and F. G. Viens, *Handbook of High-frequency Trading and Modeling in Finance*, vol. 9. John Wiley & Sons, 2016.
- [141] R. Srivastava, I. Choi, and T. Cook, “The commercial prospects for quantum computing,” tech. rep., Networked Quantum Information Technologies, 2016.
- [142] D. Venturelli and A. Kondratyev, “Reverse Quantum Annealing Approach to Portfolio Optimization Problems,” *arXiv:1810.08584*, 2018.
- [143] N. Elsokkary, F. S. Khan, D. La Torre, T. S. Humble, and J. Gottlieb, “Financial Portfolio Management using D-Wave Quantum Optimizer: The Case of Abu Dhabi Securities Exchange,” tech. rep., Oak Ridge National Lab, 2017.
- [144] Z. Bian, F. Chudak, W. G. Macready, and G. Rose, “The Ising model: teaching an old problem new tricks,” 2010. D-Wave systems.
- [145] H. Markowitz, “Portfolio selection,” *The Journal of Finance*, vol. 7, no. 1, pp. 77–91, 1952.
- [146] Y. Cao, S. Jiang, D. Perouli, and S. Kais, “Solving set cover with pairs problem using quantum annealing,” *Scientific Reports*, vol. 6, p. 33957, 2016.
- [147] N. Jones, “The quantum company: D-Wave is pioneering a novel way of making quantum computers—but it is also courting controversy,” *Nature*, vol. 498, no. 7454, pp. 286–289, 2013.
- [148] M. A. Nielsen and I. L. Chuang, *Quantum computation and quantum information*. Cambridge University Press, Cambridge, 2000.
- [149] T. Boothby, A. D. King, and A. Roy, “Fast clique minor generation in chimera qubit connectivity graphs,” *Quantum Information Processing*, vol. 15, no. 1, pp. 495–508, 2016.
- [150] J. King, S. Yarkoni, J. Raymond, I. Ozfidan, A. D. King, M. M. Nevisi, J. P. Hilton, and C. C. McGeoch, “Quantum annealing amid local ruggedness and global frustration,” *arXiv:1701.04579*, 2017.
- [151] S. Xu, X. Sun, J. Wu, W.-W. Zhang, N. Arshed, and B. C. Sanders, “Quantum walk on a chimera graph,” *New Journal of Physics*, vol. 20, no. 5, p. 053039, 2018.

- [152] A. Glos and T. Januszek, “Impact of global and local interaction on quantum spatial search on chimera graph,” *arXiv:1807.09347*, 2018.
- [153] K. V. Mardia, “Measures of multivariate skewness and kurtosis with applications,” *Biometrika*, vol. 57, no. 3, pp. 519–530, 1970.
- [154] L. Baringhaus and N. Henze, “A consistent test for multivariate normality based on the empirical characteristic function,” *Metrika*, vol. 35, no. 1, pp. 339–348, 1988.
- [155] A. W. Van der Vaart, *Asymptotic statistics*, vol. 3 of *Cambridge Series in Statistical and Probabilistic Mathematic*. Cambridge university press, 1998.
- [156] P. Pal and P. Vaidyanathan, “Multiple level nested array: An efficient geometry for $2q$ th order cumulant based array processing,” *IEEE Transactions on Signal Processing*, vol. 60, no. 3, pp. 1253–1269, 2012.
- [157] R. Stelzer, “Multivariate continuous time Lévy-driven GARCH processes,” in *5th International Conference on Lévy Processes: Theory and Applications*, p. 89, 2007.
- [158] R. Stelzer, “Multivariate COGARCH (1, 1) processes,” *Bernoulli*, vol. 16, no. 1, pp. 80–115, 2010.
- [159] A. M. Lindner, “Continuous time approximations to garch and stochastic volatility models,” in *Handbook of Financial Time Series*, pp. 481–496, Springer, 2009.
- [160] C. Z. Yao, B.-Y. Sun, and J. N. Lin, “A study of correlation between investor sentiment and stock market based on Copula model,” *Kybernetes*, vol. 46, no. 3, 2017.
- [161] A. Sklar, “Fonctions de répartition à n dimensions et leurs marges.,” *Publications de l’Institut de Statistique de l’Université de Paris*, 1959.
- [162] H. Pham, “Recent studies in software reliability engineering,” in *Handbook of Reliability Engineering*, pp. 285–302, Springer, 2003.
- [163] S. Wu, “Construction of asymmetric copulas and its application in two-dimensional reliability modelling,” *European Journal of Operational Research*, vol. 238, no. 2, pp. 476–485, 2014.
- [164] R. Kilgore and D. Thompson, “Estimating joint flow probabilities at stream confluences by using copulas,” *Transportation Research Record: Journal of the Transportation Research Board*, no. 2262, pp. 200–206, 2011.
- [165] Y. Zhang, M. Beer, and S. T. Quek, “Long-term performance assessment and design of offshore structures,” *Computers & Structures*, vol. 154, pp. 101–115, 2015.
- [166] A. Onken, S. Grünewälder, M. H. Munk, and K. Obermayer, “Analyzing short-term noise dependencies of spike-counts in macaque prefrontal cortex using copulas and the flashlight transformation,” *PLoS Computational Biology*, vol. 5, no. 11, p. e1000577, 2009.

- [167] P. Laux, S. Wagner, A. Wagner, J. Jacobeit, A. Bardossy, and H. Kunstmann, “Modelling daily precipitation features in the Volta Basin of West Africa,” *International Journal of Climatology*, vol. 29, no. 7, pp. 937–954, 2009.
- [168] C. Schoelzel and P. Friederichs, “Multivariate non-normally distributed random variables in climate research—introduction to the copula approach,” *Nonlinear Processes in Geophysics*, vol. 15, no. 5, pp. 761–772, 2008.
- [169] H. D. Bandara and A. P. Jayasumana, “On characteristics and modeling of P2P resources with correlated static and dynamic attributes,” in *Global Telecommunications Conference (GLOBECOM 2011)*, pp. 1–6, 2011.
- [170] J. C. Strelen, “Tools for dependent simulation input with copulas,” in *Proceedings of the 2nd International Conference on Simulation Tools and Techniques*, p. 30, 2009.
- [171] A. Erdely, “A subcopula based dependence measure,” *arXiv:1610.00780*, 2016.
- [172] B. Schweizer and E. F. Wolff, “On nonparametric measures of dependence for random variables,” *The Annals of Statistics*, pp. 879–885, 1981.
- [173] P. K. Trivedi and D. M. Zimmer, “Copula modeling: an introduction for practitioners,” *Foundations and Trends in Econometrics*, vol. 1, no. 1, pp. 1–111, 2007.
- [174] P. Embrechts, F. Lindskog, and A. McNeil, “Modelling dependence with copulas,” *Rapport technique, Département de mathématiques, Institut Fédéral de Technologie de Zurich, Zurich*, 2001.
- [175] S. Cambanis, S. Huang, and G. Simons, “On the theory of elliptically contoured distributions,” *Journal of Multivariate Analysis*, vol. 11, no. 3, pp. 368–385, 1981.
- [176] S. Kotz and S. Nadarajah, *Multivariate t-distributions and their applications*. Cambridge University Press, 2004.
- [177] B. V. de Melo Mendes and R. M. de Souza, “Measuring financial risks with copulas,” *International Review of Financial Analysis*, vol. 13, no. 1, pp. 27–45, 2004.
- [178] G. Szegö, “Measures of risk,” *Journal of Banking & Finance*, vol. 26, no. 7, pp. 1253–1272, 2002.
- [179] M. Semenov and D. Smagulov, “Portfolio risk assessment using copula models,” *arXiv:1707.03516*, 2017.
- [180] A. D. El Maliani, M. El Hassouni, N.-E. Lasmar, Y. Berthoumieu, and D. Aboutajdine, “Color texture classification using rao distance between multivariate copula based models,” in *International Conference on Computer Analysis of Images and Patterns*, pp. 498–505, 2011.

- [181] A. Belghith, C. Collet, and J. P. Armspach, “Change detection based on a support vector data description that treats dependency,” *Pattern Recognition Letters*, vol. 34, no. 3, pp. 275–282, 2013.
- [182] S. Demarta and A. J. McNeil, “The t copula and related copulas,” *International Statistical Review*, vol. 73, no. 1, pp. 111–129, 2005.
- [183] S. Matthias and M. Jan-Frederik, *Simulating copulas: stochastic models, sampling algorithms, and applications*, vol. 6 of *Series in Quantitative Finance*. World Scientific, 2nd ed. ed., 2017.
- [184] N. Naifar, “Modelling dependence structure with Archimedean copulas and applications to the iTraxx CDS index,” *Journal of Computational and Applied Mathematics*, vol. 235, no. 8, pp. 2459–2466, 2011.
- [185] K. Domino and T. Błachowicz, “The use of copula functions for modeling the risk of investment in shares traded on the Warsaw Stock Exchange,” *Physica A: Statistical Mechanics and its Applications*, vol. 413, pp. 77–85, 2014.
- [186] K. Domino and T. Błachowicz, “The use of copula functions for modeling the risk of investment in shares traded on world stock exchanges,” *Physica A: Statistical Mechanics and its Applications*, vol. 424, pp. 142–151, 2015.
- [187] G. W. Peters, T. A. Myrvoll, T. Matsui, I. Nevat, and F. Septier, “Communications meets copula modeling: Non-standard dependence features in wireless fading channels,” in *IEEE Global Conference on Signal and Information Processing (GlobalSIP)*, pp. 1224–1228, 2014.
- [188] Q. Zhang, J. Li, and V. P. Singh, “Application of Archimedean copulas in the analysis of the precipitation extremes: effects of precipitation changes,” *Theoretical and applied climatology*, vol. 107, no. 1-2, pp. 255–264, 2012.
- [189] G. Tsakiris, N. Kordalis, and V. Tsakiris, “Flood double frequency analysis: 2D-Archimedean copulas vs bivariate probability distributions,” *Environmental Processes*, vol. 2, no. 4, pp. 705–716, 2015.
- [190] X. Zeng, J. Ren, Z. Wang, S. Marshall, and T. Durrani, “Copulas for statistical signal processing (Part I): Extensions and generalization,” *Signal Processing*, vol. 94, pp. 691–702, 2014.
- [191] R. F. Silva, S. M. Plis, T. Adalı, and V. D. Calhoun, “A statistically motivated framework for simulation of stochastic data fusion models applied to multimodal neuroimaging,” *NeuroImage*, vol. 102, pp. 92–117, 2014.
- [192] A. J. McNeil and J. Nešlehová, “Multivariate Archimedean Copulas, d-Monotone Functions and l_1 -Norm Symmetric Distributions,” *The Annals of Statistics*, pp. 3059–3097, 2009.

-
- [193] C. Genest and R. J. MacKay, “Copules archimédiennes et familles de lois bidimensionnelles dont les marges sont données,” *Canadian Journal of Statistics*, vol. 14, no. 2, pp. 145–159, 1986.
- [194] A. J. McNeil, “Sampling nested Archimedean copulas,” *Journal of Statistical Computation and Simulation*, vol. 78, no. 6, pp. 567–581, 2008.
- [195] M. Hofert, “Sampling archimedean copulas,” *Computational Statistics & Data Analysis*, vol. 52, no. 12, pp. 5163–5174, 2008.
- [196] D. G. Clayton, “A model for association in bivariate life tables and its application in epidemiological studies of familial tendency in chronic disease incidence,” *Biometrika*, vol. 65, no. 1, pp. 141–151, 1978.
- [197] M. M. Ali, N. Mikhail, and M. S. Haq, “A class of bivariate distributions including the bivariate logistic,” *Journal of Multivariate Analysis*, vol. 8, no. 3, pp. 405–412, 1978.
- [198] P. Kumar, “Probability distributions and estimation of Ali-Mikhail-Haq copula,” *Applied Mathematical Sciences*, vol. 4, no. 14, pp. 657–666, 2010.
- [199] A. W. Marshall and I. Olkin, “Families of multivariate distributions,” *Journal of the American Statistical Association*, vol. 83, no. 403, pp. 834–841, 1988.
- [200] W. Feller, *An introduction to probability theory and its applications. Vol. II*. John Wiley & Sons, New York, 1971.
- [201] M. Hofert and D. Pham, “Densities of nested archimedean copulas,” *Journal of Multivariate Analysis*, vol. 118, pp. 37–52, 2013.
- [202] M. Hofert, “Efficiently sampling nested Archimedean copulas,” *Computational Statistics & Data Analysis*, vol. 55, no. 1, pp. 57–70, 2011.
- [203] K. Domino and A. Glos, “Introducing higher order correlations to marginals’ subset of multivariate data by means of Archimedean copulas,” *arXiv:1803.07813*, 2018.
- [204] K. Domino, “The use of the Higher Order Singular Value Decomposition of the 4-cumulant’s tensors in features selection and outlier detection,” *arXiv:1804.00541*, 2018.
- [205] J. Bezanson, J. Chen, S. Karpinski, V. Shah, and A. Edelman, “Array operators using multiple dispatch: A design methodology for array implementations in dynamic languages,” in *Proceedings of ACM SIGPLAN International Workshop on Libraries, Languages, and Compilers for Array Programming*, p. 56, 2014.
- [206] T. Schmidt, “Coping with copulas,” in *Copulas – From Theory to Applications in Finance*, pp. 3–34, 2007.

- [207] M. Geng, H. Liang, and J. Wang, "Research on methods of higher-order statistics for phase difference detection and frequency estimation," in *Image and Signal Processing (CISP), 2011 4th International Congress on*, vol. 4, pp. 2189–2193, 2011.
- [208] J. R. Latimer and N. Namazi, "Cumulant filters-a recursive estimation method for systems with non-gaussian process and measurement noise," in *Proceedings of the 35th Southeastern Symposium on System Theory*, pp. 445–449, 2003.
- [209] J. C. Arismendi and H. Kimura, "Monte Carlo approximate tensor moment simulations," *Numer. Linear Algebra Appl.*, vol. 23, pp. 825–847, 2016.
- [210] E. Jondeau, E. Jurczenko, and M. Rockinger, "Moment component analysis: An illustration with international stock markets," *Swiss Finance Institute Research Paper*, no. 10-43, 2015.
- [211] G. Birot, L. Albera, F. Wendling, and I. Merlet, "Localization of extended brain sources from EEG/MEG: the ExSo-MUSIC approach," *NeuroImage*, vol. 56, no. 1, pp. 102–113, 2011.
- [212] H. Becker, L. Albera, P. Comon, M. Haardt, G. Birot, F. Wendling, M. Gavaret, C.-G. Bénar, and I. Merlet, "EEG extended source localization: tensor-based vs. conventional methods," *NeuroImage*, vol. 96, pp. 143–157, 2014.
- [213] J. Gabelli and B. Reulet, "High frequency dynamics and the third cumulant of quantum noise," *Journal of Statistical Mechanics: Theory and Experiment*, vol. 2009, no. 01, p. P01049, 2009.
- [214] M. D. Schatz, T. M. Low, R. A. van de Geijn, and T. G. Kolda, "Exploiting symmetry in tensors for high performance: Multiplication with symmetric tensors," *SIAM Journal on Scientific Computing*, vol. 36, no. 5, pp. C453–C479, 2014.
- [215] A. Gut, *An Intermediate Course in Probability*. Springer, 2009.
- [216] K. Domino, Ł. Pawela, P. Gawron, and T. Kelman, "SymmetricTensors.jl: Framework for symmetric tensors." <https://github.com/ZKSI/SymmetricTensors.jl>, 2018.
- [217] P. Głomb, K. Domino, M. Romaszewski, and M. Cholewa, "Band selection with Higher Order Multivariate Cumulants for small target detection in hyperspectral images," *arXiv:1808.03513*, 2018.
- [218] S. M. Qasim, S. Abbasi, S. Alshebeili, B. Almashary, and A. A. Khan, "Fpga based parallel architecture for the computation of third-order cross moments," *International Journal of Computer, Information and Systems Science, and Engineering*, vol. 2, no. 3, pp. 216–220, 2008.
- [219] J. Muthuswamy and N. V. Thakor, "Spectral analysis methods for neurological signals," *Journal of Neuroscience Methods*, vol. 83, no. 1, pp. 1–14, 1998.

- [220] E. Pereda, R. Q. Quiroga, and J. Bhattacharya, “Nonlinear multivariate analysis of neurophysiological signals,” *Progress in Neurobiology*, vol. 77, no. 1-2, pp. 1–37, 2005.
- [221] C. Rabotti, *Characterization of uterine activity by electrohysterography*. PhD thesis, Eindhoven University of Technology, 2010.
- [222] M. Domino, B. Pawlinski, M. Gajewska, T. Jasinski, M. Sady, and Z. Gajewski, “Uterine EMG activity in the non-pregnant sow during estrous cycle,” *BMC Veterinary Research*, vol. 14, no. 1, p. 176, 2018.
- [223] M. Domino, B. Pawlinski, and Z. Gajewski, “The linear synchronization measures of uterine EMG signals: Evidence of synchronized action potentials during propagation,” *Theriogenology*, vol. 86, no. 8, pp. 1873–1878, 2016.
- [224] M. Domino, B. Pawlinski, and Z. Gajewski, “Biomathematical pattern of EMG signal propagation in smooth muscle of the non-pregnant porcine uterus,” *PLoS One*, vol. 12, no. 3, p. e0173452, 2017.
- [225] J. Morton, “Algebraic models for multilinear dependence,” 2009. NSF Workshop Future Directions in Tensor-Based Computation and Modeling.
- [226] P. Głomb, M. Romaszewski, M. Cholewa, and K. Domino, “Application of hyperspectral imaging and machine learning methods for the detection of gunshot residue patterns,” *Forensic Science International*, vol. 290, pp. 227–237, 2018.
- [227] O. Dalby, D. Butler, and J. W. Birkett, “Analysis of gunshot residue and associated materials—a review,” *Journal of Forensic Sciences*, vol. 55, no. 4, pp. 924–943, 2010.
- [228] I. S. Reed and X. Yu, “Adaptive multiple-band CFAR detection of an optical pattern with unknown spectral distribution,” *IEEE Transactions on Acoustics, Speech, and Signal Processing*, vol. 38, no. 10, pp. 1760–1770, 1990.
- [229] B. Schölkopf and A. J. Smola, *Learning with kernels*. MIT Press, 1998.
- [230] K. Domino and P. Gawron, “Algorithm for an arbitrary-order cumulant tensor calculation in a sliding window of data streams,” *Int. J. Appl. Math. Comput. Sci.*, vol. 29, no. 1, 2019.
- [231] K. Domino and P. Gawron, “CumulantsUpdates.jl: Updates of high order cumulant tensors,” 2018. <https://github.com/ZKSI/CumulantsUpdates.jl>.
- [232] M. Domino, K. Domino, and Z. Gajewski, “An application of higher order multivariate cumulants in modelling of myoelectrical activity of porcine uterus during early pregnancy,” *Biosystems*, vol. 175, pp. 30–38, 2019.

- [233] H. Eswaran, H. Preissl, J. D. Wilson, P. Murphy, and C. L. Lowery, "Prediction of labor in term and preterm pregnancies using non-invasive magnetomyographic recordings of uterine contractions," *American Journal of Obstetrics and Gynecology*, vol. 190, no. 6, pp. 1598–1602, 2004.
- [234] R. Fanchin and J. M. Ayoubi, "Uterine dynamics: impact on the human reproduction process," *Reproductive Biomedicine Online*, vol. 18, pp. S57–S62, 2009.
- [235] F. Sammali, N. P. M. Kuijsters, B. C. Schoot, M. Mischi, and C. Rabotti, "Feasibility of transabdominal electrohysterography for analysis of uterine activity in nonpregnant women," *Reproductive Sciences*, pp. 1124–1133, 2018.
- [236] D. Devedeux, C. Marque, S. Mansour, G. Germain, and J. Duchêne, "Uterine electromyography: a critical review," *American Journal of Obstetrics and Gynecology*, vol. 169, no. 6, pp. 1636–1653, 1993.
- [237] Z. Gajewski, M. Blitek, J. Klos, K. Gromadzka-Hliwa, B. Pawlinski, A. Andrzejczak, and A. Ziecik, "Oviductal and uterine myometrial activity during periovulatory period in the pig," *Reprod. Dom. Anim*, vol. 1, pp. 41–47, 2004.
- [238] E. Oczeretko, A. Kitlas, M. Borowska, J. Światecka, and T. Laudański, "Uterine contractility: visualization of synchronization measures in two simultaneously recorded signals," *Annals of the New York Academy of Sciences*, vol. 1101, no. 1, pp. 49–61, 2007.
- [239] R. E. Garfield and W. L. Maner, "Biophysical methods of prediction and prevention of preterm labor: uterine electromyography and cervical light-induced fluorescence—new obstetrical diagnostic techniques," *Preterm. Birth*, pp. 131–144, 2007.
- [240] C. Rabotti and M. Mischi, "Propagation of electrical activity in uterine muscle during pregnancy: a review," *Acta Physiologica*, vol. 213, no. 2, pp. 406–416, 2015.
- [241] M. Domino, K. Domino, B. Pawlikowski, M. Sady, M. Gajewska, and Z. Gajewski, "Computational multivariate modeling of electrical activity of porcine uterus during spontaneous and hormone-induced estrus," *Experimental Physiology*, 2019.
- [242] K. Domino, "CumulantsFeatures.jl: Cumulants based features selection and outlier detection." <https://github.com/ZKSI/CumulantsFeatures.jl>, 2018.
- [243] L. R. Tucker, "Some mathematical notes on three-mode factor analysis," *Psychometrika*, vol. 31, no. 3, pp. 279–311, 1966.
- [244] L. De Lathauwer, B. De Moor, and J. Vandewalle, "A multilinear Singular Value Decomposition," *SIAM Journal on Matrix Analysis and Applications*, vol. 21, no. 4, pp. 1253–1278, 2000.
- [245] W. Krzanowski, *Principles of multivariate analysis*, vol. 22 of *Oxford Statistical Science Series*. OUP Oxford, 2000.

-
- [246] L. De Lathauwer and J. Vandewalle, “Dimensionality reduction in higher-order signal processing and rank- (r_1, r_2, \dots, r_n) reduction in multilinear algebra,” *Linear Algebra and its Applications*, vol. 391, pp. 31–55, 2004.
- [247] B. Savas and L.-H. Lim, “Quasi-Newton methods on Grassmannians and multilinear approximations of tensors,” *SIAM Journal on Scientific Computing*, vol. 32, no. 6, pp. 3352–3393, 2010.